F44620-71-C-0067

AD-740880

CONSOLIDATED SEMIANNUAL PROGRESS REPORT

NO. 14

Covering Research Activity During the Period

31 March 1971 through 1 October 1971

Prepared By
The
Electronic Sciences Laboratory
of the
School of Engineering
University of Southern California
Los Angeles, California 90007

UNCLASSIFIED
Security Classification

DOCUMENT CONTROL DATA - R & D

(Security classification of title, body of abstract and indexing annotation must be entered when the overall report is classified)

1. ORIGINATING ACTIVITY (Corporate author)	2a. REPORT SECURITY CLASSIFICATION
Electronic Sciences Laboratory University of Southern California Los Angeles, California 90007	Unclassified
	2b. GROUP

3. REPORT TITLE

CONSOLIDATED SEMIANNUAL PROGRESS REPORT NO. 14 #13 AD. 728242

4. DESCRIPTIVE NOTES *(Type of report and inclusive dates)*

Scientific ---------- Interim

5. AUTHOR(S) *(First name, middle initial, last name)*

Z. A. Kaprielian

6. REPORT DATE	7a. TOTAL NO. OF PAGES	7b. NO. OF REFS
13 April 1972	172	

8a. CONTRACT OR GRANT NO. F44620-71-C-0067	9a. ORIGINATOR'S REPORT NUMBER(S)
b. PROJECT NO. 4751	
c. 61102F	9b. OTHER REPORT NO(S) *(Any other numbers that may be assigned this report)*
d. 681305	AFOSR - TR - 72 - 0919

10. DISTRIBUTION STATEMENT

Approved for public release; distribution unlimited.

11. SUPPLEMENTARY NOTES	12. SPONSORING MILITARY ACTIVITY
TECH, OTHER	JSEP through AFOSR (NE) 1400 Wilson Boulevard Arlington, Virginia 22209

13. ABSTRACT

This document is Semiannual Progress Report No. 14 issued by the Electronic Sciences Laboratory, University of Southern California, Los Angeles, California. It summarized the research activity during the period of 1 April 1971 to 31 October 1971.

DD FORM 1 NOV 65 1473

TABLE OF CONTENTS

---

* Supported by Joint Services Electronics Program.

ACKNOWLEDGEMENT

This document is Semiannual Progress Report No. 14 issued by the Electronic Sciences Laboratory, University of Southern California, Los Angeles. It summarizes the research activity conducted during the period 1 April 1971 through 1 October 1971.

The Laboratory hereby acknowledges the following support:

Contract or Grant	Agency
AF-AFOSR-71-2066	Air Force Office of Scientific Research
AF-AFOSR-71-2075	Air Force Office of Scientific Research
AF-AFOSR-71-2087	Air Force Office of Scientific Research
AF-AFOSR-71-2088	Air Force Office of Scientific Research
F19628-71-C-0220	Air Force Cambridge Research Laboratories
F44620-71-C-0667	Air Force Office of Scientific Research
AFOSR-68-1555	Air Force Office of Scientific Research
GJ 28787	National Science Foundation
GK-4056	National Science Foundation
GK-5751	National Science Foundation
GK-12796	National Science Foundation
GK-14190	National Science Foundation
GK-15787	National Science Foundation
GK-17042	National Science Foundation
GK-19283	National Science Foundation
GK-20258	National Science Foundation
GK-23886	National Science Foundation
GK24877	National Science Foundation
GK-24520	National Science Foundation
GK-25144	National Science Foundation
GP-19109	National Science Foundation
GP-29031	National Science Foundation

Contract or Grant	Agency
GP-29049	National Science Foundation
DAHC-04-69-C-0003	Department of the Army (ARPA)
DAHC-15-71-G-6	Department of the Army (ARPA)
DA-ARO-D 31-124-70-G15	U.S. Army Research Office, Durham
DA-ARO-D 31-124-71-G34	U.S. Army Research Office, Durham
DA-ARO-D 31-124-71-G37	U.S. Army Research Office, Durham
DA-ARO-D 31-124-71-G104	U.S. Army Research Office, Durham
DA-ARO-D 31-124-71-G51	U.S. Army Research Office, Durham
N00014-67-A-0269-0006	Office of Naval Research
N00014-67-A-0269-0007	Office of Naval Research
N00014-67-A-0269-0010	Office of Naval Research
N00014-67-A-0269-0018	Office of Naval Research
N00014-67-A-0269-0019	Office of Naval Research
N00014-67-A-0269-0020	Office of Naval Research
N00014-67-A-0269-0022	Office of Naval Research
NAS 5-21505	National Aeronautics and Space Administration
NGR-05-018-022	National Aeronautics and Space Administration
NGL-05-018-044	National Aeronautics and Space Administration
NGR-05-018-104	National Aeronautics and Space Administration
NGL-05-018-118	National Aeronautics and Space Administration
AM 15145-02	Department of Health, Education and Welfare
GM 01724-05	Department of Health, Education and Welfare
GM 16197-03	Department of Health, Education and Welfare
GM 16437-03	Department of Health, Education and Welfare
GM 39547-03	Department of Health, Education and Welfare
RR 07012	Department of Health, Education and Welfare
AT (04-3)-113 #19	Atomic Energy Commission
AT (04-3)-113 #22	Atomic Energy Commission
AT (04-3)-113 #23	Atomic Energy Commission
PF-019	California Institute of Technology
PF-304	California Institute of Technology

PARTICIPATING PERSONNEL OF THE UNIVERSITY OF SOUTHERN CALIFORNIA ELECTRONIC SCIENCES LABORATORY

DIRECTOR

Z. A. Kaprielian

FACULTY, VISITING FACULTY AND RESEARCH ASSOCIATES

Anderson, R.
Andrews, H. C.
Azen, S. P.
Bekey, G. A.
Bellman, R. E.
Bergman, R.
Breuer, M. A.
Buell, J. M.
Cady, J. R.
Card, R. E.
Carlson, F. R.
Chandler, W. J.
Copley, S.
Crowell, C. R.
Davisson, L. D.
Daybell, M. D.
DeShazer, L. G.
Dunk, A. C.
Esquivel, A. L.
Faust, W. L.
Fenner, W. R.
Gabrielian, A.
Gagliardi, R. M.
Gershenzon, M.
Gilbert, P.
Ginsburg, S.
Goldstine, J.
Golomb, S. W.
Grodins, F. S.
Habib, A.
Halloran, M. H.
Harris, T. E.
Hellwarth, R. W.
Hibbard, T. W.
Hurrell, J. P.
Jain, A.
Johnson, E. S.
Kruger, R.
Kalaba, R.
Kashef, B.
Kashef, R.
Kell, C.
Kim, J-K.
Kim, K.S.
Kim, Y. B.
Kleitz, M.
Kroger, F. A.
Kuehl, H. H.
Lakin, K. M.
Lamont, J. W.
Langdon, T.
Lindsey, W. C.
Louisell, W. H.
Maloney, J.
Marburger, J. H.
Marsh, D.
Meisel, W. S.
Merritt, M. J.
Meyer, G.
Moore, G. P.
Munushian, J.
Murr, L. E.
Nahi, N. E.
Narayanan, G.
Neustadt, L. W.
Nich, S.
Ohlson, J. E.
Olive, D. W.
Osaki, S.
Parks, J.
Payne, R. T.
Penne, R. F.
Porto, S.P.S.
Pratt, W. K.
Ramon, U.
Reed, I. S.
Reichert, J. D.
Reswick, J. B.
Roohk, V.
Rusch, W.V.T.
Sato, T.
Scholtz, R. A.
Shlichta, P. J.
Silverman, L. M.
Singh, H.
Smit, J.
Smith, J. D.
Smith, S. W.
Smith, T. I.
Soong, T. T.
Spitzer, W. G.
Steele, D. F.
Steier, W. H.
Stover, H. L.
Su, Y-H.
Swerling, P.
Sworder, D. G.
Tooper, R. F.
Ung, M. T.
Vasudevan, G.
Wagner, W. G.
Wang, R.
Weber, C. L.
Welch, L. R.
Whelan J. M.
Wilcox, W. R.
Williams, L. J.
Wittry, D. B.
Wolf, M. B.
Yamashiro, S.
Yates, F. F.
Zobrist, A.

LECTURERS AND GRADUATE RESEARCH ASSISTANTS

Agarwal, V. K.
Allen, G. D.
Allred, W. P.
Alyassini, M.
Assefi, T.
Austin, J. W.
Axwelband, E. L.
Baenziger, G. P.
Baker, J. E.
Basu, R.
Beguwala, M.M.E.
Bottlik, I. P.
Bower, H. H.
Bowman, C. K.
Brandsma, M.
Brewer, J. H.
Cady, L. D.
Cervenka, P. O.
Chang, C. E.
Chang, S-J.
Chao, T. C.
Chen, C-K.
Chen, D-Y.
Chen, K-H.
Chen, W-H.
Cheng, I-C.
Chern, S. S.
Chiao, S-M.
Chiu, K-Y.
Choi, L. L.
Colbert, T.
Culbertson, G.
Dutt, B.
Farrukh, U.
Fordyce, W. E.
Franco, C. A.
Frohlich, A.
Galanoudes, V.
Gonzalez, D.
Guha, J. K.
Hale, R. L.
Hartmann, U. G.
Hawk, W. E.
Hon, D. T.
Horylev, R. J.
Hsiung, S-K.
Huang, C-H.
Hyman, E.
Joiner, R., Jr.
Joshi, S.
Joseph, T. R.
Kahyai, K.
Kao, K.
Karush, R.
Kazakos, D.
Kazakos, P. P.
Kazangey, T.
Khalaf, A.
Klement, R.
Ko, D.C.C.
Kosai, K.
Krol, J. G.
Kung, J. K.
Kuo, V.H.S.
Lambrigtsen, B.
Larson, R. W.
Lederman, S.
Leung, P. C.
Levy, M. E.
Lin, M-C.
Lin, W-N.
Lioio, R. J.
Lindholm, C.
Liporace, L.
Mack, D. R.
Mancill, C.
Mangis, M. S.
Mark, J. G.
McCormack, M.
McHard, R. W.
Miller, D. S.
Mohanty, N. C.
Naraghi, M.
Newnam, B. E.
Nourai, F.
Nuttahi, D. E.
Okuto, Y.
Otaguro, W. S.
Outwater, J. E.
Parker, R. D.
Paterson, W. L.
Penunuri, D.
Perlman, M.
Potash, H.
Powell, S. R.
Proffitt, W. P.
Rao, P.A.D.
Rao-Sahib, T.
Reader, C.
Rim, C.
Rounsavell, T.
Schlosser, G.
Schrey, A. F.
Selim, F. A.
Seo, J.
Sen, S.
Shei, S-A.
Shortwell, C. P.
Smith, D. R.
Smith, J. M.
Smith-Palliser, A.
Sun, C.
Swaminathan, V.
Tang, C-H.
Tejada-Flores, L.
Tolivar, A.
Trivedi, A.
Tee, G. J.
Tuey, D. B.
Turner, G. B.
Vassilakis, G.
Vijayakumar, P.S.
Vydyanath, H.
Wang, K-L.
Ware, J. E., Jr.
Weilin, S. A.
Wilczynski, D.
Yee, J. F.
Yeo, Y-K.
Yeh, L. S.
Yip, V. F-S.
Yu, J. W.
Ziai, E.

TECHNICAL SUPPORT PERSONNEL

Akachi, T. M.
Asa, M. L.
Duplex, J. J.
Emerson, J. C.
Goldstein, J.
Haller, B.
Hellock, L.
Hill, R. M.
Howland, D. L.
Huff, S. G.
Lum, F.
Lunden, R.
Lloyd, H.
Maran, J. W.
Maunders, E. A.
Mikhel, R. E.
Morris, L.
Mueller, G.
Owen, H. R.
Pearson, C.
Pocock, H.
Reichik, M.
Sanders, M. A.
Savage, J. W.
Soberay, W. G.
Thill, R. J.
Thornton, H. J.
Watts, J. C.
Wong, G.
Wong, R.
Yasuda, C.
Yoshida, J.

ADMINISTRATIVE

Alexander, R. Z.
Armstrong, J.
Baker, W. P.
Blood, L. J.
Collins, K.
Daruty, K.
Dillon, E. P.
Enriquez, A.
Estrada, M.
Gursel, N.
Hoagland, J.
Lee, L.
Leslie, C. J.
Lopez, F.
Luginbuehl, A.
Lum, G. T.
Lyness, C. J.
Mahoney, A. M.
Marshall, J. W.
Nihei, J. T.
Osborne, D. M.
Patterson, A.
Pendleton, A. K.
Pester, B. A.
Pratt, A. K.
Reuter, A. M.
Redmon, B.
Rice, G. L.
Roth, R. J.
Rothman, B. A.
Salas, V. J.
Strouse, B.
Stuart, J. H.
Tierney, M.
Ward, R. A.
Webster, L. M.
White, L. A.
Wilcox, S. L.
Wilkinson, C.
Zoitl, M. V.

1. SOLID STATE

1.1 SEMICONDUCTORS

1.1.1 Localized Vibrational Mode Absorption of Ion Implanted Silicon in GaAs

GK-10633, National Science Foundation

F19628-68-C-0169, Air Force Cambridge Research Laboratories

AFOSR-71-2075, Air Force Office of Scientific Research

F44620-71-C-0067, Joint Services Electronics Program

W. G. Spitzer, L. H. Skolnik, A. Kahan*, and R. G. Hunsperger**

Introduction

Recent infrared absorption studies have reported localized vibrational modes (LVM) for ion implanted species in semiconductors. In particular, the vibrational modes of oxygen and carbon implanted into silicon (refs. 1 and 2) and of aluminum and phosphorus implanted into GaAs (ref. 3) have been observed. In the present discussion we present some results for GaAs implanted with Si. This case is of interest not only because of the technological importance of GaAs:Si, but also because of the variety of point defects in which Si impurities in GaAs are known to participate. Vibrational modes have been previously identified for Si substitutional on a Ga site Si_{Ga}, Si substitutional on an As site Si_{As}, Si_{Ga} - Si_{As} nearest neighbor pairs,

* Air Force Cambridge Research Laboratories, Bedford, Massachusetts.

** Hughes Research Laboratory, Malibu, California.

and Si_{Ga} - Cu_{Ga} and Si_{Ga} - Li_{Ga} second neighbor pairs (refs. 4, 5, 6).

When GaAs: Si is grown from a near-stoichiometric melt, the resulting material is always n-type; however, the carrier concentration saturates at 5-10 x 10^{18} cm^{-3} while the solid solubility of Si is 1-2 x 10^{20} cm^{-3} (ref. 7). This electrical behavior is explained in terms of three defect species: Si_{Ga} which is a donor, Si_{As} an acceptor, and Si_{Ga} - Si_{As} pairs of unknown but probably neutral electrical behavior.

Experimental Results and Discussion

Liquid nitrogen temperature infrared absorption spectra of several Si implanted GaAs samples have been measured. The techniques of implantation and measurement have been discussed previously (ref. 3). Figure 1 shows representative liquid nitrogen temperature spectra for a sample implanted with a fluence of 4.2 x 10^{16} Si/cm^2 on each side at room temperature and at an energy of 1.5 MeV. The sample was annealed for 1 hr. periods at 100°C intervals from 200 to 500°C, at 50°C intervals to 800°C, and at 900°C. Infrared absorption measurements were made after each anneal. Similar results were obtained for a 1.0 MeV implant. The product of the absorption coefficient and implant layer thickness is given as a function of frequency, where the absorption of the GaAs lattice has been subtracted. Therefore, the bands are those produced by the Si implantation alone. The integrated intensity, $\int(\alpha x)d\nu$ of each band shown in Fig. 1 is proportional to the areal concentration of the particular species responsible for that band.

After the 400°C anneal stage the sample was encapsulated with a 1000 Å SiO_2 layer at 425°C to inhibit the loss of As upon higher temperature annealing and also to reduce the possibility of Si outdiffusion. The 1000 Å SiO_2 layer is sufficiently thin that its absorption in the spectral region of interest is negligible (ref. 9) and infrared absorption measurements could be made without removing the layer.

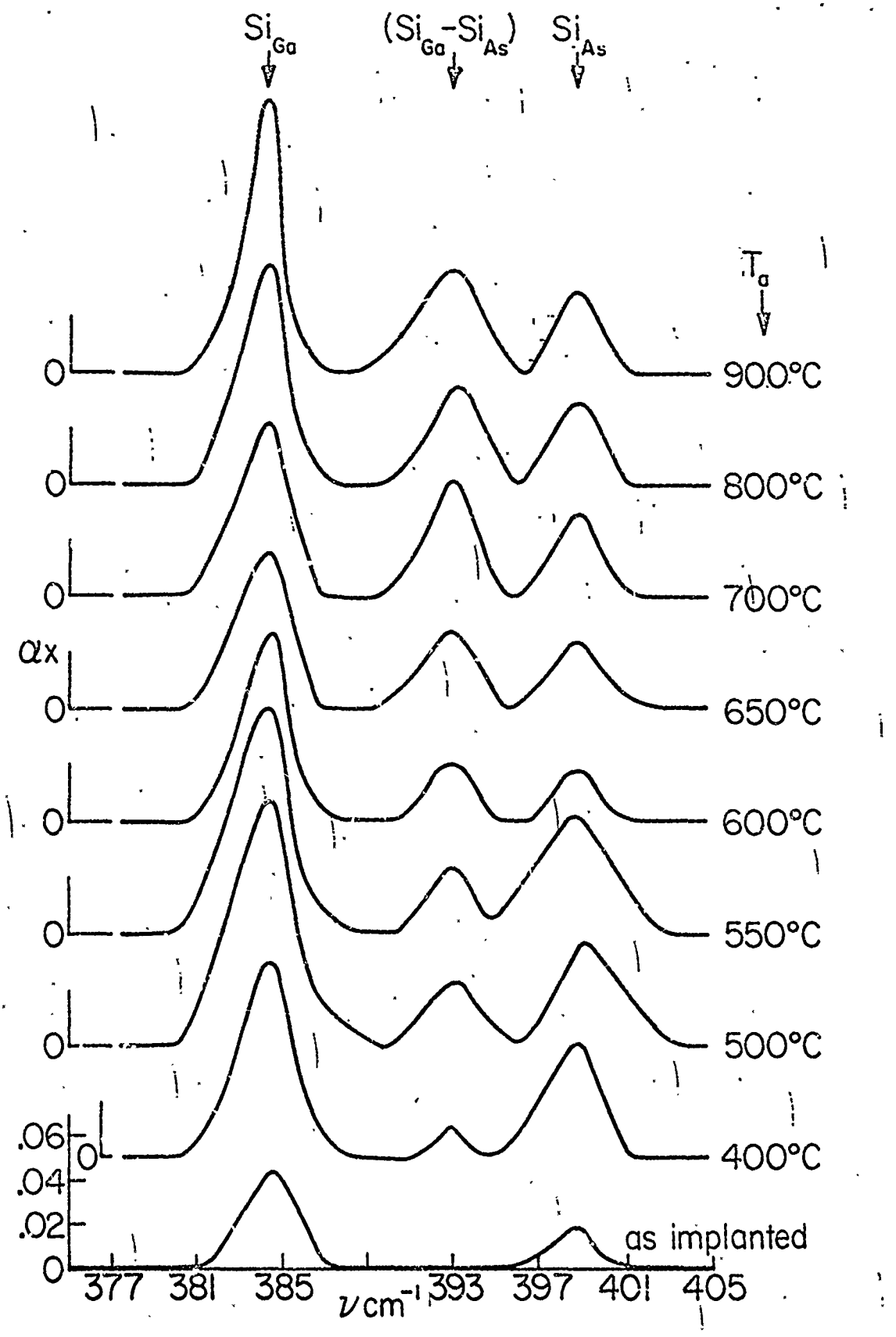

Figure 1: Selected liquid nitrogen temperature absorption spectra of GaAs implanted at room temperature with 4.2×10^{16} Si/cm^2 on each side of 1.5 MeV. All anneals were for one hour and and at temperatures as described in the text. The Si_{Ga}, Si_{As}, and Si_{Ga}-Si_{As} pair) bands are seen at 384 cm^{-1}, 399 cm^{-1} and 393 cm^{-1} respectively, The αx scale on the lowest spectrum applies equally to all the spectra.

It had previously been established on phosphorus implanted samples that any Si contamination from the film was below our optical detection limits. The SiO_2 layer was grown in a silane gas oxidation system with a SiH_4: O_2 ratio of 1:100. Thus an excess of free Si included in the layer is not expected. Furthermore, growth of undoped GaAs in quartz boats produces material with low [Si] and therefore, no significant Si contamination of the sample was expected from the SiO_2 film.

Before annealing above room temperature, two bands are observed, one at $\sim 384\ cm^{-1}$ previously attributed to the Si_{Ga} donor defect and the other near $399\ cm^{-1}$ from the Si_{As} acceptor species (refs. 4, 5, 6). Both bands grow with anneal temperature to 400°C where a weak band near $393\ cm^{-1}$ is first detected. The $393\ cm^{-1}$ band is due to the doubly degenerate out-of-phase transverse vibration of the $(Si_{Ga}-Si_{As})$ pair defect which has C_{3v} symmetry (ref. 6). The bands continue to increase with anneal temperature until 500-550°C and decreases with further increases in anneal temperature until ~650°C. A similar behavior is noted for the Si_{As} band at $399\ cm^{-1}$ which peaks at ~550°C and shows a sharp decrease in intensity after 600°C annealing. The $(Si_{Ga}-Si_{As})$ pair band, however, shows no such large decrease but rather remains nearly constant in strength between the 500 to 600°C annealing stages. Upon annealing at temperatures above ~650°C, the integrated absorption of all three bands are seen to increase.

These results are shown quantitatively in Fig. 2 for each of the bands of Fig. 1. The scale on the right side of the graph giving the Si_{Ga} and Si_{As} areal concentrations was obtained from the reported absorption cross section measurements on melt grown GaAs:Si of known [Si] (ref. 6). From these absorption cross sections, one finds $\int \alpha x\, d\nu = 1.7 \times 10^{-17}\ N\ (Si)$, where N(Si) is either the Si_{Ga} or Si_{As} areal concentration and the integration is over the Si_{Ga} or Si_{As} LVM band. Unfortunately, there are no reliable cross section measurements

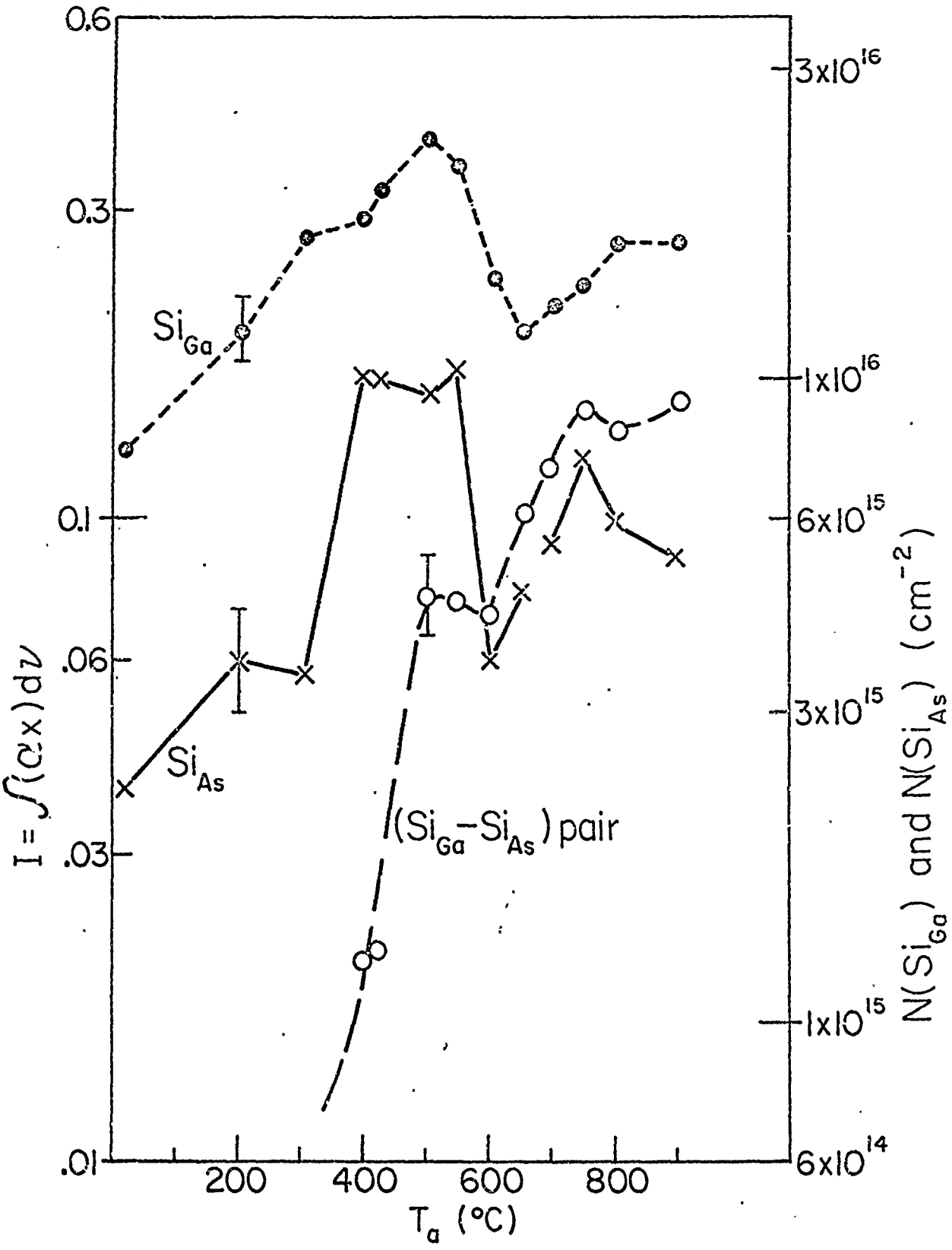

Figure 2: Integrated αx of the localized mode bands and Si defect concentrations as a function of anneal temperature for the sample whose spectra are shown in Figure 1.

for the (Si_{Ga} - Si_{As}) pair band, and one cannot therefore quantitatively relate the sum of the integrated absorptions to the total silicon concentration. If the spatial distribution of the implanted Si is assumed to be approximately Gaussian, then based on the LSS model (ref. 10) one estimates an average [Si] of $\sim 1 \times 10^{21}$ cm^{-3}. Therefore, under these implant conditions, the Si solubility in melt grown crystals has probably been exceeded.

There are several points of interest in the results shown in Figs. 1 and 2. The increase with temperature up to $\sim 500^{\circ}C$ of $\int \alpha x \, d\nu$ for both the Si_{Ga} and Si_{As} band is presumably related to annealing of lattice disorder introduced by the implantation. Both the 384 cm^{-1} and 399 cm^{-1} bands are the $\Delta n = 1$ transitions from the vibrational ground state of the Si_{Ga} and Si_{As} species, where each has tetrahedral (T_d) point group symmetry. The first excited state of the T_d oscillator is triply degenerate ($^3\Gamma_5$) and the degeneracy can be split by perturbations which lower the point group symmetry. Although the observed line widths in Fig. 1 are larger than those observed in grown samples (see Fig. 3), the bands are well resolved with no measurable evidence for fine structure. Therefore, it appears reasonable to conclude that the annealing of disorder increases the number of Si species which reside in substitutional sites of nearly tetrahedral symmetry. This result is similar to that of the P and Al in GaAs (ref. 3) and is in qualitative agreement with previous electrical studies of GaAs implanted with Si (ref. 8). The decrease in the Si_{Ga} and Si_{As} concentrations for anneal temperatures above $\sim 550^{\circ}C$ is not well understood. Clearly the decrease is not the result of direct formation of pairs by a $Si_{Ga} + Si_{As} \rightarrow (Si_{Ga} - Si_{As})$ process since the 393 cm^{-1} pair band shows little change from $500^{\circ}C$ to $600^{\circ}C$. Similar annealing effects were observed in the other Si-implanted samples all of which were implanted with energies and fluences within a factor of two of the sample in Fig. 1 and 2.

Because of these results, the room temperature carrier concentration of melt grown, heavily Si-doped GaAs ($[Si] \approx 10^{19}$ - 10^{20} cm^{-3}) was measured by using the plasma resonance method through a set of anneals similar to those of Fig. 1. Preliminary results indicate that $n_e = [Si_{Ga}] - [Si_{As}]$ decreases substantially in the 400-600°C range, a result which is qualitatively consistent with the data of Fig. 1 and 2. The recovery in n_e predicted by Fig. 2 for annealing at $T_A \geq$ 650°C is also observed in grown samples. This annealing effect on n_e is not observed in samples for which $[Si] \lesssim 1\text{-}2 \times 10^{18}$ cm^{-3}. The similarity of the results for the melt doped and ion implanted samples suggests that the mechanism responsible for the Si_{Ga} and Si_{As} decrease is not directly related to the implantation processs but is rather a general result for heavily Si-doped GaAs.

The changes in line widths of Fig. 1 are also of interest. In Fig. 3 we reproduced the 650°C and 900°C curves of Fig. 1 along with the spectrum of a melt doped sample where the $[Si] \sim 10^{20} cm^{-3}$. The thickness used for the grown sample was chosen such that the value of αx (peak) at 384 cm^{-1} is the same as the 900°C anneal curve. The line narrowing of the 384 band between 650 and 900°C anneal is clear. The 399 and particularly the 393 cm^{-1} bands are both broader than the same bands in the grown material. The details of line shape in the implant spectra should, however, be viewed with considerable reservation as the measured absorption is small and the possible errors quite large (see error bars in Fig. 2). These results are also similar to those reported for P and Al implants in GaAs (ref. 3). For the case of P in GaAs, crude calculations indicate that line broadening from inhomogeneous elastic strain fields as well as frequency shifts arising from macroscopic variations in local [P] cannot account for the observed increases. Further, calculations of the splitting of the triply degenerate mode due P_{As} - P_{As} second neighbors indicated frequency shifts an order of magnitude larger than the observed line

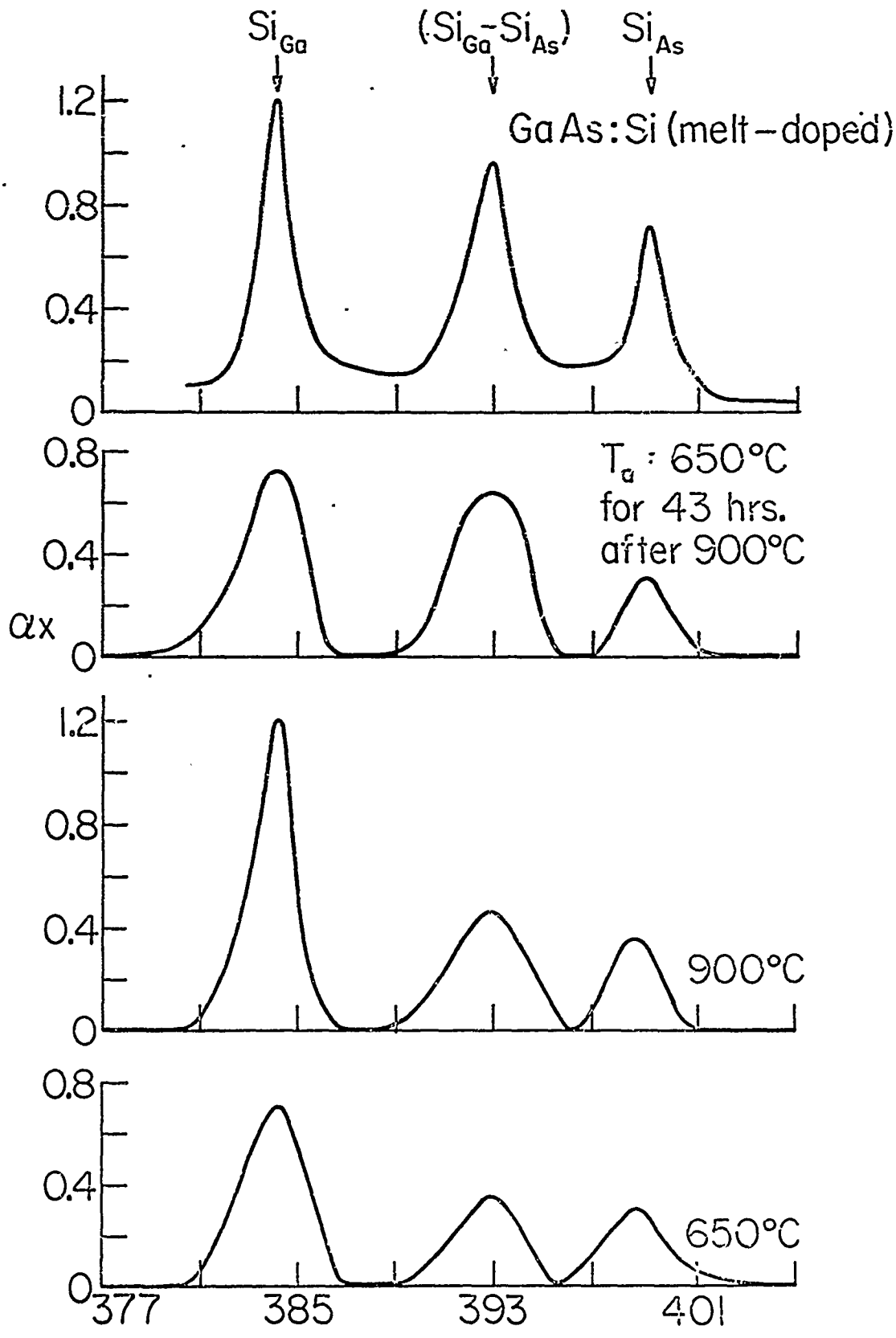

Figure 3: Cyclical annealing experiment for the Si implanted GaAs sample whose spectra are shown in Figure 1. The spectrum of a melt doped, Cu compensated sample where $[Si]\sim10^{20}cm^{-3}$ (see fef. 6) is shown for comparison.

width increases (ref. 3). Similar conclusions are expected to apply to the Si implants. The most likely source for the increased line widths is therefore residual radiation damage in the vicinity of the implanted Si (e.g., vacancies or other defects) causing distortions in tetrahedral bonding symmetry. These defects can result in changes in effective first neighbor force constants of the Si thus producing changes in line width and shifts in the central local mode frequency (ref. 11).

Figure 3 also shows the data for the Si implant of Figs. 1 and 2 when reannealed at 650°C for 43 hours after the 1 hr. anneal at 900°C. The Si_{As} (399 cm^{-1}) band shows little measurable change. The large increase in strength of the (Si_{Ga} - Si_{As}) pair band indicates that we are probably far from equilibrium for pair formation even after the 1 hr. anneal at 900°C. Moreover, since the Si_{As} band shows only little change while the Si_{Ga} band increases after the 900°C anneal, it would appear that the [(Si_{Ga} - Si_{As}) pair] is increasing via a net change in Si species which is not yet identifiable as isolated Si_{Ga} or Si_{As}. The apparent reversibility of the line width of the 384 cm^{-1} band is also of interest as it indicates that the defects responsible for the increased line width of this band at 650°C may not have their origin in the damage from the implantation. This result along with the decrease in $\int(\alpha x)d\nu$ for this band between 500° and 650°C, and the annealing effects on n_e of the heavily Si-doped melt grown GaAs are suggestive of a pairing mechanism between Si_{Ga} and some thermally generated defects. These defects paired on 1st or possibly 2nd neighbor sets can introduce large frequency shifts in the Si_{Ga} LVM frequency and hence these paired species are lost from the 384 band. Point defects on more distant sites produce broadening effects. A similar vacancy pairing process has been offered to explain annealing effects in heavily Te-doped GaAs (ref. 12). Another possible explanation for the changes in $\int(\alpha x)d\nu$ and n_e is Si precipitation. This would require precipitation at ~500°C and would not afford any simple explanation of line width changes. However, some

Si mobility at temperatures as low as $T \sim 400^{\circ}C$ may be inferred from the formation and growth of the (Si_{Ga} - Si_{As}) pair band. Further experiments are needed before one can do more than speculate on these possible mechanisms.

From Fig. 2 the difference between the Si_{Ga} and Si_{As} area concentrations after the $500^{\circ}C$ anneal is $\sim 1.4 \times 10^{16} cm^{-2}$. If this density of excess donors is assumed to be distributed over the Si penetration depth of ~ 1 micron, then an $n_e \sim 10^{20} cm^{-3}$ would be expected. With this carrier concentration, the plasma frequency, ν_p, is $\sim 2000\ cm^{-1}$ (ref. 13) and the sample should be nearly totally reflecting in the region $\nu \sim 300\text{-}400\ cm^{-1}$ where the present optical measurements are made. However, it is observed that the carrier concentration is not given by $[Si_{Ga}] - [Si_{As}]$. In several cases sheet resistance was measured and carrier concentrations were obtained from Hall measurements (van der Pauw method). In the high energy, high fluence implant cases studied here the electrical properties do not show the same annealing behavior as those samples of ref. 8 mentioned previously. Indeed, although the $[Si_{Ga}]$ is always greater than $[Si_{As}]$ in the present work, (see Fig. 2) the layers frequently show p-type conductivity even after the high temperature annealing. Moreover, while the LVM bands do not show any measurable dependence upon whether or not the sample is encapsulated with SiO_2 during annealing, the electrical properties of samples with similar annealing histories often show considerable variation between the encapsulated and non-encapsulated cases. The electrical data and concentrations of different Si species have no apparent correlation. While difficulties such as poor electrical isolation of the substrate, substrate annealing effects, and the variation in [Si] with depth make electrical data quantitatively uncertain, it appears likely that the conductivity is controlled by residual damage in the layer rather than the implanted species themselves.

It is known that the damage caused by implanting GaAs with

a dose of ions large enough to create an amorphous layer does not completely anneal out at 900°C, (ref. 14) although this residual damage has not been observed to strongly affect the electrical characteristics of the implanted layer. Thermally induced damage, produced by annealing GaAs in vacuum at 600°C without a protective SiO_2 coating, has been observed to result in conversion of conductivity type from n to p (ref. 15).

Although much of the quantitative results presented here should be regarded as tentative, this study provides additional evidence of the importance of the localized vibrational mode technique for investigating some implanted ions in semiconductors.

References

1. H. J. Stein and W. Beezhold, Appl. Phys. Letters 17, 442 (1970).

2. J. A. Borders, S. T. Picrau, and W. Beezhold, Appl. Phys. Letters 18, 509 (1971).

3. L. H. Skolnik, W. G. Spitzer, A. Kahan, and R. G. Hunsperger, J. Appl. Phys., to be published.

4. O. G. Lorimor and W. G. Spitzer, J. Appl. Phys. 37, 3687 (1966).

5. W. G. Spitzer and W. Allred, Appl. Phys. Letters 12, 5 (1968).

6. W. G. Spitzer and W. Allred, J. Appl. Phys. 39, 4999 (1968).

7. C. Kolm, S. A. Kulin and B. L. Averbach, Phys. Rev. 108, 965 (1957).

8. J. Sansbury and J. F. Gibbons, Appl. Phys. Letters 14, 311 (1969); J. Sansbury and J. F. Gibbons, International Conference on Ion Implantation in Semiconductors, Thousand Oaks, California, May, 1970, published in Radiation Effects 6, (1970).

9. J. R. Ligenza and W. G. Spitzer, Phys. and Chem. Solids 14, 131 (1960).

10. See J. W. Mayer, L. Eriksson, and J. A. Davies, Ion Implantation in Semiconductors (Academic Press, New York, 1970), Chapter 2.

11. R. C. Newman, Advances in Physics 18, 545 (1969).

12. C. Fuller, K. Wolfstirn, and H. Allison, J. Appl. Phys. 38, 4339 (1967).

13. An extrapolation of the data of Fig. 2 of K. Okada and T. Oku, Japan J. Appl. Phys. 6, 276 (1967).

14. R. G. Hunsperger and E. D. Wolf, J. Electrochemical Soc., to be published.

15. J. S. Harris, Y. Nannichi, and G. L. Pearson, J. Appl. Phys., 40, 4575 (1969).

1.1.2 Materials Preparation

DAHC 15-71-G6, Advanced Research Projects Agency

GK 17042, National Science Foundation

PRF 4528-AC6, American Chemical Society

F44620-71-C-0067, Joint Services Electronics Program

Research Corporation, New York City, New York

W. R. Wilcox, W. Allred, P. J. Shlichta, N. Brovko,

C. Chang, K. Chen, A. Khalaf, V. Kuo, M. Lin,

W. L. Paterson, L. Skolnik, and V. Yip

Introduction

Solids and single crystals play an important role in many aspects of modern technology. For example, modern electronics would be impossible without single crystal semiconductors. Crystallization is involved in the human body, both in bone and teeth formation and in conditions such as gouty arthritis and urinary stones. Much is unknown about crystallization and about the relation of properties to crystallization conditions.

The objectives of the materials preparation program are:

(1) To investigate crystal growth phenomena; (2) To develop new crystal growth techniques; (3) To relate properties of solids to preparative conditions; and (4) To study dissolution of solids.

Present Status of Research

1.1.2.1 Crystal Growth of Semiconductors

W. Allred, L. Skolnik, V. Yip, C. Chang and W. R. Wilcox

All operational problems with our new Czochralski technique for growth of bulk GaAs crystals have been solved. Single crystals of low dislocation density are now grown routinely. We are having purity problems with the crystals, but attribute these to the impure boron oxide employed and to the crucible. High purity boron oxide and different crucibles will be tried.

The apparatus for liquid encapsulation floating zone melting has been constructed. The technique has been tried on GaAs, and looks promising.

An improved drying technique has been developed for the boron oxide to be used for the above growth methods. The boron oxide is slowly heated in a vacuum oven and then melted in a dry nitrogen atmosphere. Nitrogen gas is bubbled through the melt from about 800°C to 1300°C. The rate of removal of moisture from the melt was found to decrease exponentially, as expected.[1] At room temperature the rate of pickup of moisture from the air at first decreased with the square root of time and then became constant. This corresponds to formation and then breakup of a surface film, as observed under the microscope. The film is boric acid. This surface moisture is removed in a vacuum at room temperature with two rate constants, one rapid and one slow.

The travelling heater method of growing bulk crystals from solution is under investigation. Gallium arsenide crystals are being

grown under a variety of conditions. An organic analog is also being studied because of the lower temperature of operation and its transparency. We have found that the solution zone is displaced upward from the heater because of free convection effects. Because of this the upper interface tends to be concave while the lower interface tends to be flat, which is probably the desirable growth condition.

1.1.2.2 Silicon Nitride

W. L. Paterson

Silicon nitride films have been deposited by chemical vapor deposition onto silicon substrates. Apparatus has been constructed for measuring the electrical properties of these films. Transients in leakage current are being studied as a function of stored charge, film thickness, and temperature in an attempt to elucidate the charge storage and conduction mechanisms in silicon nitride and to relate these to applications as computer memories. The theories of conduction and of thermally-stimulated currents (glow curves) are being studied to enable interpretation of experimental data. A computer program is being written to permit transformation of glow curves to information on charge traps.

1.1.2.3 Crystallization of Sodium Urate

A. Khalaf, M. Lin and W. R. Wilcox

Sodium urate crystallization is necessary for development of gouty arthritis. Previously proposed mechanisms for a severe gout attack have invoked the concept that the solubility of sodium urate decreases as pH falls.[2] We have shown theoretically, however, that the solubility of sodium urate actually increases as the pH falls.[3] This has been confirmed experimentally in all details by workers at the UCLA Medical School. In Reference 3 all prior data for equilibria involving uric acid and sodium urate has been rationalized, including activity

coefficient corrections.

As mentioned in the previous progress report, nucleation of sodium urate is being studied with a programming microscope hot stage. The supersaturation ratio necessary for nucleation at 37°C was unaffected by additions of synovial fluids from a gout patient, but was greatly increased by synovial fluid from a rheumatoid patient. This indicates the presence of a nucleation inhibitor in the rheumatoid patient, which corresponds with the clinic observation that patients with rheumatoid arthritis rarely if ever develop gout even when excess sodium urate is present in their bodies. Alcohol slightly increased the supersaturation ratio required for nucleation.

X-ray powder patterns of sodium urate have been taken as a function of crystallization rate. The size of the peaks diminished as the crystallization rate increased, with a rapidly crystallized powder showing no peaks. This confirms previous observations of "amorphous" sodium urate. We are attempting to discern the true nature of amorphous sodium urate, which has been found to rarely cause inflammation when injected into points and tissues, unlike crystalline sodium urate. We are also attempting to grow mm size crystals of sodium urate to permit determination of its crystal structure in cooperation with Dr. Bau of the chemistry department.

1.1.2.4 Pushing of Foreign Particles by a Solidifying Interface

V. Kuo and W. R. Wilcox

The goal of this project is to develop methods for removing particles from materials and for separating particle mixtures.

The presence of bubbles was found to greatly increase trapping of particles by freezing organics. This could be avoided by a vacuum treatment before solidification. Convex interfaces led to enhancement of trapping between the interface and the container. Some

dependence of trapping on crystal orientation was observed. A mixture of two materials was successfully separated into bands by solidifying with an increasing rate while the particles rested on the horizontal interface. Stirring has been found to enhance particle pushing. The influence of stirring conditions is being studied in detail. The dependence of interfacial temperature gradient on crystal dimensions has been determined theoretically.[4]

1.1.2.5 Movement of Solvent Inclusions in a Temperature Gradient

K. Chen and W. R. Wilcox

Thermal gradient induced movement of inclusions of water and of water-alcohol mixtures in alkali halides was studied above 100°C. Under some conditions boiling occurred on the hot side of the inclusion with condensation on the cool side, generally resulting in movement away from the heat source. Movement rates and directions are being studied as a function of inclusion, crystal, and temperature level.

1.1.2.6 The Influence of Ozone on Corrosion

N. Brovko and W. R. Wilcox

Ozone arises from photochemical processes in polluted air. In order to determine its influence on metallic corrosion, stainless steel, aluminum and copper were exposed to sea water and to 2% H_2SO_4 both in the absence and in the presence of ozonated air. The most dramatic effect was obtained with aluminum in 2% H_2SO_4. Deep pits were formed with ozone while no pits were formed without ozone. The weight loss was over 300% larger with ozone. The corrosion rate in other cases was only slightly higher in the presence of ozone.

1.1.2.7 Theory of Crystal Growth

W. R. Wilcox

If one regards the crystal surface as stationary, then crystal growth generates a flow through the crystal-fluid interface. The flow velocity in the crystal is the growth rate. The corresponding velocity in the fluid at the interface we call the crystallization flow, which is not equal to the crystal growth rate.[5] The exact relationship between growth rate and crystallization flow depends on whether the diffusion flux is referred to the mass average velocity, the mole average velocity, or the volume average velocity. These results have been applied to calculation of growth rate, segregation and constitutional supercooling in solution and vapor growth as well as in high purity melt growth.

1.1.2.8 General Structure Theory

P. J. Shlichta

As reported previously, Hadamard matrices (orthogonal matrices having only +1 and -1 elements) have been generalized to three and four dimensions[6]. Thus the m x m x m matrix $|P|$ is Hadamardian if $\sum_{i=1}^{m}\sum_{j=1}^{m} P_{ija} P_{ijb} = m^2 \delta_{ab}$ where i and j are any two coordinate axes of the matrix. It can be shown that any m^3 matrix is Hadamardian if either (a) all m^2 layers in one direction are Hadamardian and mutually orthogonal, (b) all m^2 layers in two directions are Hadamardian, or (c) the matrix is a tensor product of two smaller Hadamard matrices. Since all row-permutations of a Hadamard matrix are mutually orthogonal, it follows from (a) that every m^2 Hadamard matrix generates at least one m^3 Hadamard matrix. Similar rules obtain for the generation of four-dimensional Hadamard matrices. It, therefore, seems reasonable to assume that the number of Hadamard matrices increases with dimensionality.

Hadamard matrices bear an intersting relation to random binary matrices in that the only definable property of the former is that the correlation between any two rows or columns of the former (i.e., zero) is equal to the mean expectation value of the correlation between any two rows or columns of the latter. Thus a Hadamard matrix is a paradigm of a random binary matrix. Therefore, it should be possible to develop an iterative search program for refining any random binary matrix into a Hadamard matrix.

At present, an investigation is being initiated into the application of higher-dimensional Hadamard matrices to error-correcting data transmission, secure coding, and error-free matrix switches.

1.1.2.9 Control Growth in Centrifugal and Graviational Fields

It has been shown that, when a saturated solution of relatively dense ions is spun in an ultracentrifuge, the resultant concentration gradient is sufficient to cause crystal growth or even spontaneous nucleation[7]. A program has been initiated to apply this technique to the measurement of the critical supersaturation for homogeneous nucleation. A nuclei-free solution is spun in an analytical ultracentrifuge and its schlieren pattern is observed up to the onset of nucleation. Similar observations are made on a seeded solution so as to determine the equilibrium saturation as a function of centrifugation-induced hydrostatic pressure. Preliminary results, using average values for the hydrostatic component of index-of-refraction gradient, indicate that a KBr solution can sustain long-term supersaturations of over 6%. Present efforts are being directed to refining the data analysis.

During this investigation it was noted that tetramethylammonium chloride solutions showed virtually no equilibrium concentration gradient

in a centrifugal field. Since such a system should be immune to concentration-difference convection currents, it should be virtually unaffected by gravity and might be regarded as a simulation of crystal growth under zero-gravity conditions. Preliminary experiments on the growth of tetramethylammonium chloride crystals, by solvent evaporation or by slow cooling of saturated solutions, do indeed exhibit many of the phenomena predicted for zero-gravity conditions.

References

1. C. Chang and W. R. Wilcox, Mat. Res. Bull. (in press).
2. J. E. Seegmiller, Hospital Practice 1 (Dec., 1966).
3. W. R. Wilcox and A. Khalaf (in preparation).
4. V. Kuo and W. R. Wilcox, J. Crystal Growth (in press).
5. W. R. Wilcox, J. Crystal Growth (in press).
6. P. J. Shlichta, Bull. Am. Phys. Soc. 16, 825 (1971).
7. P. J. Shlichta and R. E. Knox, J. Crystal Growth 3-4, 808 (1968).

Recent Publications

1. R. J. Baughman, R. A. Lefever and W. R. Wilcox, J. Crystal Growth 8, 317 (1971).
2. W. R. Wilcox and P. J. Shlichta, J. Appl. Phys. 42, 1823 (1971).

1.1.3 Experimental Analysis of Impurity Energy Levels in Semiconductors

DA-ARO-D-31-124-71-634, U.S. Army Research Office - Durham

C. R. Crowell, C. L. Anderson, M. Beguwala, and K. Nakano

We are attempting to demonstrate the extent to which capacitance-voltage studies of Schottky diodes can be used to show the presence of deep-lying impurities and to measure the properties which are important in characterizing semiconductor materials and devices (namely the energy levels, capture cross-sections and concentrations of each species of impurity or defect). One of the great advantages of the Schottky barrier approach is that the level characterization should be virtually independent of bulk doping.

The theoretical work of Crowell and Nakano has been completed and accepted for publication. This work provides a simple model which outlines how the capacitance makes the transition between the low and high frequency asymptotes and shows the depth of information which is present in the capacitance-frequency relationship at a single temperature. At the same time, however, the model stylizes behavior in the low frequency region and is unable to treat the case of extremely high frequencies when the deep level and free electron responses are comparable. These limitations arose primarily because we attempted to orthogonalize capacitive and conductive effects. Beguwala and Crowell are developing an improved theory which overcomes all the above limitations and provides added insight. In this approach the contributions of all impurities to the complex impedance of a Schottky barrier can be expressed in a simple differential equation in which it is shown that the effects (both capacitive and conductive) of the deepest

levels are determined in part by all the shallower levels. At appreciable reverse bias a single deep level plus shallow ionized levels can best be characterized by a bias dependent and frequency independent capacitance in series with a parallel R-C combination which is bias independent and only slightly frequency dependent. This result shows great promise of providing an excellent correlation with experimental results which have never successfully been interpreted in terms of a two element model which is applicable to both the high and low frequency asymptote.

The capacitance measuring system being developed by Anderson and Crowell is nearing completion. The C-V relationship can now be scanned automatically for either capacitance or conductance or impurity profile and point-by-point C-ω measurements have been done. The Princeton Applied Research Model 124 phase-sensitive detector was found to need factory adjustment and selection of components (now completed) before being able to be swept in frequency without appreciable phase error. Frequency scanning, a remote access probe and improved data presentation are planned for the future.

Sample surface preparation facilities have been improved and In doped Si acquired from two sources. We plan to use Pt-n-type Si barriers for the In study. In addition, we plan to verify the work of Saxena (who found $\approx .90$ eV hole barriers for the Hf-p type Si) so that the parameters of hole traps in Si may be determined.

During the reporting period two manuscripts (see references) were prepared for journal publication.

References

1. C. R. Crowell and K. Nakano, "Deep Level Impurity Effects on the Frequency Dependence of Schottky Barrier Capacitance", (currently undergoing minor revision, but accepted for publication in Solid State Electronics).

2. G. I. Roberts and C. R. Crowell, "Capacitive Effects of Au and Cu Impurity Levels in Pt-n Type Si Schottky Barriers", (to be submitted to Solid State Electronics).

1.1.4 Avalanche Multiplication in Semiconductors

AF-AFOSR 69-1622, Joint Services Electronics Program

C. R. Crowell, C. L. Anderson and Y. Okato

Carrier multiplication through impact ionization of electron-hole pairs is an essential mechanism in the operation of many semiconductor devices. The widespread use of avalanche multiplication as an amplification process in the rapidly expanding solid state microwave amplifier field makes a thorough understanding of this process essential.

Our theoretical work has suggested that much of the existing published data are in error by an order of magnitude at high electric fields. This is the range in which IMPATT diodes must operate for higher frequency operation. If correct, the theoretical estimates suggest that avalanche multiplication in this field range is a sufficiently slowly varying function of field that the turn-on feature in the IMPATT diode will be progressively less efficient as the frequency increases. At the same time the increasing stability in multiplication rates should make high-gain stable multiplication possible. This research is intended to provided direct guidelines for device applications of multiplication at high fields. The use of Schottky barrier structures in this work will also provide a unique separation of the effects of electron and hole multiplication rates.

Anderson and Crowell[1,2] have determined the threshold energy for impact ionization which is applicable to any semiconductor for which impact ionization which is applicable to any semiconductor for which energy band data are available. Previous estimates of threshold energies, based on free electron model, were simply three-halves the band gap. In most instances the true minimum threshold is much closer to the bandgap energy. A manuscript on this work has been written and revised during the past six months and will be published shortly.

Okuto and Crowell[3] have investigated the widely used Baraff theoretical calculations of ionization coefficient and have shown that these curves exhibit an anomalous non-monotonicity of energy utilization in the high field regime. They have also examined the available experimental data for silicon, germanium, gallium arsenide, and gallium phosphide in a format which allows comparison of the experimental data with theoretical curves which exhibit asymptotically correct energy utilization in the high and low field ranges. For gallium phosphide a re-examination of (4) shows good agreement between them, and experiment (cf. Fig. 1 and Fig. 1, p. 42 of previous report). In the case of silicon in the high field asymptote existing experimental data are clearly in error since it appears that about 90% of the energy gained from the field is unaccounted for in the experimental results.

Experimental facilities for the investigation of avalanche multiplication in silicon are nearly complete. In recent months Anderson has developed nearly complete facilities for the preparation of silicon samples for avalanche multiplication studies. These facilities include a sample polishing and grinding apparatus and an oxide furnace for wet or dry oxidation of silicon slices for surface passivation techniques. In addition, Anderson and Crowell have designed and have partially completed a variable frequency capacitance-voltage assembly which will allow direct plotting of impurity densities within the silicon substrates. This will provide the accurate knowledge of impurity profiles necessary for determination of the electric field distributions in the devices. The construction of a vacuum insulated high voltage optical dewar has been completed. It will be used with the existing Spex spectrometer for selective photo-excitation of electrons or holes in avalanche Schottky barrier structures at temperatures from 77°K to 300°K.

We are undertaking to investigate avalanche multiplication in high resistivity n and p layers in a punched-through (essentially depleted of free charge carriers) Schottky barrier configuration. These devices

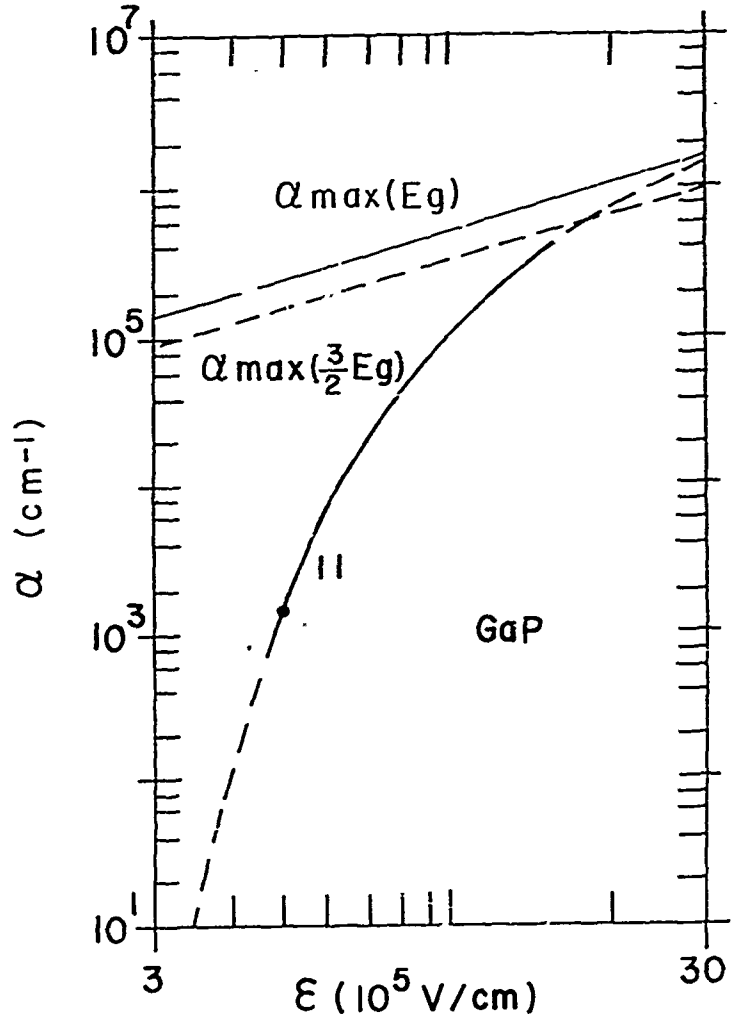

Figure 1:

Ionization rate, α, as a function of the electric field, ε, for electrons (e) and holes (h) in selected semiconductors at 300°K.

Legend: ——— experimental --------- theoretical fit.

• point used to determine mean free path fitting parameter

α_{max}(Eg) - theoretical maximum

α imposed by energy conservation

$\alpha_{max}(\frac{3}{2}$ Eg)

-------- theoretical maximum α for threshold ionization energy of $\frac{3}{2}$ Eg .

should provide a much more accurately defined electric field configuration than p-n junction structures. The analysis photoinjection of carriers into the Schottky structures is presently under investigation. Crowell and Sze[5] have analyzed the problem of quantum mechanical reflection at the Schottky barrier including the effects of image force in the semiconductor and dielectric shielding in the metal. Crowell and Anderson are extending this analysis to include the effect of transverse momentum conservation at the metal-semiconductor interface. Computation of the theoretical results is presently in progress and experimental verification of this analysis will be undertake by Anderson.

References

1. C. L. Anderson and C. R. Crowell, Bull. APS II, 15, 1615 (1970). (Abstract only).
2. C. L. Anderson and C. R. Crowell, to be published in Phys. Rev.
3. Y. Okuto and C. R. Crowell, Bull. APS II, 15, 1615 (1970). (Abstract only). Also submitted to Phys. Rev.
4. R. A. Logan and H. G. White, J.A.P. 36, 3945 (1965).
5. C. R. Crowell and S. M. Sze, J.A.P. 37, 2683 (1966).

1.1.5 Radiative Recombination in Semiconductors

F44620-71-C-0067, Joint Services Electronics Program

DA-ARO-D-31-124-70-G 15, U.S. Army Research Office - Durham

GK 12796, National Science Foundation

M. Gershenzon, W. Hawk, E. S. Johnson, K. Kosai, J. Liu, F. Selim, G. Turner, and H. Wang

Introduction

It is desirable to obtain efficient luminescence covering a

wide spectral range from semiconductor host materials in order to develop LED devices and semiconductor lasers with improved figures of merit, particularly in the visible spectrum. Therefore, we are examining light emission from relatively new semiconductors (GaN, AlN, AlP), as well as optimizing radiative recombination in some well-established semiconductors (CdS, Si) and semiconductor alloys ($In_xGa_{1-x}P$, $Al_xGa_{1-x}P$).

Present Status of Work

1.1.5.1 GaN, AlN

M. Gershenzon, E. S. Johnson, F. Selim

Gallium nitride is a very wide gap (3.4 eV) semiconductor, which has shown efficient photoluminescence in both the ultra-violet and visible ranges. Because of the extremely high N_2 pressures required for direct growth from the elements, it has been grown by a quasi-equilibrium vapor method, reacting GaCl at $\sim 1000^{\circ}C$ with NH_3. The single crystal films grown on sapphire substrates are extremely heavily doped (10^{18} - 10^{20} cm^{-3}) with native donors. Attempts to produce p-type conductivity have not been successful. There is evidence that the incorporation of the native donors is associated with lattice strain due to the use of the sapphire substrate. Therefore, we are trying to grow GaN on other substrates. AlN, in particular, is isostructural with GaN, has almost the same lattice constant as GaN and is more stable than GaN.

AlN single crystal films, $\sim 2\mu$ thick, were grown epitaxially on sapphire substrates by the pyrollysis of $Ga(CH_3)_3$ in the presence of NH_3. GaN was then grown on this film by our standard halide vapor phase technique. However, the resulting crystals have not yet shown any improvement in resistivity over those grown directly on sapphire.

In addition, we have tried to grow mixed $Al_xGa_{1-x}N$ on

sapphire by the same vapor technique. To date the crystals have shown no evidence that any Al was being incorporated both through resistivity and absorption edge measurements.

1.1.5.2 AlP

M. Gershenzon, J K. Liu, H. L. Wang

Aluminum phosphide, a wide-gap III-V semiconductor, has a bandgap of ~ 2.5 eV and is therefore capable of emitting visible light including blue. Solution growth of AlP is possible but only produces small crystals.[1] The vapor growth technique which is simpler and more versatile has been chosen as our approach.[2]

Construction and calibration of a system for the growth of AlP by halide vapor phase transport has been completed. The system consists of a 3-zone independently controlled furnace and an all-alumina reaction tube and associated gas pressure, flow and mixing controls. So far we have been able to grow whiskers, platelets and small crystals nucleated on silicon or sapphire substrates. X-ray measurements showed that the lattice constant of the whiskers was about 5.46 $\mathring{A}$. However, the crystals were too small to allow well-defined electrical and optical measurements. We will try to produce better single crystal AlP epi-layers of reasonable thickness, so that these various electrical and optical measurements can be made. Next, we will try to dope the AlP to produce both n and P type material, as well as P-N junctions.

References

1. S. Z. Beer, Trans. Met. Soc. AIME, 242, 424, 428 (1968).

2. D. Richman, J. Electrochem. Soc. 115, 945 (1968).

1.1.5.3 Luminescence Associated with Native Defects in CdS

M. Gershenzon and G. Turner

Cadmium sulfide is potentially a very useful light emitter because it has a direct band gap in the visible energy region. When the purest material obtainable is photo-excited at low temperatures, many sharp luminescence lines occur, some of which are due to unintentional impurities. CdS also contains native defects, however, which should effect the luminescence. F. A. Kroger and co-workers have recently shown that sulfur vacancies predominate at high temperatures and high cadmium pressures and have given an equation for predicting their concentrations. Our research is aimed at making samples with controlled concentrations of this defect and relating the luminescence to the concentration.

A preliminary experiment has demonstrated the feasibility of the approach. A series of samples, cut from the same boule were annealed at high temperature and cadmium pressure, and rapidly quenched. Some of these were then re-annealed at lower temperature and pressure and one was annealed a third time at high temperature and pressure.

All samples were photoluminescent at low temperature and the luminescence changed greatly with preparation conditions. The last sample, after undergoing the complete cycle, was almost identical to the first, indicating a reproducible experiment. An angle-lapped sample showed that the quenching was rapid enough.

1.1.5.4 Novel Radiative Recombination Centers in Si

M. Gershenzon, K. Kosai and E. S. Johnson

Silicon as the most technologically useful semiconductor has been extensively studied and is well understood. Radiative recombination processes, however, have received little attention, mainly because the

radiation is in the infrared and often inefficient. We are investigating the possible existence of radiative processes in silicon similar to those mechanisms which are known to be responsible for efficient emission in GaP, a compound very similar to Si in band structure. Two impurity systems, the Li-In and Li-Au nearest neighbor pairs, are being studied currently as possible isoelectronic traps, in analogy to the efficient Zn-O complex in GaP. [1]

Li-In Pairs. A crystal of float-zone Si has been grown with In concentrations from 8×10^{14} to 2×10^{16} In/cm^3. Absorption measurements give an oscillator strength for the exciton bound to neutral In in good agreement with that previously reported. [2] Photoluminescence due to excitons bound to neutral In [3] has been observed in these samples near liquid helium temperature. Before lithium diffusing the In-doped samples, we are studying the photoluminescence due to Li which has been diffused into 600 ohm-cm float-zone grown Si. Samples containing from 2×10^{14} to 4×10^{16} Li/cm^3 show two series of sharp lines beginning at 1.1327 eV and 1.0931 eV and decreasing in energy. We have tentatively identified these series as involving emisson of TA and TO momentum conserving phonons, respectively. The exact recombination mechanism remains to be established.

Li-Au Pairs. Au-doped samples in the concentration range 10^{14} to 10^{16} Au/cm^3 were prepared from 600 ohm-cm float zone silicon using high temperature diffusion techniques. The intrinsic silicon photoluminescence was quenched by the presence of gold and no new luminescence was introduced. A sample with a Au concentration of 3×10^{16}/cm^3 was diffused with Li to a concentration of 4×10^{17}/cm^3. Photoluminescence measurements taken near liquid helium temperature reveal a new radiative center dependent on the presence of both Li and Au. Emission from this new center consists of sharp bands occuring at 0.7653 and 0.7580 eV accompanied by considerable phonon replication at lower energies. The general form of the new spectrum resembles

both that of the Bi isoelectronic trap in GaP[5] and that of the strong radiative centers introduced into silicon by high-energy particle bombardment.[6]

References

1. T. N. Morgan, B. Welber, and R. N. Bhargava, Phys. Rev. 166, 751 (1968); C. H. Henry, P. J. Dean, and J. D. Cuthbert, Phys. Rev. 166, 754 (1968).

2. P. J. Dean, W. F. Flood, and G. Kaminsky, Phys. Rev. 163, 721 (1967).

3. P. J. Dean, J. R. Haynes, and W. F. Flood, Phys. Rev. 161, 711 (1967).

4. G. J. Sprokel and J. M. Fairfield, Jour. Electrochem. Soc. 112, 200 (1965).

5. F. A. Trumbore, M. Gershenzon, and D. G. Thomas, Appl. Phys. Letters 9, 4 (1966).

6. R. J. Spry and W. D. Compton, Phys. Rev. 175, 1010 (1968); M. V. Bortnik, V. D. Tkachev, and A. V. Yukhnevich, Soviet Physics - Semiconductors, 1, 290 (1967).

1.1.5.5 Radiative Recombination in $Ga_{(1-x)}In_xP$ and $Ga_{(1-x)}Al_x$ Alloys

M. Gershenzon and W. Hawk

The III-V alloy $Ga_{1-x}In_xP$ is being studied in this laboratory in order to better understand its luminescence properties and their variation with the parameter x. Previously we have grown alloys and measured the photoluminescence of samples for values of x between 0% and 3%. In this region, the well-known spectra of GaP shifted, broadened, and decreased in efficiency as x is increased.

Our present objective is to extend our present photoluminescence data to higher indium dopings where shifts from the GaP spectra should be

more easily measurable than they are in our present data.

Individual spectral lines in our samples can be followed in indium doping only out to 3% indium for edge emission lines and to 1% indium for the donor-acceptor pair spectra. A different growth technique and a different photoluminescence measurement method were tried in order to extend the data to larger x.

By growing $Ga_{1-x}In_xP$ epitaxially on GaP substrates, we have been able to observe donor-acceptor spectral lines in alloys greater than 1% indium. This improvement seems to be due to a decrease of strain in the crystal: epitaxial growth is done at a much slower growth rate than that for solution growth so that stresses due to non-equilibrium in the growth process are reduced, and, epitaxial growth results in smaller gradients in indium concentration in the alloy--thus reducing stresses due to a gradient in crystal lattice constant.

Another means of enhancing donor-acceptor pair spectra is to perform the photoluminescence at slightly higher temperatures. At 4.2°K the luminescence of our alloys is dominated by excitons bound to donor impurities. By increasing the temperature, the bound excitons should be ionized and therefore removed as luminescence centers, thus increasing the relative efficiency of the competing donor-acceptor pair lines.

Using a helium gas flow dewar to perform measurements in the region of 20°K, we have been able to observe donor-acceptor lines which were not observable at 4.2°K in our alloy samples. Using these methods, we now intend to carry our luminescence measurements out as far as possible in indium dopings.

In addition, we have now grown the alloy $Ga_{1-x}Al_xP$ and we hope to compare its luminescence with that for $Ga_{1-x}In_xP$.

1.1.6 Electron Microprobe Laboratory

D. B. Wittry, K. Y. Chiu, R. E. Gauldin, P. A. Sullivan, H. C. Marciniak, W. Lin, T. S. Rao-Sahib

1.1.6.1 Selected Area Electron Spectrometry

DAHC 15-71-G6, Advanced Research Projects Agency
F 44620-71-C-007, Joint Services Electronics Program

D. B. Wittry and R. E. Gauldin

In this work, an electron spectrometer is being used below the camera chamber of the transmission electron microscope to obtain information from selected areas of the electron microscope image. The electron spectrometer has been installed on the reconditioned Hitachi HU-10 electron microscope and preliminary tests indicate that the microscope and the spectrometer are operating satisfactorily.

With suitable modification of the high voltage power supply, it will be possible to perform the electron spectrometry experiments with the HU-10 instrument as well as with the HU-125. A system is being designed to modulate the accelerating voltage of the HU-10 in order to provide the energy sweep for the spectrometer. While the HU-10 does not employ a feedback regulated high voltage power supply it seems feasible to use a voltage programmable 2KV power supply in series with the high voltage supply. This auxilliary supply will be programmed by the analog output signal of the digital signal averager. Thus, the energy sweep will be proportional to the digital address of the signal averager. By using this auxilliary power supply it will also be possible to provide feedback controlled voltage regulation of the electron accelerating voltage over a limited dynamic range. The accelerating voltage as sensed by a voltage divider can be compared with a reference and the error signal can be applied at the input of the

operational amplifier of the auxilliary power supply. This additional voltage regulation should provide the required stability of the electron accelerating voltage.

It is planned to use this system to investigate concentration inhomogeneities in III-V semiconductors

1.1.6.2 Scanning Electron Mirror Microscopy

F 44620-71-C-0067, Joint Services Electronics Program

P. A. Sullivan and D. B. Wittry

As described in previous reports, an electron probe microanalyzer has been modified for use as a scanning electron mirror microscope. Axial alignment of the electron-optical column was retained by inserting a deflection bridge between the condenser and objective lenses to separate the incident and reflected electron beams. The reflected beam is accelerated toward a scintillation detector which provides a video signal as the beam is scanned over the sample surface.

The new deflection bridge, described in the last report, has been tested. A strong reflected electron signal was detected by the scintillation detector. However, there is still a problem in obtaining good resolution. Careful alignment of the bridge and the use of a stigmator may improve the resolution and work on these points is in progress.

A dual 10 amp constant current power supply was constructed for excitation of the coils in the deflection bridge but requires modification to prevent oscillation. An octapole stigmator was fabricated and an appropriate current supply was built. A new high voltage cable to the sample stage was installed and insulated sample holders were fabricated. An aperture assembly was constructed and installed below the condenser lens. It allows external selection of one of three apertures.

Future work will concentrate on obtaining a well-focused beam with proper alignment of the deflection bridge. When good scanning electron mirror pictures can be obtained then surface potentials of several II-VI compound semiconductors will be investigated.

1.1.6.3 The X-Ray Continuum from Thick Target

GK 3904, National Science Foundation (expired)

T S. Rao-Sahib and D. B. Wittry

In X-ray analysis with the electron probe microanalyzer, the X-ray continuum can contribute significantly to the total X-ray intensity. In addition, calculation of corrections due to excitation of characteristic X-ray lines by the continuum depend greatly upon a knowledge of the continuum intensity as a function of depth, atomic number, excitation potential and photon energy. The present work is concerned with theoretical and experimental determination of the intensity of the X-ray continuum as a function of atomic number.

The intensity of the X-ray continuum from thick targets has been generally believed to obey Kramers' equation[1]

$$I_\nu = 1.46 \times 10^{-32} Z(E_o - E_\nu) \text{ ergs/electron} \qquad (1)$$

where I_ν is the energy per unit frequency interval, Z is the atomic number of the target, E_o and E_ν are the incident electron and photon energies, respectively, in KeV. This equation was based on a classical calculation of the scattering cross-section, and the Thomson-Whiddington law for the retardation of the incident electrons in the target. It predicts that the X-ray continuum intensity should be proportional to the atomic number Z of the target. However, investigations in this laboratory have not confirmed this simple proportionality. In general, intensity was found

to vary as $I_\nu \propto Z^n(E_o - E_\nu)^{1.1}$, where n depends on Z, E_o, E_ν, and can range from 1.2 - 1.37.

A new calculation was made for the continuum intensity from thick targets using the quantum-mechanical Sommerfeld cross-section[2] and the Bethe retardation law, with the continuous slowing down approximation. The Sommerfeld cross-section was used in its equivalent empirical function form as given by Kirkpatrick and Wiedmann[3]. The empirical function was modified to provide a better fit to the values calculated from the full Sommerfeld equation. The continuum intensity calculated was found to describe experimental observations more accurately than Kramers equation. The results of this calculation and experimental confirmations are discussed in greater detail in ref. (4).

Our calculations have shown that the observed Z^n dependence of the intensity is primarily due to the influence of the mean ionization potential J. This fact suggests that careful measurement of the X-ray continuum would enable a choice to be made between the multitude of J values currently being used in the Bethe retardation law.

Nineteen elements, ranging in atomic number from 6 to 92, were examined. The continuum intensity was measured and corrections were applied for absorption and the atomic number effect as described in previous progress reports. Intensities were measured at 1.128 Å with beam voltages of 20 KV, 30 KV, and 50 KV and at 1.998 Å with beam voltages of 10 KV, 30 KV, and 50 KV. The corrected intensities were compared with theoretical intensities calculated using the Sommerfeld cross-section, Bethe retardation law and (1) Duncumb-da Casa J values; (2) Berger-Seltzer J values; (3) J = 11.5Z. In general, it was found that the use of Duncumb-da Casa J values gave intensities which are too large for Z > 40. The best overall fit was obtained by the Berger-Seltzer J values and by J = 11.5 Z, the latter formula proving somewhat superior in the range 12 < Z < 22. Our results for carbon (Z = 6) are inconclusive, and are subject to reinterpretation in the light of a possible density effect.[5]

The continuum at 1.128 Å and 1.998 Å was also measured as a function of $(E_o - E_\nu)$ for selected elements, and compared with the theoretical voltage dependence curves calculated using the various sets of J values. Agreement between theory and experiment was not as good as in the case of the Z-dependence of intensity, but the results support the previous conclusions regarding the J-values.

The generally good agreement between theory and experiment shows the validity of the absorption and atomic number corrections. At 1.998 Å and 50 KV, f(x) goes as low as 0.44 (for Sb, Z = 51) and 0.35 (for U, Z = 92). The good agreement obtained even in this case shows that the same absorption correction function applies quite well to both characteristic radiation and the continuum. Additional work which has been done on continuum intensities up to 9.671 Å also indicates that the spatial distribution of characteristic radiation and the continuum is nearly the same. The irregular behavior which was previously reported[6] in the range 4Å - 8 Å can be attributed to sources of additional intensity; e.g., radiation from the optical instrumentation caused by backscattered electrons, and fluorescence from the X-ray diffracting crystals.

As would be expected from the difference in cross-section, the atomic number correction for the continuum is different from that for characteristic radiation. The difference can amount to about 6% for $E_o/E_\nu = 2$ and high values of Z. Because of this factor and also absorption effects, it is important in X-ray analysis that the peak intensity and background be measured on the same specimen.

Since previous calculations of fluorescence excited by the continuum have been based on Kramers' equation it appears that these calculations will have to be modified. The efficiency of production of the continuum may be expected to depend on Z and E_o in a more complicated manner than the simple proportionality to the product $Z(E_o - E_\nu)$ as predicted by the Kramers theory.

References

1. H. A. Kramers, Phil. Mag. 46, 836 (1923).

2. A. Sommerfeld, Ann. d. Phys. 11, 257 (1931).

3. P. Kirkpatrick and L. Wiedmann, Phys. Rev. 67, 321 (1945).

4. T. S. Rao-Sahib and D. B. Wittry, Proc. 6th International Conf. on X-Ray Optics and Mic oanalysis, 1971, Osaka, Japan (to be published).

5. T. Ichinokawa, Proc. 4th National Conf. on Electron Microprobe Analysis, Pasadena, California (1969).

6. T. S. Rao-Sahib and D. B. Wittry, Proc. 5th National Conf. on Electron Probe Analysis, New York, 1970.

1.1.6.4 Cathodoluminescence of Semiconductors

DAHC 15-71-G6, Advanced Research Projects Agency

H. C. Marciniak and D. B. Wittry

This project has been concerned with the understanding of radiative recombination mechanisms in semiconductors by observing cathodoluminescence spectra at low temperatures and by studying the temperature dependence of various peaks in the spectrum.

The investigations are being made with the aid of a clean vacuum electron beam column.[1] After factory rework of the Joule Thompson refrigerator and by using a thermocouple soldered to the specimen holder, specimen temperatures of 27°K were recorded.

Some results obtained on GaP at 27°K with an accelerating voltage of 50 KV, a beam current of 5 nA and a spot size of 10 μM are shown in Fig. 1.

It was expected that donor-acceptor pair recombination as reported by Thomas, et al.,[2] at 1.6°K might be observed between

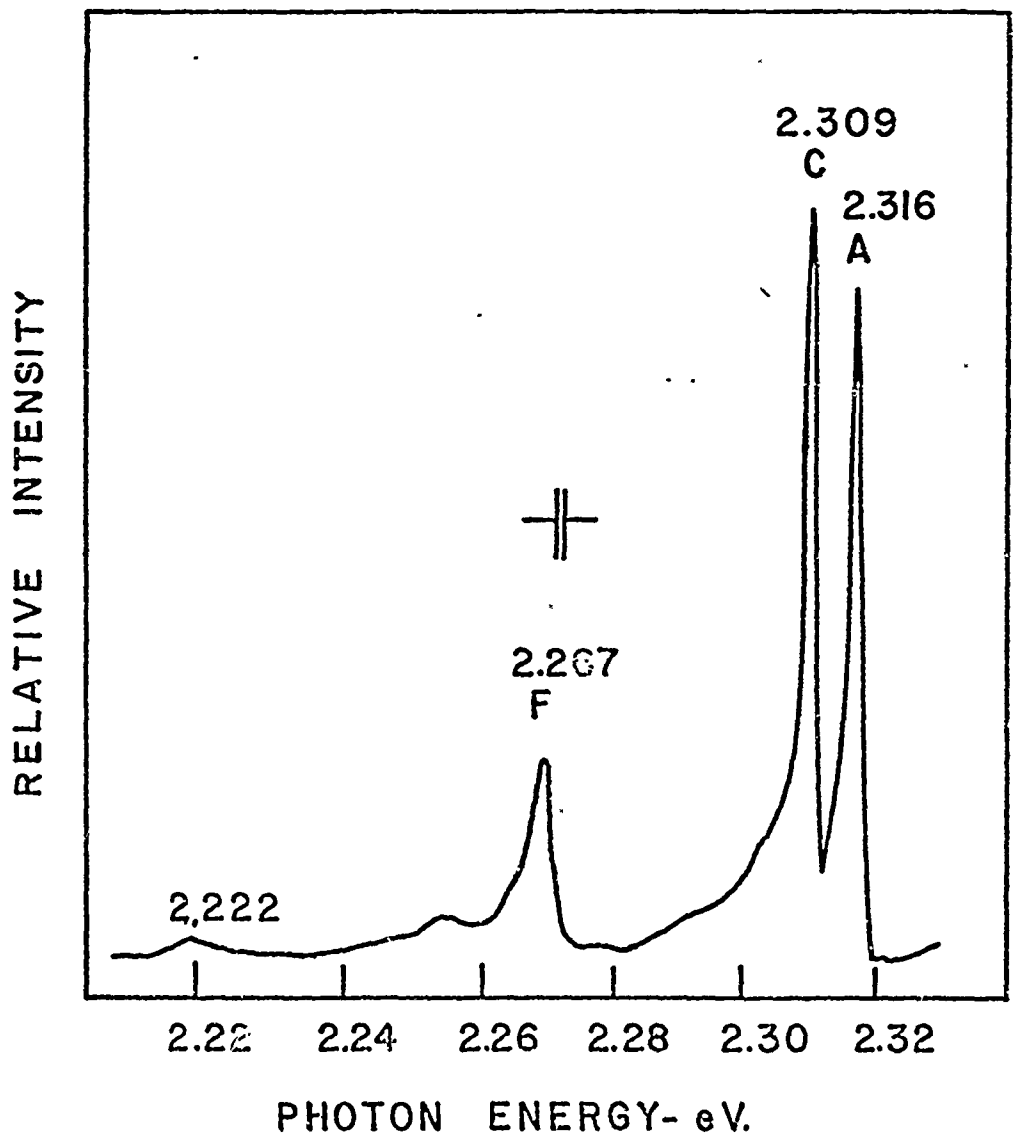

Figure 1. Cathodoluminescence Spectrum of GaP at 27°K

2.2 eV and 2.3 eV. However, donor-acceptor pair recombination showing spectra of resolved peaks in GaP has not yet been reported above 20°K. Shown in the figure is the 'A' line due to the nitrogen bound exciton and the C bound-exciton line due to neutral sulfur donors.[3] The F line is due to recombination at pairs of isoelectronic nitrogen traps.[3] The other peaks could be phonon-replicas of the A line as discussed by Dean and Thomas.[4]

We are now attempting to study recombination mechanisms in GaP_xAs_{1-x} alloys and are using the electron probe microanalyzer to determine the exact composition of these alloys.

References

1. H. C. Marciniak and D. B. Wittry, to be published in Rev. Sci. Instrum., Dec. 1971.

2. D. G. Thomas, J. J. Hopfield and K. Colbow, "Light from Distant Pairs," p. 67 in Radiative Recombination in Semiconductors (Paris, 1964).

3. M. Gershenzon, "Electroluminescence from p-n Junctions," p. 625-627, in Luminescence of Inorganic Solids (New York, 1966).

4. P. J. Dean and D. G. Thomas, Phys. Rev. 150, 690 (1966).

1.1.6.5 Stimulated Emission of Recombination Radiation with Electron Beam Excitation

DAHC-15-71-G6, Advanced Research Projects Agency

W. N. Lin and D. B. Wittry

In this work attempts are being made to observe stimulated emission by electron beam excitation without feedback from a resonant cavity structure.

New crystals of heavily doped n-type GaAs have been tried.

At room temperature the radiation observed (within a cone perpendicular to the surface) gave no indication of super-radiance similar to that reported by Casey and Kaiser[1]. We are now trying to determine whether the results of Casey and Kaiser[1] were influenced by the emergence angle of the photons by using tilted specimens having similar doping level as the specimens used by Casey and Kaiser.

The construction of a sample cooling system has been completed. With liquid nitrogen cooling, the lowest sample temperature obtained was about 93°K. Investigations of stimulated emission effects will be made at this temperature as well as at room temperature.

Reference

1. H. C. Casey, Jr., and R. H. Kaiser, Appl. Phys. Letters 8, 113 (1966).

1.1.6.6 Electron and Photon Interactions at Semiconductor Surfaces

F 44620-71-C-007, Joint Services Electronics Program

K. Y. Chiu and D. B. Wittry

In this work, an electron spectrometer is being used in the EMX for studying semiconductor surface photovoltaic effects. As indicated in last semiannual report, the construction of the electron spectrometer has now been completed. Preliminary experiments are being made on a special sample for calibration of the energy scale.

The collector-voltage characteristic is usually nonlinear and difficult to define since it depends to some extent on the potential distribution on the specimen as well as on the voltages. It is hard to deduce the voltage of the specimen from observation of collector output. An experimental technique[1] based on the use of a control loop will be

used to provide better linearity in the determination of surface voltages.

Reference

1. J. P. Flemming, J.Sci. Instrum, Ser. 2, 4, 1179-1182, 1968.

1.2 QUANTUM ELECTRONICS AND LASERS

1.2.1 Coherent Optical Devices

F 44620-71-C-006, Joint Services Electronics Program
NGL-05-018-044, National Aeronautics and Space Administration

W. H. Steier, C. T. Wittig, S. Nieh, D. Gonzales, R. Basu, and R. Joiner

Introduction

The purpose of this work is the development and study of devices for the control and modulation of visible and infrared coherent energy. The work currently in progress is outlined below.

$LiNbO_3$ Parametric Oscillator

A pulse pumped Nd-YAG laser is under construction for use as the pumping source for the parametric oscillator. The output power of the CW pumped laser was not sufficient to achieve threshold for the singly resonant oscillator. The CW pumped laser had only a few percent gain per pass and hence the insertion of the intracavity $LiIO_3$ doubler significantly reduced the output power. The severe thermal gradients in the laser rod during CW pumping also caused a distortion in the output beam so that a pure TEMoo mode could not be obtained. Both of the problems should be overcome by the use of pulse pumping.

The pulse pumped laser is shown in Figure 1. High pressure krypton lamps in a single ellipse cavity are used. These lamps efficiently match the absorption bands of Nd-YAG. Resonant charging techniques are used in the lamp circuits to reduce the DC voltage requirements on the power supply. The acousto-optic Q switch has a 35° cut $LiNbO_3$ transducer bonded to the quartz prism. The

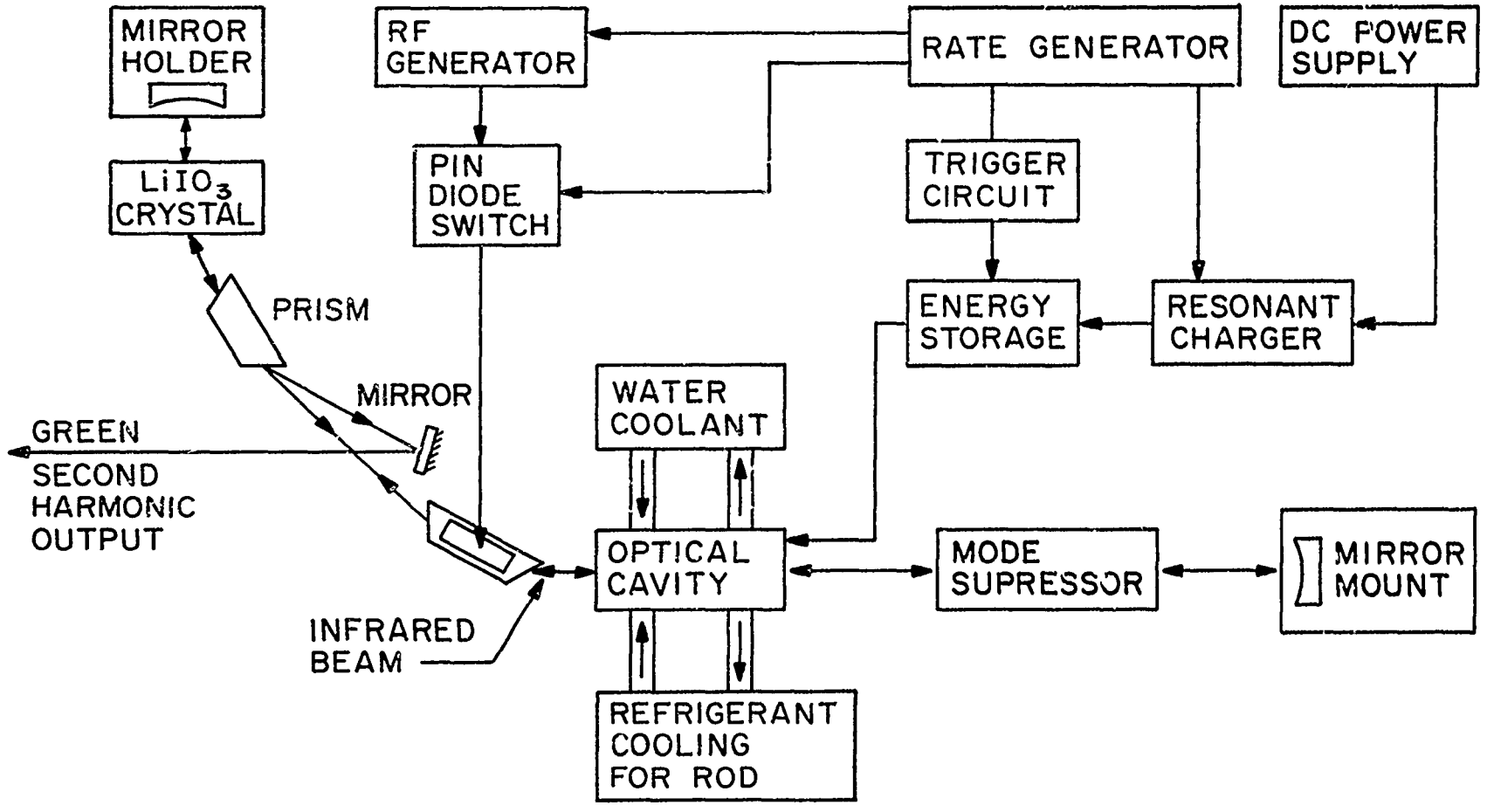

Fig. 1: Block diagram of laser

additional prism in the cavity allows for better line selection in the laser and is needed because of the high gain of the pulsed system. The prism is also used to conveniently couple the green power from the cavity by making use of the dispersion of quartz. The prisms also serve to linearly polarize the 1.06 energy.

The laser rod has a measured 3 db gain at 1.06μ with a 6 joule input to the lamp. The lamps can be pulsed at rates up to 100 Hz. The Q switch has a measured deflection efficiency of 90% at 6328 Å with an input of 10 watts at 28 MHz. This will correspond to 32% deflection efficiency at 1.06μ.

Theoretical Study of the Limits of Angle Tuning

We have extended our studies of the tuning band and the threshold increase of angle tuned parametric oscillators by taking into account double refraction in the near field limit. An expression for the threshold increase due to a non-colinear interaction is derived and this result is related to the bandwidth of angle tuning of a singly resonant parametric oscillator. We have considered angle tuning in two cases: i) at 90° to the optic axis where double refraction is negligible, and ii) at 43° to the optic axis where double refraction is important. Two methods of angle tuning have been considered for a singly resonant oscillator with $LiNbO_3$ as a nonlinear crystal. In a) the nonlinear crystal is rotated and the mirrors remain fixed and in b) the crystal and mirrors rotate as a unit.

Our calculation predicts the following: 1) angle tuning is not attractive for operation at 90° to the optic axis because of the limited band widths possible. The bandwidth is either limited by the threshold increase or the crystal aperture. Voltage tuning is more attractive in this case and a wideband fast tuning system might consist of a combination of step temperature tuning and voltage fine tuning between the steps.

2) Wideband angle tuning is possible around an axis which is not along one of the crystal axes. The preferred oscillator design would have one curved mirror and one flat mirror and tune by rotation of the crystal only. This oscillator design has a very small threshold increase and consequently the bandwidth is limited by either the crystal aperture or the bandwidth of the mirror reflectivity.

Pulsed Ion Lasers

The pulsed Xe ion laser was described in the previous report. By using an intra-cavity quartz prism several individual lines could be selected which spanned most of the visible spectrum. The power output in a single line ranged from a few hundred watts to 2 KW. The laser was found to have very high gain on most transistions and intra-cavity elements had a small effect on the power output.

Measurement of the angular divergence of the output beam showed a large number of transverse modes oscillating. An iris inside the cavity reduced the mode structure but greatly reduced the output power because of the inefficient use of the plasma volume. No significant improvement in the output beam could be achieved with different mirror combinations. This multi-transverse mode output beam makes the pulsed ion laser a poor source for pumping of parametric oscillators. Only the power in the lowest order mode is useful for pumping and this was found to be not sufficient to achieve threshold in the parametric oscillator. The pulse pumped Nd-YAG laser described above will be used as the pump.

A series of low signal gain measurements have been made in pulsed Xe and Ar. A separate plasma tube was used as a probe oscillator for measuring the gain in the larger bore amplifier tube. The gain was measured as a function of radial position, and time from the initiation of the discharge. Measurements were made on several transitions in both Ar and Xe.

1.2.2 Study of Laser-Irradiated Thin Films

F19628-71-C-0220, Air Force Cambridge Research Laboratories

L. G. DeShazer, E. A. Maunders, B. E. Newnam and H. R. Owen

During this report period we measured the damage thresholds of several "state-of-the-art" dielectric thin film coatings supplied by Spectra-Physics and Bausch & Lomb/Herron Optical, and the results are of great interest. The laser damage at 6943 Å to these high-quality coatings clearly showed that the damage was strongly dependent on the radial gradient of the power density in the laser beam and not on the peak power density. This conclusion was derived from measurements of the thresholds as the diameter of the laser beam was varied. Heretofore, experiments to determine this beam-size dependence have resisted analysis due to a large variety of difficulties at the high powers (above one gigawatt/cm^2) necessary for laser damage. Now we seemed to have overcome these difficulties by obtaining and thoroughly characterizing a 20 MW TEM_{00} ruby laser beam, and by acquiring the best coatings available.

Both reflecting and anti-reflecting coatings were tested. Spectra-Physics Corp. supplied two 99% reflecting (at 6943 Å) coatings on glass substrates and Herron Optical Co. supplied three anti-reflecting vee-coatings on glass substrates. The results of the tests are shown in Figure 1. The solid curve is drawn through the data for the best anti-reflection coating. The dashed curve follows the highest threshold 99% reflector. Both the enormous threshold values and the increase in threshold as the laser beam spot size was increased should be noted. Additionally, we found that a "baked" AR coating damaged at lower powers, by about 20%, at the same spot sizes (black square on figure).

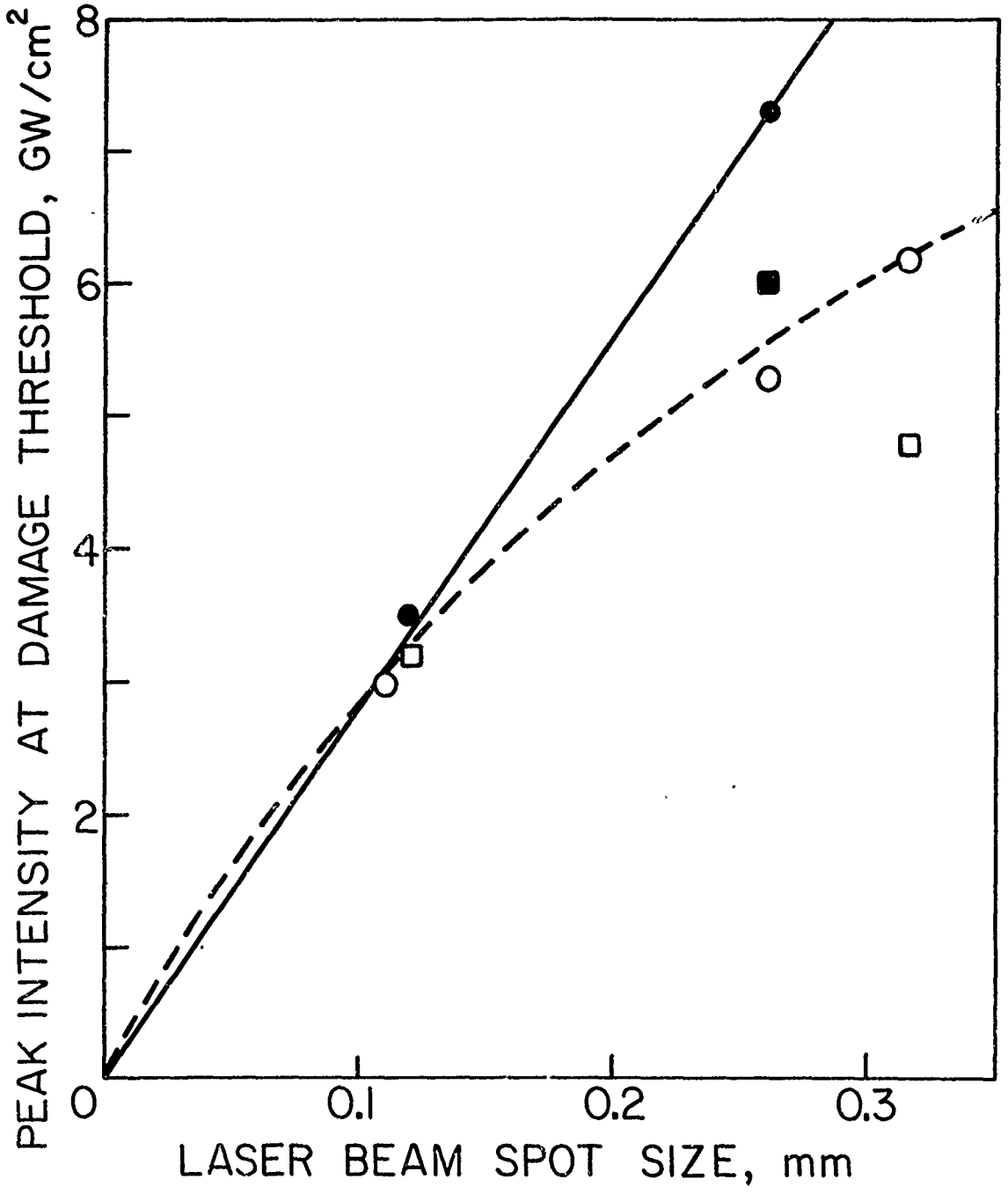

Figure 1. Peak Intensity Damage Thresholds Versus Laser Beam Spot Size for Dielectric Thin Film Coatings.

We are presently obtaining additional data points to more thoroughly determine the curves.

The data obtained to date does show that the damage was strongly dependent on the radial gradient of the laser power density and not on the peak power density. Two possible physical mechanisms which predict an intensity gradient stress in the coatings are electrostriction and thermostriction. Electrostrictive forces result from the gradient of the electric-field-squared (intensity), and thermostrictive forces from temperature gradients. Because our laser beam had a near Gaussian radial dependence, calculation of the relative magnitudes of electro- and thermo-strictive forces is possible. We are collecting the various physical constants of the coating materials with which to perform these calculations.

Our results indicate that caution must be exercised in quoting the breakdown limits of coatings in terms of peak intensity (GW/cm^2) or energy density ($joules/cm^2$) alone, because it is not the pertinent beam parameter to specify damage initiation. We believe that the intensity gradients in the laser beam will be that pertinent parameter; in the present tests, intensity gradients of the order of 250 GW/cm^3 caused damage.

It should be indicated that this is a new point-of-view towards thin film damage, and accounts for some past anomalies and confusions in laser work. Thus the present coatings can take enormous powers, exceeding 10 GW/cm^2, if the intensity gradients are kept to a low level. On the other hand, the analysis indicates that the same coatings will damage at low powers (100 MW/cm^2) if the gradients a·e large. Most users of lasers do not measure the intensity gradients in their laser beams so at present this measure of damage, even though proper, might be difficult to be related to a particular laser apparatus. For instance, multimode performance of a laser is known to give "hot spots" and hence large intensity gradients in the beam.

1.2.3 Transient Behavior of Transverse Modes in High-Power Pulsed Lasers

AFOSR-71-2066, Air Force Office of Scientific Research

L. G. DeShazer and B. E. Newnam

We are investigating theoretically and experimentally the transient behavior of transverse modes in high-power Q-switched laser oscillators. This research will cover an important deficiency in the present characterization of "single-mode" pulsed lasers emitting high powers, a characterization that is urgently needed in order to achieve the total capability of giant-pulse lasers in optical systems. During the tenure of this program, a computer analysis will derive for high-power Q-switched lasers the transverse patterns, which will be compared to experimental patterns of a giant-pulse ruby laser.

Initial experiments have been performed for cavity Fresnel numbers from 0.3 to 3.4. These experiments were conducted in order to develop the necessary diagnostic tools, and measured the oscillator output at specified distances in the near and far fields of diffraction. At each Fresnel number and distance, a pinhole aperture (0.09 mm diameter) was translated in the plane perpendicular to the incident laser beam to obtain a point-by-point mapping of the spatial distribution of intensity. The energy passing through the pinhole was detected by a very fast photodiode and displayed on a fast oscilloscope (Tektronix 519) as power versus time. A portion of the laser beam is deflected before reaching the pinhole and is displayed on the same oscillogram as the reference. Therefore, the relationship of a small spatial portion of the laser beam is compared to the total output.

From these experiments we have been able to suggest good criteria which will delineate the existence of the transient behavior of transverse modes in high power pulsed lasers. One such criterion

that had been proposed by us is that the transient behavior will be negligible when the product of initial gain and Fresnel number is less than a certain dimensionless number of the order of 20. This criterion has been difficult to assess since the initial gain of the high-power pulsed laser is difficult to accurately determine. Now, a better criterion has been demonstrated. It is that the transient behavior will be negligible when the product of the pulsewidth (FWHM) and the inverse of the Fresnel number is greater than 25 nanoseconds. This criterion is now being fully explored.

1.2.4 Advanced Nonlinear Absorption Devices for Laser Systems

NGL-05-018-044, National Aeronautics and Space Administration

L. G. DeShazer and J. W. Austin

Even though saturable absorbers have been used in laser systems as passive switches and modulators since 1964, the operation of these absorbers in conjunction with optical resonators has not been adequately described before. The features of this problem are succinctly contained in the problem of a Fabry-Perot resonator containing a saturable absorber. Such a device is called a saturable resonator. Previous treatments of saturable resonators have neglected the optical resonance effects and have used unsuitable models for the saturable absorbers. Now, a general steady-state solution to the performance of the saturable resonator has been obtained and applied to several experimental configurations. This solution was accomplished by first considering a Fabry-Perot interferometer containing an unsaturable absorber. The transmittance, reflectance and absorptance for this case were determined as a function of the phase difference

arising from round trip cavity transits. These quantities are parametrized by the mirror reflectivity and the transmittance of the absorber. Next, the absorber was considered to be saturable and was realistically characterized by the model of Huff and DeShazer[1] with some modifications. Most saturable absorbers exhibit a residual absorption and this residual absorption must be included in any model chosen for a saturable absorber. It was just this neglect of the residual absorption that made most previous treatments of the problem in error. The behavior of a saturable absorber was characterized by two parameters which are functions of the transition rates and absorption cross-sections. One of these parameters controls the residual absorptivity and shape of the saturation curve while the other determines the intensity range of saturation. Since the transmittance of the saturable absorber is a complicated transcendental function of the incident intensity, the solution must be done numerically with the aid of a computer. The results of these calculations show the existence of the bistable operation of a saturable resonator under certain conditions. The criteria for bistable operation were obtained and found to be dependent on mirror reflectivity, weak-signal absorber transmittance and the absorber parameter involved with the residual absorption. It was determined that this parameter had to be greater than 8.5 in order to get bistable operation.[2]

A single mode giant pulse ruby laser was used to determine the characteristics of several saturable resonators. A search was also conducted to find saturable absorbers which meet the criteria for bistable operation while at the same time obeying the steady-state assumption. The change of the transmission with incident intensity was measured for the organic dyes cryptocyanine and 1, 1'-Diethyl-2, 2'-Dicarbocyanine Iodide (DDI) dissolved in various organic solvents, as well as a Cd:Se:S glass. For the organic dye it was found that the parameters were highly dependent on the solvent. Those absorbers which met the bistable criteria were the semiconductor glass, and both DDI and cryptocyanine

dissolved in either acetone or acetonitrile. Experimental results follow the theory but on-resonance matching difficulties have hindered observation of bistable operation for those saturable absorbers which were found to meet the criteria, however, very noticeable pulse shaping was obtained in many cases. The saturable resonator was also tried as a laser cavity dumping device but here large residual absorption and resonance matching problems limited its usefulness.

References

1. L. Huff and L. G. DeShazer, "Saturation of Optical Transitions in Organic Compounds by Laser Flux," J. Opt. Soc. Am. 60, 157 (1970).

2. J. W. Austin, "Laser Saturable Resonators and Criteria for Their Bistable Operation," Ph.D. dissertation, Univ. So. Calif., 1971.

1.2.5 Laser and Spectral Properties of Rare Earth Crystals

AF-AFOSR-69-1622A, Joint Services Electronics Program

Union Carbide Corporation (Partial Support)

L. G. DeShazer, J. K. Guha, and L. M. Hobrock

Rare earth ions in crystalline or glass hosts are commonly used as a laser active media but only a few of these ions have an energy level structure that provides a natural population inversion in a four level system at room temperature. The significant characteristics of such a system are a predominantly radiative decay of the initial level and a rapid depletion of the final level by nonradiative processes. For such a system to be of use as a room temperature continuous laser it is further required that the final level be many kT above the ground state and thus have a negligible thermal population. The rare earth ion with a four level system most commonly used to obtain laser action is triply ionized neodymium (Nd^{3+}) which lases in the near infrared, 1.06 microns.

Another rare earth ion that exhibits all the requirements for a four level system is thulium (Tm^{3+}) in yttrium orthoaluminate ($YAlO_3$) which provides laser energy at 2.34 microns. At present this is the only room temperature four level solid state laser in the middle infrared.

The complete energy level diagram of 1% at. Tm^{+3}: $YAlO_3$ was determined spectroscopically up to 27,900 cm^{-1}. The site symmetry of (Tm^{3+}) was identified as C_s and such a low symmetry electrostatic field splits the levels into 2J + 1 sublevels. $YAlO_3$ is a distorted perovskite and it is shown that the splittings of the sublevels can be derived from an O_h symmetry, as an ideal perovskite, with a C_s distortion.

To obtain sufficient pumping of (Tm^{3+}) for laser action the crystal was co-doped with chromium (Cr^{3+}). When Cr^{3+} is doped in yttrium aluminum garnet (YAG) the ^2E level is approximately at 14,400 cm^{-1} which is near to the $^3F_3$ level of thulium, but in ($YAlO_3$) the ^{2}- level of Cr^{3+} is shifted down to approximately 13,800 cm^{-1} and lies very close to the $^3F_4$ level at 12,800 cm^{-1}. With the ^2E level in Cr^{3+} so nearly matched in energy with the initial laser level ($^3F_4$) in Tm^{3+} excellent energy transfer is obtained. Time resolved fluorescence measurements were used to determine the fluorescence lifetimes of the $^3F_4$, $^3H_4$, and $^1G_4$ levels of Tm^{3+}: $YAlO_3$ and from this data it was determined that the aforementioned energy transfer was nonradiative. The measured lifetimes are 630 μ sec., 4.7 m sec., and 261 μ sec. for the $^3F_4$, $^3H_4$ and $^1G_4$ levels respectively. These results were compared with values predicted from the Judd-Ofelt theory and the agreement between experiment and theory is extremely good.

Pulsed room temperature laser action was obtained[1] in the middle infrared with 1% at Tm^{3+}:$YAlO_3$ sensitized with 0.09% at Cr^{3+}. The laser spectra was obtained and it revealed that laser action occurred on two transitions at 2.349 and 2.346 microns. From fluorescence and

absorption spectra these transitions were identified and it was determined that both emissions initiated from the lowest sublevel of the $^3F_4$ and terminated on the two lowest sublevels of the $^3H_5$ level.

Reference

1. L. M. Hobrock, Ph.D. Dissertation, University of Southern California, 1971.

1.2.6 Optical Experiments with Laser Sources

DAHC 04-69-C-0003, U.S. Army Research Office, Durham, N.C.

W. L. Faust

I. Introduction

Work proceeded under the above title and contract for the three year period beginning Aug. 20, 1968 and terminating Aug. 19, 1971. In this report the final phases of the project effort are described as well as some measures of reorientation of our work, to accommodate objectives of a new research program being formulated.

II. Light Scattering Associated with Impurities in Semiconductors (with D. T. Hon)

As discussed in the previous report, we have worked on two entirely distinct types of excitation which give Raman scattering, apart from the pure-crystal phonons. These are local-mode vibrational scattering from isoelectronic substituent impurities, and effects on the Raman spectrum arising from free carriers (due to non-isoelectronic impurities).

Our earliest studies of local modes[1] were done with a visible laser source, in the transparent III-V semiconductor GaP. In

the previous report we described successful extension of the method to the host GaAs. This host required use of a 1.06 μ laser source. With the methodology now established, this effort is in the process of being shifted into Prof. Spitzer's research effort. The next development will be study of ion-implanted samples, for which this seems to be a very appropriate analytical technique.

In first-order Raman scattering from lattice vibrations and/or from free carriers, only small R-vector excitations need be considered. The carriers may then be treated as a spatially-continuous plasma contributing to the linear dielectric properties, and in principle to the nonlinear ones also. In the previous report we sketched a simple approximate treatment (valid for small damping) which predicted interaction between the LO phonons and the plasmons. Mooradian[2] had shown previously that this led to repulsion between the modes, and presumptively to mixed-modes exchanging character with increasing carrier concentration. We indicated roughly how, for a highly damped plasma, the plasma resonance might not be observable. We have now completed and are preparing for publication an analysis of this theoretical problem: calculation of the full spectrum of scattered intensity $I(\omega)$ (where ω is the Raman shift), and the structure of the mixed-"modes". The method, which involves repeated use of Nyquist's theorem in several contexts, is valid for arbitrarily large damping. Using carrier concentration and damping constant values consistent with determinations from independent Hall and resistivity measurements, we can fit the $I(\omega)$ for various GaP samples. All the features due to the large damping in GaP are explained.

III. CO_2 Laser, Apparatus Development (with E. Vasconcellos)

In previous reports we described construction and operation of a non-Q-switched laser and of a Q-switched laser (respectively NQS and QS), and of a local-mode resonance experiment performed with

these lasers. For future work we need only a single source. Therefore, we have adapted one laser for either QS or NQS operation, with easy changeover; and the second laser is subsequently to be applied as an amplifier. Without amplification, the first laser presently generates either i) a cw 30 watt single frequency beam (this requires a custom-built copper-substrate diffraction grating for line selection; a conventional grating would be destroyed immediately) or ii) a 360 pulse/sec., 20 kilowatt, 300 nanosecond beam, also grating tuned. For a third mode of operation, iii) we are presently fabricating a special pyramidal spinning-mirror device for high repetition-rate Q-switching. In conventional systems, Q-switching at feasible repetition rates entails a loss of average power by a factor of twenty. We hope to obtain perhaps half the cw power by pulsing at ~3 kHz.

All work on the transversely-excited CO_2 laser system has been abandoned.

IV. Materials Study

A. Measurement of Low-Level Absorption by Calorimetry

We are instrumenting to apply the 30 watt cw CO_2 beam described in Section III to a study of wavelength-structure in the absorption due to multiple-phonon generation in various materials attractive as 10μ windows.

B. Observation of Large-R Phonon Populations by Sidebands on Visible Fluorescence (with M. Gundersen)

1. We are continuing our work to observe phonons produced in GaP by an H_2O laser. Thus far we have been able to produce exciton fluorescence with considerable phonon sideband structure, similar to spectra obtained by prior workers. However, we have not yet attempted the full experiment with the infrared laser beam as well as the visible beam to excite fluorescence.

2. We intend to seek evidence for specific phonons produced in BaF_2 by a Q-switched CO_2 laser beam, through multiphonon generation. The fluorescent impurity Sm^{++} will be used for phonon side bands. It will be excited by the same pulsed visible ion laser which we have placed in operation for the experiment immediately above. This work, together with item A above, is of interest for 10μ window development for ultra-high power CO_2 laser sources.

References

1. D. T. Hon, W. L. Faust, W. G. Spitzer, and P. F. Williams, Phys. Rev. Letters 25, 1184 (1970).

2. A. Mooradian and G. B. Wright, Phys. Rev. Letters 16, 999 (1966); ibid., 19, 849 (1967).

1.2.7 Theory of Infrared Absorption in Low Absorption Materials

R. W. Hellwarth

Background

A major block to scaling up the output power of existing types of high-power infrared lasers is the lack of any window that will pass a large (10-100 cm diam.) output beam without warping so badly from thermal distortions that it distorts the beam phase front unacceptably. The origin of the small infrared absorption that causes the thermal distortion is not yet understood in those materials (alkali halide crystals, certain II-VI crystals, certain chalcogenide glasses, and high resistivity germanium) which, so far, are believed to be the best for windows in the 10.6 and 2-5 micron regions of greatest importance. One mechanism widely mentioned as likely to be responsible for the low absorption is multi-phonon absorption. However, theoretical predictions

on this basis cannot yet be made well enough to see if it accounts for observed absorption values. Since these values seem lately to be changing as crystal preparation techniques change, theoretical interpretations must be made warily.

Objectives

The purpose of this project is to calculate what each of several physical mechanisms will contribute to infrared absorption in the aforementioned materials that are most likely to exhibit the small absorption for given material strength and cost. We will try to interpret observed absorption values by our theory, and, if that effort is unsuccessful, to at least place a limit on how low absorption could possibly be in an ideal crystal in which only these mechanisms operated.

Approach

The research will be theoretical, applying existing theories of some absorption mechanisms, developing new theories where required, and calculating numerical predictions from these theories.

Present Status of Work

This project has just been initiated in September of 1971. We are presently performing a review of the problem, isolating possibly important absorption mechanisms, and finding which materials seem most promising as high power infrared windows.

1.2.8 Laser Studies of Relaxation Processes

J. H. Parks

This report discusses work progressing in three areas: 1) molecular relaxation, 2) laser induced damage, and 3) the study of e.m. wave propagation in a laser amplifier.

1.2.8.1 Molecular Relaxation in Gases and Liquids

AF-AFOSR, Joint Services Electronics Program
Frederick Gardner Cottrell Grant

J. H. Parks, N. Alyassini, T. Pacala, A. Scalabrin, L. Singer, R. Brown

1.2.8.1.1 Decay of N_2 Triplet Metastables

The radiative and diffusion relaxation rates of N_2 molecules in the first excited triplet metastable state $A^3\Sigma_u$ are not known to within an order of magnitude.[1] This is primarily due to the fact that the molecular symmetry rules out the use of direct radiative processes to monitor molecules leaving this state. These relaxation rates are important to obtain since these excited states (6 e.v.) can exist for 10^{-3} to 10^{-1} sec. and may be directly involved in chemical reactions in the atmosphere.

The excited triplet $A^3\Sigma_u$ is the lower electronic state of many pulsed laser transitions in the first positive bands of N_2.[2] In this experiment these laser transitions will be used to optically pump the $A^3\Sigma_u$ metastable population produced in a second N_2 discharge cell placed within the laser cavity. The side emission from the absorbing N_2 cell is monitored as the laser pulse probes the cell at different times after the cell discharge terminates. The variation of the spontaneous emission intensity will be directly proportional to the decay of the $A^3\Sigma_u$

population. This experiment takes advantage of an indirect radiactive process to obtain the various relaxation rates.

In the initial experiments we are concentrating on the following measurements.

(i) The lifetime of N_2 molecules in the vibrational level $A^3\Sigma_u$ (v = 0) is determined primarily by diffusion since the radiative decay is $\tau_R \sim 0.1$ sec. The laser lines in the vibrational band $B^3\pi_g$ (v = 2) → $A^3\pi_u$ (v = 0) at 7700 A^o will be used to measure the diffusion of v = 0 molecules.

(ii) Molecules in $A^3\Sigma_u$ (v = 1) can undergo vibrational energy transfer to v = 0 during collisions. Probing the population with the laser lines in the band $B^3\pi_g$(v = 3) → $A^3\Sigma_u$ (v = 1) at ~ 7600 A^o will allow a direct radiative measurement of vibrational relaxation.

These laser transitions have been produced in a crossed-field N_2 discharge[3] and measurements are presently underway.

1.2.8.1.2 Time Resolved Spectroscopy of Benzophenone

The N_2 amplifier is suitable for observing fast relaxation processes in many large molecules. A technique developed to obtain the individual fluorescence and phosphorescence spectra has been applied to the radiative decay of Benzophenone ($C_6H_5COC_6H_5$). This molecule is often employed to probe photochemical processes because intersystem crossing to the lowest triplet state occurs with close to unit probability. For this reason it is used as a triplet sensitizer and quencher, and as a method of determining intersystem crossing efficiencies in other systems.

The results of these studies[4][5] have clarified earlier

observations[6][7] concerning the time delayed component of the fluorescent spectrum. It is believed that these experimental techniques represent the first direct observation of the processes producing this delayed fluorescence.

1.2.8.1.3 Tuneable Ultraviolet Lasers

At present tuneable laser sources do not extend below $\sim 3500\ A^{o}$. The possibilities in materials studies and gas phase spectroscopy which will become available when lasers having $\lambda_L < 3000\ A^{o}$ are developed, are exciting many efforts towards these shorter wavelengths. Our particular interest is the study of nonradiative relaxation processes in molecules such as Benzene and Napthalene. A project is presently underway to generate a tuneable ultraviolet laser source in the $2400\ A^{o}$ - $2700\ A^{o}$ wavelength range by using a ruby laser and a dye laser to produce a tuneable sum frequency.

When the intense radiation from a Q-switched ruby laser at frequency ω_R is combined with the output of a dye laser at ω_R in an ADP crystal, the resulting nonlinear interaction will produce radiation at the sum frequency $\omega_S = \omega_R + \omega_D$. The wave vector phase matching condition $\vec{K}_S = \vec{K}_R + \vec{K}_D$ will be satisfied by temperature tuning the indices of refraction. Since this can be accomplished in ADP for collinear propagation of $\vec{K}_R$ and $\vec{K}_D$, longer crystals can be used to achieve more efficient conversion to the sum frequency. Using the data available for ADP, we calculate that a coumarine dye laser tuned through the spectral range 4000 -5000 A^{o} will generate ultraviolet radiation 2400 - 2700 A^{o}. Phase matching can be maintained by varying the ADP crystal temperature between $0^{o}C$ - $75^{o}C$.

A Korad K-15 ruby laser has been redesigned to produce ~ 200 MW peak powers and we convert approximately 10% of this to the second harmonic for use as a dye laser pump source. The ADP oven

is completed and provides a uniform temperature over the crystal length to within $\pm 0.05^{\circ}C$. We are presently constructing the tuneable dye laser source which will then allow the first experiments in sum-frequency generation.

1.2.8.2 Laser Induced Damage Studies

F19628-71-C-0220, Air Force Cambridge Research Laboratories

J. H. Parks, R. Owens, N. Alyassini, A. Scalabrin, T. Colbert

1.2.8.2.1 Damage in Thin Dielectric Films

This laboratory is undertaking the characterization of ultraviolet laser damage as part of a joint effort to investigate the physical processes leading to structural and optical damage in thin dielectric films.[8] This research is an integral part of a general emphasis on ultraviolet physics presently underway and bears upon the need for damage resistance in ultraviolet dielectric reflectors. In particular, we are concerned with the deterioration of the optical properties of dielectric thin films as well as structural damage, both of which are induced by laser irradiation.

An experiment is in progress to measure the threshold of structural damage at 3472 Å and determine if it differs significantly from the damage threshold at 6943 Å. This provides a careful study of laser induced damage at an ultraviolet wavelength, and also may indicate the dispersive behavior of a damage mechanism. The experimental optics will allow the ruby and ultraviolet beams to be separated after emerging from the KDP doubling crystal and then simultaneously focused upon different areas of the sample. This allows the damage resulting from both wavelengths to occur during a single Q-switched

light pulse. Each wavelength is independently attenuated and the spatial or temporal characteristics observed to measure any increased non-uniformity caused by the nonlinear doubling process. The optical components for this experiment are being assembled and a study of damage in ZnS films is expected to begin shortly. The electronics to monitor the pulse peak power will include an ITT FW114 photodiode and a Tektronix 519 oscilloscope.

In addition to the ultraviolet damage studies, we are extending our capability to investigate these processes in the 5 micron region. This is particularly important in view of the fact that a strong effort is underway to produce high power CO lasers at these wavelengths. Studies to indicate the utility of various materials for dielectric mirrors and optical windows would be useful to this laser development. We are planning to generate difference frequencies in the 5μ region with an experimental arrangement similar to that described in section (1.2.8.1.3). In this case, however, the nonlinear materials being considered are Pronstite and Lithium Iodate (LiO_3) which have better transmission characteristics at these infrared wavelengths.

1.2.8.2.2 Damage at the Surface of Bulk Materials

It has been observed[9] in studies of bulk damage in glasses and other transparent dielectric materials that surface damage usually occurs only on the exit surface of the sample. Although this has lead to much speculation on the specific process involved, attention has not been directed to more detailed studies of this experimental observation. Since this type of damage is involved when high peak power radiation is passed through lenses and optical windows, we are investigating the physics of this damage behavior.

The experiment consists of reflecting a 6328 A^o He/Ne laser from the exit face of a fused silicia or glass disk (1" dia x 1/4" thk) as a Q-switched ruby laser pulse is passing through the disk. By

monitoring the change in reflected 6328 A^{o} laser power, we have been able to observe power changes which are related to a decrease in the refractive index. The possibilities of thermal heating or sound wave propagation are being investigated. This technique is also being applied to thin film damage processes.

1.2.8.3 Electromagnetic Wave Propagation in Laser Amplifiers
AF-AFOSR 69-1622, Joint Services Electronics Program

J. H. Parks, D. Chen, A. Scalabrin

1.2.8.3.1 Frequency Coupling in High Gain Amplifiers

The current development of extremely high gain optical amplifiers may find important application in laser communication technology. These devices, operating on visible and near infrared transitions, could be useful as multi-channel amplifiers for a set of frequencies lying within the radiative linewidth. This possibility requires an understanding of electromagnetic wave propagation through high gain optical frequency amplifiers. Theory indicates that the problem of crosstalk, familiar at radio frequencies, has an optical analog which arises through the nonlinear interaction between waves of different carrier frequencies traveling through the high gain medium. The following experimental technique is designed to observe this frequency coupling as a function of the amplifier gain. Since this research can lead to an assignment of carrier frequencies which minimizes crosstalk, this study can provide useful design parameters for laser communication systems.

Emphasis is being placed on dye laser amplifiers since they produce very high gains, are inherently broadband ($\sim$100-500 A^{o}), and saturate at high power levels. Consider a continuous Argon laser at frequency ω_A which is being amplified by a dye laser amplifier. If a dye laser at frequency ω_D is also passed through the amplifier and tuned through ω_A.

the Argon laser amplification will show a modulation when both ω_A and ω_D are within the homogeneous linewidth. The frequency range, $\Delta\omega = (\omega_D - \omega_A)$, over which modulation is observed determines this linewidth and also provides the range within which frequency coupling can occur in the amplifier. This measurement is particularly important in the liquid phase organic systems because long range (~ 100 A°) dipole-dipole interactions[10] have been observed to be an essential interaction mechanism between these large molecules. These interactions which determine the homogeneous linewidth have not been measured before with as much sensitivity as the above technique will provide. This experiment is presently underway as a study of the saturated absorption of Perylene. We are choosing to develop this technique with this absorbing molecule and then proceed to studies in amplifying media.

1.2.8.3.2 Amplification of a Broadband E.M. Field

In this study a semi-classical theory[11] has been derived which describes the amplification and saturation behavior of a broad band electromagnetic field as it propagates through a high gain gas amplifier. This case is of particular interest because an adequate theoretical description has not been developed which treats the nonlinear coupling among the components of a broad band field as it builds up from radiative noise. A recent paper[12] which considers the broad band amplifier concentrates on the variation of the field bandwidth with intensity but neglects the detailed behavior of these coupling processes. This theory relates to the optical amplifier problem since a high gain broadband device will necessarily generate a significant amplified spontaneous emission field internally. It is important to understand how these internally generated fields will couple energy away from the signal we wish to amplify.

The theory is formulated in terms of the density-matrix equations of motion and is applied to both an inhomogeneous and a

homogeneous amplifier lineiwdth. The electromagnetic field and the induced polarization are represented as Fourier integrals and equations for the amplitude and phase are written assuming the quasi-Fourier components are varying slowly as the field is amplified. The full expression for the polarization, including amplitudes and phases, is calculated to third order in the field. The linear polarization treats each field component independently and leads to a gain induced narrowing of the field bandwidth. As the field strength increases, the nonlinear interaction reduces the gain available for each field component and, in addition, introduces amplitude and phase coupling among these components. The extent of this interaction between field components is determined by the atomic homogeneous linewidth. When the amplifying transition has a Doppler broadened linewidth, computer solutions indicate that the power spectrum broadens in the presence of these saturation effects even when the phases are assumed to be randomly distributed. The amplitude coupling, which still remains in this approximation, reduces the saturation of individual broad band field components by diffusing the energy throughout the field bandwidth. An amplifier with a homogeneous, collision broadened linewidth continues to gain narrow the field bandwidth in the saturation region, when the phases remain randomly distributed. However, the general expression for the nonlinear polarization including phase terms contains a frequency dependence related to saturation rebroadening.

1.2.8.3.3 Propagation of Two Vector Waves in a Laser Amplifier

The interaction between two fields which are <u>not</u> propagating along parallel directions is another process related to e.m. propagation in a high gain gas amplifier. The interaction between two parallel travelling waves has been extensively studied for the case when the frequencies of <u>both</u> waves lie <u>within</u> the natural width of the amplifying transition.

However, similar interactions can occur even when the frequency difference is greater than the natural width if these waves are travelling at an angle with respect to one another. This suggests a new frequency coupling between waves within the broad Doppler bandwidth which has not been suggested or studied previously.

The calculation presently underway follows the theoretical guidelines described above in Section (1.2.8.3.2). The total field is assumed to be a sum of two monochromatic fields $\vec{E}_1(w_1, \vec{k}_1)$ and $\vec{E}_2(w_2, \vec{k}_2)$ having frequencies w_1, w_2 and wave vectors $\vec{k}_1$ and $\vec{k}_2$. In the nonlinear regime we have been able to relate the results to simple, clear physical mechanisms although the mathematical forms are somewhat complex. We have observed that there are resonant interactions with the atomic high gain medium which lead to two interesting parametric processes. One of the terms arising from these nonlinear interactions describes the generation of a third field which propagates at an angle different from $\vec{k}_1$ and $\vec{k}_2$. Another term allows for the transformation of energy in $\vec{E}_1$ directly to $\vec{E}_2$ even when the frequencies w_1 and w_2 are widely spaced compared to the natural linewidth. It is possible that these terms are important in transverse mode-locking phenomena and also the spatial distribution of light emitted from a high gain noise amplifier.

References

1. S. N. Foner, R. L. Hudson, J. Chem. Phys. 45, 40 (1966).

2. L.E.S. Mathias, J. T. Parker, Appl. Phys. Letters 3, 16 (1963).

3. D. A. Leonard, Appl. Phys. Letters 7, 4 (1965).

4. R. Brown, J. H. Parks, L. Singer, "Prompt and Delayed Fluorescence from Benzophenone," submitted for publication.

5. R. Brown, J. H. Parks, L. Singer, "Concentration Effects on the Lifetime of the Benzophenone Triplet," submitted for publication.

6. J. Saltiel, et. al., J. Amer. Chem. Soc. 92, 410 (1970).

7. W.D.K. Clark, et. al., J. Amer. Chem. Soc. 91, 5413 (1969).

8. L. G. DeShazer and J. H. Parks, "Investigations Toward Understanding the Physics of Laser Damage to Thin Dielectric Films," presented at Third Symposium on Damage in Laser Materials, Boulder, Colorado, May 19-20, 1971 (Proceedings to be published).

9. R. W. Beck, NBS Special Publication #341, "Damage in Laser Materials".

10. An excellent discussion is found in "Photophysics of Aromatic Molecules," J. B. Birks, Lond/N.Y., Wiley Interscience 1970, p. 567.

11. J. H. Parks, A. Javan, J. Cpt. Soc. Am. 61, 658 (1971), also presented at The Esfahan Symposium on Fundamental and Applied Laser Physics, August 26 - September 5, 1971 (Proceedings to be published).

12. M. M. Litvak, Phys. Rev. A2, 2107 (1970).

1.3 MAGNETISM

1.3.1 Paramagnetic Impurities in Antiferromagnetic Crystals

F 44620-71-C-0067, Joint Services Electronics Program

J. P. Hurrell, U. Ranon and D. Bozinus

I. Introduction

Rare earth ions can affect the properties of magnetic materials because they interact appreciably with iron group elements and relax strongly to the lattice. When present in small quantities they can be used as probes to investigate the microscopic behavior of magnetics near defect locations. In higher concentrations they modify the magnetic anisotropy. This is particularly relevant to the present status of bubble devices.

The objectives of our research program are to study recent advances in the observation of interactions between rare earth ions and lattices, and to pursue the properties of paramagnetic ions in magnetic materials. In our research approach we are using the techniques of electron spin resonance, Electron Nuclear DOuble Resonance, fluorescence and Raman scattering. Progress along three major directions is discussed below.

II. Present Status of Work

A) MnF_2: Er were chosen for an ENDOR study of a paramagnetic impurity in an antiferromagnet. Many different samples with spin resonance and fluorescence were studied. A severe materials problems has been encountered in this work but finally we have acquired good samples, with high enough impurity concentrations and narrow lines, grown by a liquid phase epitaxy modification of the Bridgeman-Stockbarger method. Further annealing is required to dispose adequately the charge compensation.

B) Recent observations of Jahn-Teller effects in rare earth ions prompted us to investigate the YVO_4: Dy system with spin resonance techniques. Both the ground and first excited states were detected with g-values close to those expected in $DyVO_4$. Hence the dilute system mirrors the concentrated $DyVO_4$ system and can be used to supplement the understanding of the phase transition at low temperatures in the latter. The effects of static strains (which are the manifestation in the dilute system of the Jahn-Teller distortion in $DyVO_4$) were observed in the perpendicular plane where they cause a and b directions to become inequivalent: g-value shifts of 10% were observed. In addition, the system possesses peculiar relaxation properties. The g-values in the ground and excited states can be made equal allowing material narrowing to occur which can be inhibited by depopulating the excited state. These relaxation effects as a function of temperature are currently being monitored.

C) Raman scattering in some concentrated systems is also being investigated. We have found a slight optical window in the green region in rare earth chromites which may afford an opportunity to observe electronic Raman scattering by the rare earth ions and monitor their exchange interactions with the chromium system. Backward light scattering experiments exhibit some Raman peaks, but their detailed interpretation has yet to be completed. To investigate some of the scattering capabilities of iron group systems, some Raman experiments on $Cs_3Co\,Cl_5$ have also been initiated. The tetrahedral cobalt ion presents a unique opportunity to observe strong electronic scattering together with interesting effects on the intensity of the phonon scattering. Our preliminary results are very encouraging.

1.4 DEFECT CHEMISTRY AND SOLID STATE ELECTROCHEMISTRY

1.4.1 Defect Chemistry of CdS

No Contract Support

1.4.1.1 High-Temperature Hall Effect Measurements

F. A. Kroger and H. R. Vydyanath

Measurements have been carried out on iodine and silver doped crystals. The former were obtained by growing course polycrystalline CdS by chemical vapor transport, using iodine as the carrier, followed by slow sublimation; crystals of 10 x 10 x 3 mm were obtained. Silver doped crystals were made by diffusion of Ag into pure CdS single crystals.

Hall effect measurements on CdS-Ag at 1 atm $\geq p_{S_2} > 0.01$ atm showed an electron concentration of the order of 10^{16} cm^{-3} with $[e'] \propto p_{Cd}^{1/2}$, independent of the silver concentration for [Ag] from $1 - 5 \times 10^{18}$cm^{-3}. This indicates a compensation mechanism $[Ag^{\cdot}] \approx [Ag']$ under the condition of the experiment, and supports the expected amphoteric behavior of the silver. For the iodine doped crystals a definite pressure dependence was not found. It is probable that $[e'] \propto p_{Cd}^{1/4}$; the electron concentration increases with increasing temperature.

1.4.1.2 Chemical Diffusion Involved in Establishing Non-Stoichiometry by Heating in Sulfur Vapor

Knowledge of the relaxation time τ of the variation of the electronic conductivity of CdS-In brought about by a change in sulfur pressure should make it possible to estimate the concentration of neutral S_i^x defects.

Efforts to measure τ have so far been unsuccessful as a result of unwanted temperature variations accompanying any pressure changes.

1.4.2 Defect Chemistry of CdTe

No Contract Support

1.4.2.1 Self-Diffusion Studies in Indium Doped CdTe

F. A. Kroger and S. S. Chern

CdTe crystals containing $\pm 4 \times 10^{17}$ indium cm^{-3}, (i.e., more than the crystals originally used, which contained 10^{17} In cm^{-3}) were made by in-diffusion of In in Te_2 vapor at 700°C for ± 1 week. The cadmium self-diffusion coefficient D^*_{Cd} of these crystals at 700° and 800°C in Cd-vapor was $\approx 2 \times$ smaller than for the more weakly doped crystals. This is in line with a model in which $Cd_i^{\cdot}$ or $Cd_i^{\cdot\cdot}$ is the major Cd-carrying species under these conditions. In sulfur vapor at 800°C, D^*_{Cd} is the same as in the weakly doped crystals. At 700°C, at p_{S_2} = 1 atm, D^*_{Cd} is somewhat larger than in CdTe : 10^{17} In. This fits the model with both V''_{Cd} and $Cd_i^{\cdot}$ or $Cd_i^{\cdot\cdot}$ contributing to the diffusion of Cd, with the former slightly in excess .

These results support our contention that the independence of D^*_{Cd} on p_{Cd} reported by other workers results from the superposition of 2 mechanisms involving charged defects with opposite p_{Cd} dependence.

Attempts are being made to make even more strongly doped crystals, using In, Ga or Al as the dopant.

1.4.3 Defect Chemistry of Al_2O_3

N0014-67A-0269-0007, Office of Naval Research

1.4.3.1 EMF Measurements on Al_2O_3 + Co or Mg

F. A. Kroger and J. Yee

Attempts to repeat earlier emf measurements on pure Al_2O_3, using cells of the type

O_2, Pt | Al_2O_3 | Pt, O_2

have been unsuccessful due to the occurrence of spurious signals.

1.4.3.2 Valency Variation of Cobalt in Al_2O_3

F. A. Kroger and B. V. Dutt

Reduction of green Al_2O_3 - Co_2O_3 crystals with hydrogen at 1500°C proceeds to completion in a few hours (crystal dimensions $3 \times 3 \times 3$ mm^3 or $10 \times 5 \times 2$ mm^3) leading to crystals with a brown precipitate. Observation after 1 hour shows a reduction front marked by the presence of a brown precipitate in the layer near the surface. There is marked anisotropy of the rate of penetration, duffsion $\parallel$ c faster than diffusion $\perp$ c. (Similarly as has been found for conduction). Oxidation in O_2 or air of completely reduced crystals having a brown precipitate throughout proceeds much more slowly than reduction, complete oxidation requiring $\pm$ 1 week. This indicates that the rate determining step is different in the two processes. Possible mechanisms are as follows:

In reduction, the rate is probably governed by the diffusion of hydrogen into the crystal as H_i^x or $H_i^{\cdot}$ + e'; electrons are trapped at Co^{3+} to form Co^{2+} whenever a Co^{3+} is met; as a result a layer with reduced Co-ions forms near the surface and, since the solubility of Co^{2+} << that of Co^{3+}, a precipitate is formed. The rate of oxidation, on the other hand, may be governed by the release of electrons from Co^{2+}, thus re-forming Co^{3+}. This may happen all over the crystal. Out-diffusion of H_i^x or $H_i^{\cdot}$ + e' being rapid, we should expect no front; the hydrogen and electrons concentration is reduced throughout the crystal, and bleaching occurs everywhere at the same time.

Experimental results are still contradictory; a front was observed in the initial stage of the oxidation, while the precipitates are

being dissolved. No front was found in the final stages, although the overall absorption color was blue, i.e., not yet the green color of pure Co^{2+}.

1.4.4 Electrochemical Pressure Gauges and Pumps

1.4.4.1 Electrochemical Oxygen Pump

N0014-67-0269-0007, Office of Naval Research

F. A. Kroger and B. V. Dutt

Stabilized zirconia normally used as a solid electrolyte in oxygen pumps and sensors have the disadvantage of mechanical instability in heating and cooling cycles.

We are attempting to remedy this by using porous alumina tubes which have good mechanical stability, forming the ZrO_2-Y_2O_3 electrolyte in the pores by alternately soaking of the alumina in a solution of Zr + Y salts and heating in air.

In order to be able to have pump and/or monitor sections in an otherwise impervious Al_2O_3 tube, a 96% Al_2O_3 tube is chosen, and the 4% additional silicate is removed locally by etching with HF. Initial attempts were successful.

1.4.4.2 An Electrochemical Hydrogen Pump

No Contract Support

F. A. Kroger and A. Schrey

Potassium dihydrophosphate (KDP, KH_2PO_4) is a proton conductor. Application of a voltage over the cell

$$\overset{-}{Pt,\ H_2} \mid KH_2PO_4 \mid \overset{+}{Pt,\ H_2}$$

must be expected to remove hydrogen from the + side, evolving it on the - side, i.e., the cell works as a hydrogen pump. A proton current can no longer be sustained if H_2 is no longer present at the + side; a K^+ current can also not flow. Therefore, any rest current must be electronic in nature.

A similar polarization experiment with K metal present at the anode may reveal a small ionic K^+ current.

1.5 METALS, ALLOYS, AND LOW TEMPERATURE PHYSICS

1.5.1 Experimental Studies of Fermi Surface Topology in Metals

F44620-71-C-006, Joint Services Electronics Program

M. H. Halloran, J. H. Brewer, and R. D. Parker

Introduction

Since the electronic structure of the pure, metallic elements is now well understood in most cases, we have begun to extend certain techniques which were successful in those studies to the study of intermetallic compounds. The spectrum of compounds presents a much broader area of study and includes many materials which have interesting thermal, electronic, elastic or magnetic properties which make them useful but which can only be properly understood if their electronic band structure is known. In addition, we have been able to obtain very pure samples of the transition element vanadium, which is one of the few elements for which fairly complete experimental results have not already been attained but now appear possible.

The specific goals of the present research are to determine the Fermi surface topology and electron effective masses for intermetallic compounds $AuGa_2$, $AuIn_2$, and $MgZn_2$ as well as vanadium. The research is carried out utilizing the deHaas-van Alphen (dH-vA) effect at temperatures down to 1.1°K and magnetic fields up to 100 kOe (10T). Measurements of sample magnetization, conductivity and temperature are made using lock-in, phase sensitive detection and the analog results are converted to digital information on magnetic tape and analyzed on the IBM 320 at the University Computer Center. The magnetic fields are obtained with a superconducting solenoid. The research is divided into three areas in the discussion below--the

compounds $AuGa_2$ and $AuIn_2$, which are part of an isoelectronic sequence but which have strikingly different magnetic properties at low temperatures; the compound $MgZn_2$, which is very important as a hardening agent in aluminum alloys but which is not well understood; and vanadium, the group V transition element which has properties similar to tantalum and mobium and which is expected to have very similar electronc structure.

Present Status of Research

1. $AuGa_2$ and $AuIn_2$. The results on $AuGa_2$ were essentially completed[1] at the time of the last report. However, not all the results are yet understood. In order to help the understanding, two types of experiment were planned--one to study $AuGa_2$ under uniaxial stress and one to study the isoelectronic partner $AuIn_2$. At this time the latter experiment has been the most productive. The first accomplishment was to produce samples with a resistance ratio ($R_{293K}/R_{4.2K}$) of ~ 1000, an order of magnitude better than previously obtainable and comparable to the best $AuGa_2$. This was achieved with a horizontal Bridgman growth process, starting with .3 - .5% excess indium. The first experimental results on these samples are now being analyzed and detailed comparison with $AuGa_2$ should be possible. It is apparent already that these better samples have dH-vA signals of magnitude comparable to the best $AuGa_2$ samples and the results should have comparable completeness. At least two previously unreported Fermi surface sections have been identified. The apparatus for the pressure experiments has neen modified and those experiments will also be completed soon. By the next progress report it is hoped that this project will be complete.

2. $MgZn_2$. This research is in the very early stages, but we have succeeded in obtaining samples with resistance ratios of ~ 150 using standard Bridgman techniques, and this is twice the highest

previously reported ratio for samples which yielded limited results.[2] Oriented samples are being prepared for experiments and results should be obtained soon for comparison with recent band calculations.[3]

3. Vanadium. Using material obtained from Materials Research Corporation, we had been purifying samples with an electron-beam zone-refiner, with the best samples yielding resistance ratios of ~150, and barely observable dHvA oscillations. Earlier this year we received samples from the Bureau of Mines as well as some of their very high purity bulk material. The former consist of dendritic crystals and have enabled us to observe reasonably strong dHvA oscillations and map two sections of the Fermi surface.[4] These preliminary results are shown in Fig. 1. We are now zone-refining the bulk material to see if even better samples can be produced. The dendrites have a high density of occlusions and structural defects such as dislocations, vacancies, etc., are probably also of high density. The zone-refining process should eliminate that at the risk of introducing excessive carbon and/or oxygen. The results obtained thus far with the dendrites are in good agreement with those of other observers[5] and indicate close similarities with the Fermi surfaces[6] of tantalum and niobium.

References

1. J. C. Abele, J. H. Brewer and M. H. Halloran, Solid State Comm. 9, 977 (1971).

2. B. W. Veal and J. A. Rayne, Phys. Letters 6, 12 (1963).

3. P. Rennert and M. Taut, Phys. Stat. Sol. 41, 703 (1970).

4. R. D. Parker, J. C. Abele and M. H. Halloran, Bull. Am. Phys. Soc. 16, 838 (1971).

5. R. A. Phillips (to be published).

6. M. H. Halloran, J. H. Condon, J. E. Graebner, J. E. Kunzler and F.S.L. Hsu, Phys. Rev., B1, 366 (1970).

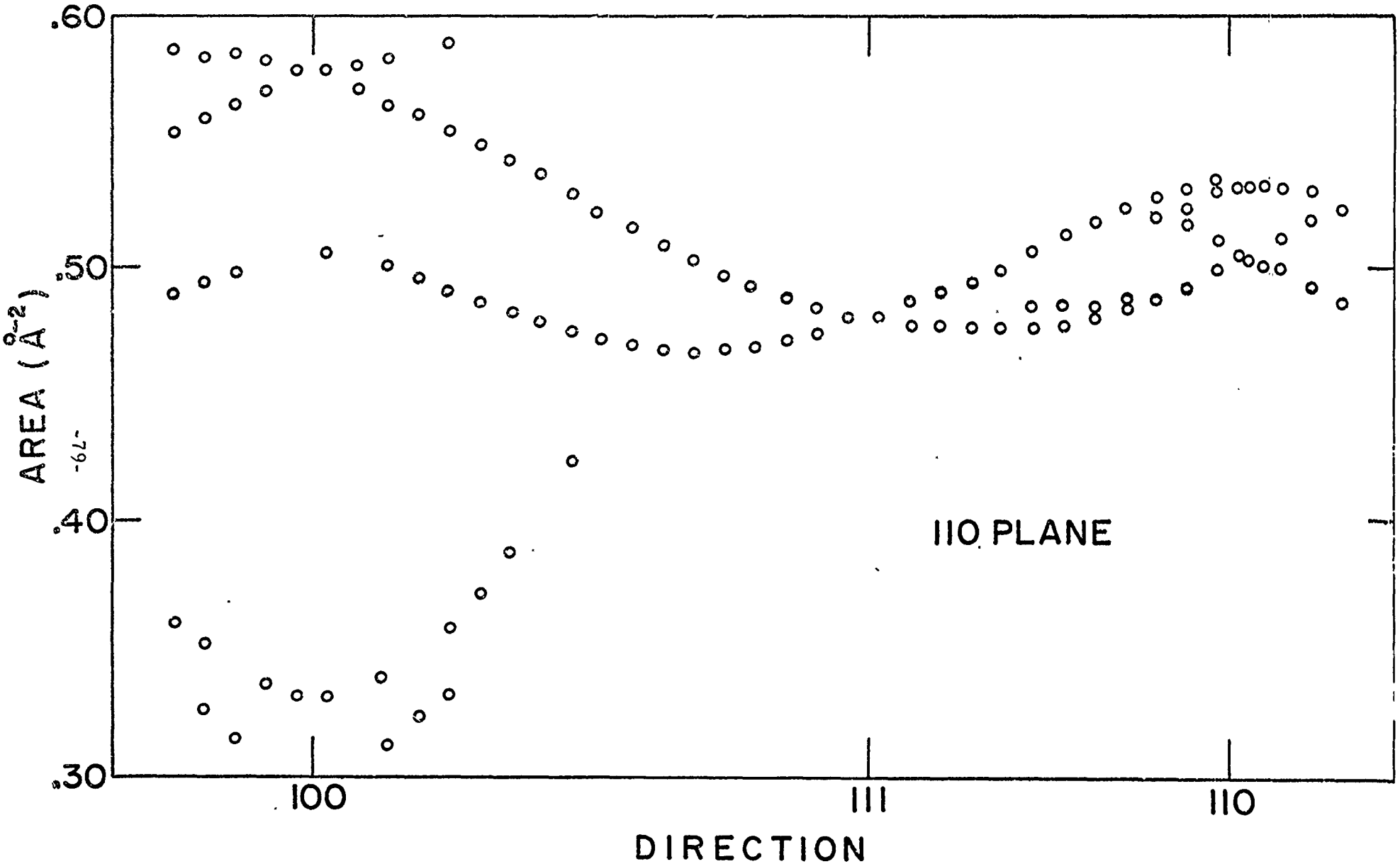

Figure 1. Extremal Fermi Surface Areas for Vanadium are Plotted as a Function of Crystallographic Orientations Within a { 110 } Plane.

1.5.2 Fundamental Studies of Nucleation and the Effects of a Magnetic Field on Nucleation and Growth of Vapor-Deposited Metal Films

AT (04-3)-113, Project #22, Atomic Energy Commission

L. E. Murr, H. P. Singh, O. T. Inal, K. P. Standhammer, and G. Wong

This research program is seeking to determine the effects of electric and magnetic fields on the growth of vapor deposited thin films; and is especially concerned with the nucleation of these films.

During the current report period, investigations of the atomic features of film growth as observed in the field-ion microscope were concluded[1,2]. The kinetics of nucleation of Sn and In films was continued with some very interesting revelations. By combining observations of nucleation in the scanning electron microscope with those obtained in the transmission electron microscope, it has been possible to clearly distinguish nucleation growth phase sequences as a function of substrate temperature. Nucleation of the vapor-liquid type has been shown to consist of three distribution modes of particle sizes characterized by primary, secondary, and tertiary nucleation. These features are clearly illustrated in Figs. 1 and 2. The variation of size distribution for nucleation at steps on the substrate have also been clearly observed in the scanning electron microscope as shown in Fig. 3.

Some preliminary investigations of the nucleation, growth, and ex-solution of immiscible metal thin-film systems has also been carried out as discussed in ref. (3); and the comparison of nucleation characteristics in single-component thin film systems has been continued[4].

Apparatus for the deposition of ferromagnetic single-component films of Ni, Co, and Fe in the presence of a magnetic field in the plane of the substrate (and perpendicular to the vapor stream) has been constructed

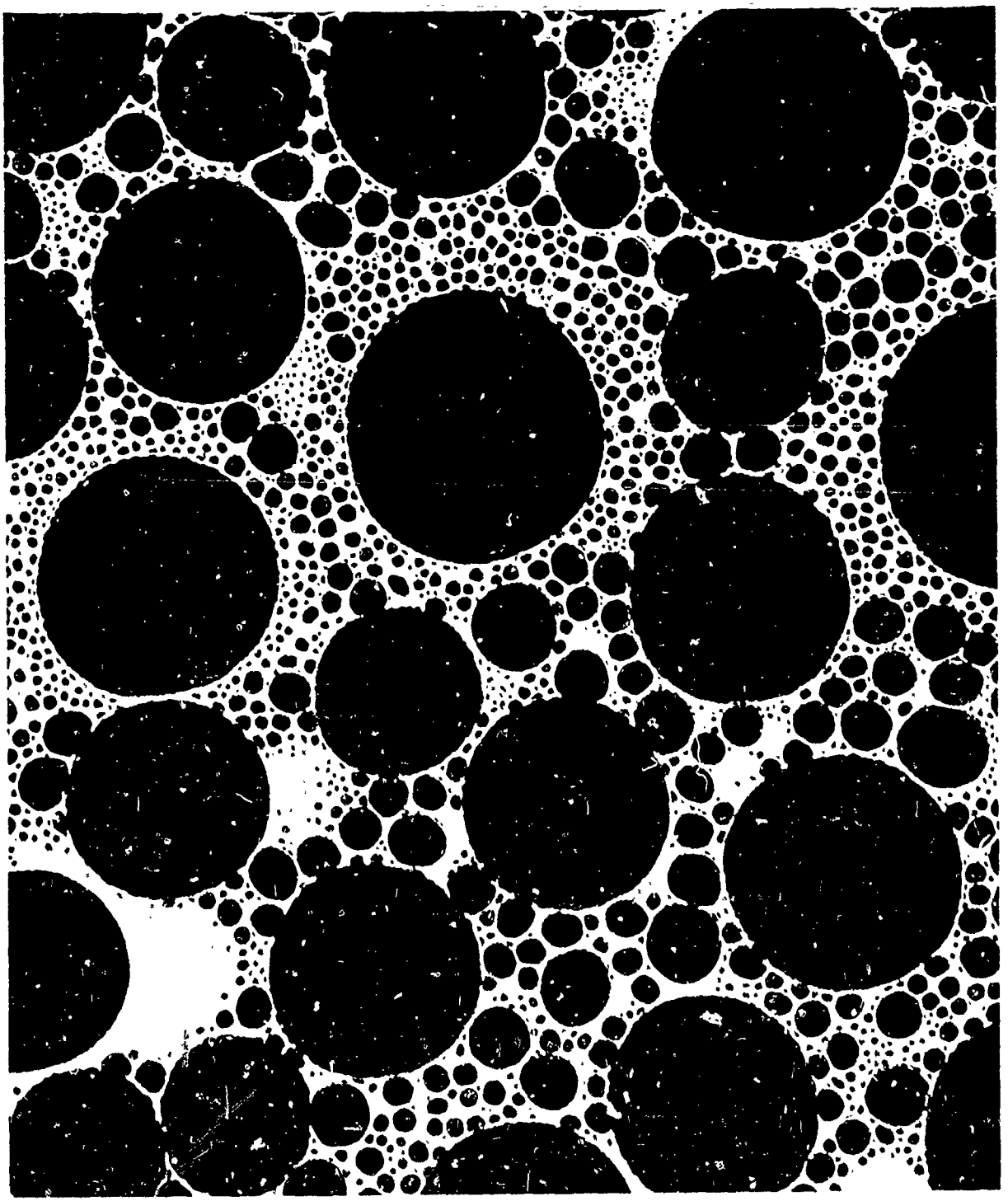

Fig. 1 Tin nuclei observed in the transmission electron microscope showing the distributions of particle sizes. Film was vapor-deposited into NaCl at 150°C. Magnification 60,000 X.

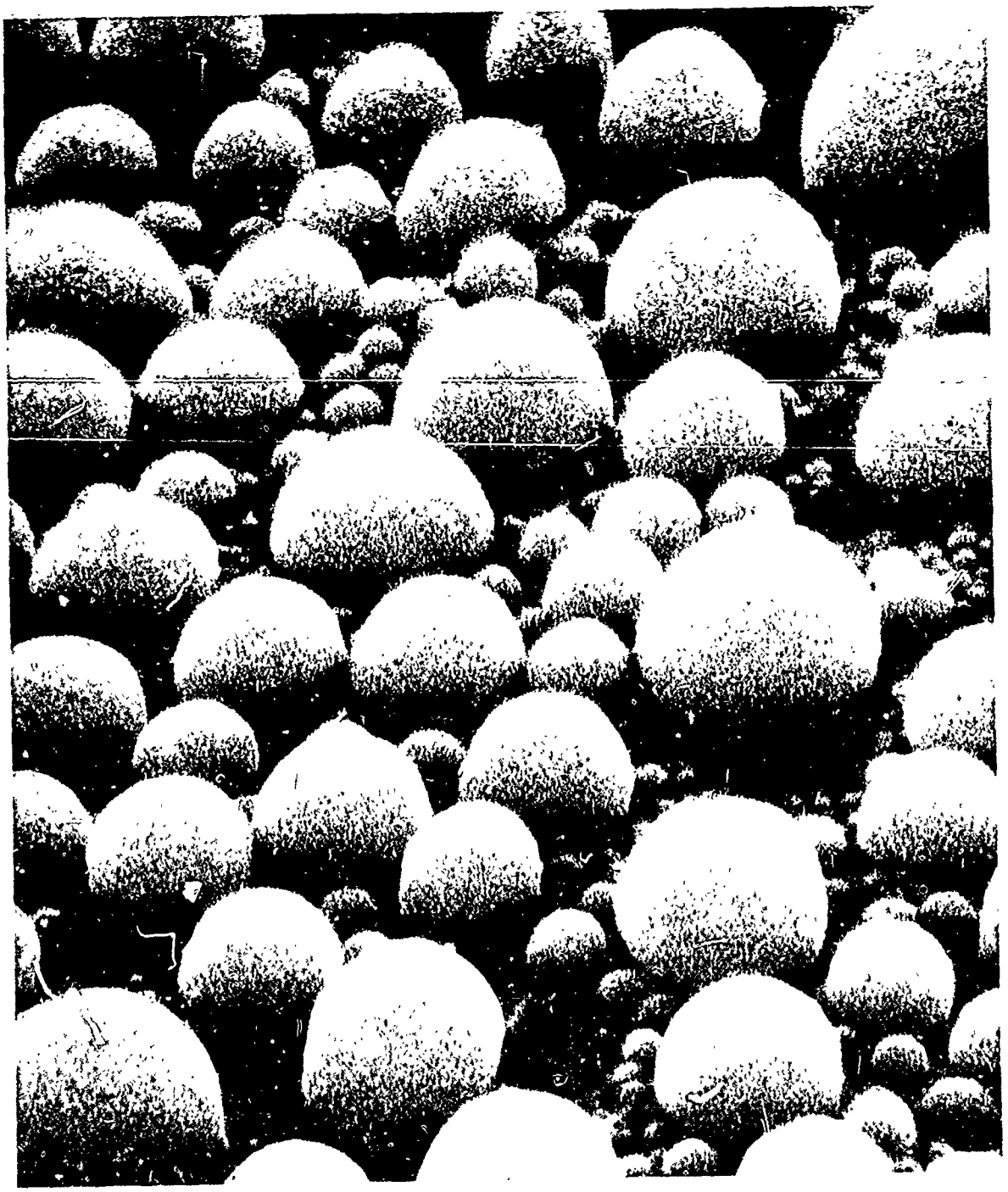

Fig. 2 Tin nuclei corresponding to Fig. 1 as observed at an oblique angle on the NaCl substrate in the scanning electron microscope. Magnification 50,000 X.

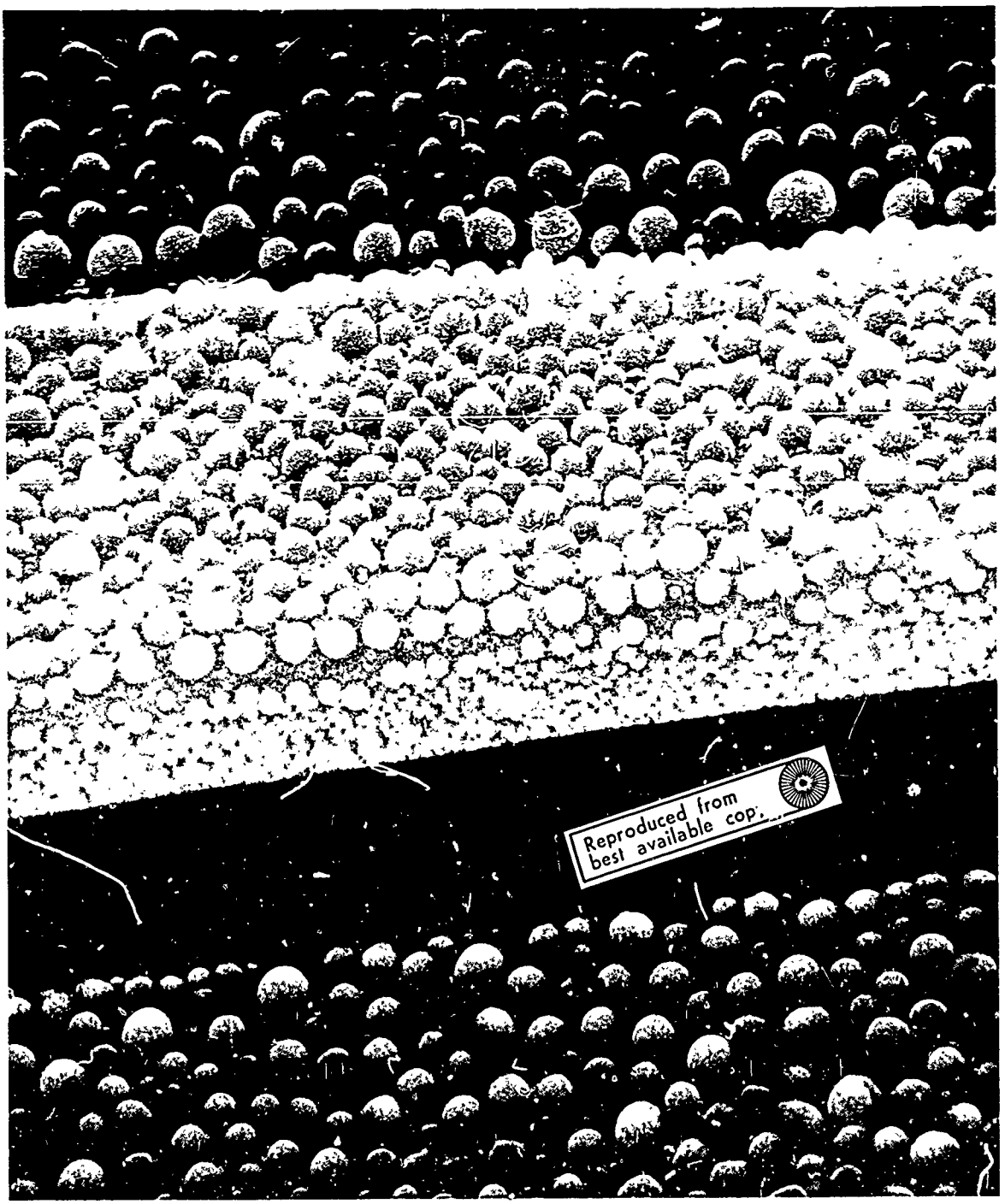

Fig. 3 Tin nuclei on a thin cleavage section on an NaCl crystal surface. Note the size distributions on the section surface and ledge-face. Scanning electron micrograph. Magnification 20,000 X.

and calibrated. A field strength of approximately 2 Kilogauss maximum can be obtained.

References

1. L. E. Murr, O. T. Inal and H. P. Singh, Proc. Electron Microscopy Society of America, p. 214 (1971).

2. L. E. Murr, O. T. Inal, and H. P. Singh, "A Field-Ion Microscope Study of Vapor-Deposited Platinum," Thin Solid Films, in the press.

3. K. P. Staudhammer and L. E. Murr, Proc. Electron Microscopy Society of America, p. 218 (1971).

4. H. P. Singh and L. E. Murr, ibid., p. 216.

1.5.3 Measurement of Interfacial Free Energies in Solid Metals and Alloys

N00014-67-A-0269-0010, NR 031-735, Office of Naval Research

L. E. Murr, R. J. Horylev, O. T. Inal and G. Wong

Aside from the direct measurement of grain boundary and related interfacial free energies, this research program has sought to investigate the general structure and properties of interfaces, including their stability, etc. The concept of interfacial torque as originally described by Murr, Horylev, and Lin[1] has also been investigated as this relates to interfacial structure and energetics.

A transmission electron microscopy study of 304 stainless steel films has been undertaken to systematically study the interrelationships of the degrees of freedom characterizing a grain boundary. From this study a configurational theory has been developed which is useful in explaining the existence of interfacial torques at twin-grain boundary intersections. The grain boundary misorientation (θ) is defined as the

relative rotation of the $< 1\bar{1}0 >$ directions in the adjacent grains of identical (110) orientation. The two remaining degrees of freedom are represented by the tilt or inclination (θ) and the asymmetry (Φ) of the grain boundary plane. Torques arise because of a difference in grain boundary energy with a change in misorientation or tilt. 90° twin configurations (twin plane along a $< \bar{1}12 >$ direction) are essentially high-torque situations, as a result of the change in misorientations ($\Delta\Theta$) between the twinned grain and its neighboring grain. 35° twins (twin plane along a $< 1\bar{1}0 >$ direction) are low-torque configurations, but can exhibit high torque anomalies when there is a sufficient variation in tilt across the intersection, $\Delta\theta$. Misorientation, Θ, appears to be the dominant torque producing parameter for high-torque configurations, and dominates the variations in grain boundary free energy. Also, a functional relationship between $\Delta\theta$ and $\Delta\Phi$ is observed for both high-torque occurrences. Spreads in the histograms for twin boundary-grain energy ratios for the two high-torque configurations were found to be due to torque terms, whereas the residual spread observed for the low-torque configuration data was attributed to variations in grain boundary energy with changes in grain boundary parameters.

The optimum mean value of the twin boundary to grain boundary energy ratio in 304 stainless steel has been computed from low-torque configuration systems to be 0.0235. The high-torque configuration data yielded a mean absolute torque equal to 84.8% of the average grain boundary energy, while absolute torque values for the anomalous high-torque and low-torque configurations were 179.8% and 4.2% respectively. The mean values for the torque contributing parameters $\Delta\Theta$, $\Delta\theta$, and $\Delta\Phi$ were 33.2°, 3.3° and 26.0°, respectively, for the high-torque configurations. The anomalous high-torque configuration twins had mean values of 8.6° and 9.4° for $\Delta\theta$ and $\Delta\Phi$, while the low-torque configuration twins had mean values of 2.3° and 5.2° for $\Delta\theta$ and $\Delta\Phi$, respectively.

This study, completed as the Ph.D. thesis by R. J. Horylev during the current report period should be useful in describing several structural and energetic features of interfaces in metallic systems. A recent study of phase transformations by Perkins and Massalski[2] has, in fact, utilized this concept as originally developed in ref. (1).

Several other areas of this study have also been summarized in references (3-5).

We are presently involved in the systematic measurement of the changes in surface and grain boundary free energy of 304 stainless steel as a function of temperature in the range 1000 - 1400°C. In addition, the formation of annealing twins and their energetics in aluminum is being pursued.

References

1. L. E. Murr, R. J. Horylev, and W. N. Lin, Phil. Mag., 22, 515 (1970).

2. A. J. Perkins and T. B. Massalski, Met. Trans., 2, 2701 (1971).

3. L. E. Murr, Proc. Electron Microscopy Soc. America, p. 218 (1971).

4. L. E. Murr, R. J. Horylev, and G. I. Wong, Surface Sci., 26, 184 (1971).

5. L. E. Murr, O. T. Inal, and G. I. Wong, Proc. 5th International Materials Symposium, Berkeley (1971).

1.5.4 Fundamental Studies of Explosive Shock Loading and High-Rate Forming

N00014-67-A-0269-0010, NR 031-735, Office of Naval Research

AF-AFOSR 69-1622A, Joint Services Electronics Program

L. E. Murr and J. A. Korbonski

The purpose of this research program is the investigation of residual microstructures of metals and alloys following explosive shock deformation or high-rate forming using the electron microscope. During the current report period, the necessary designs for modifying a gas gun for strain-rate measurements on thin sheets have been completed. In this experiment, stainless steel sheets will be formed to a pre-determined hemispherical shape by a projectile. The system design affords a wide range of velocities (strain rates) with which to form the constant strain). The formed samples will then be examined by transmission electron microscopy.

Future investigations will also examine the thermal recovery of the residual as-formed microstructures. Preliminary analysis of the range of microstructures anticipated over a strain-rate range of roughly 10^{-2} - 10^{5} sec^{-1} has been performed as discussed, for example, in an abstracted form in ref. (1).

References

1. J. A. Korbonski and L. E. Murr, "The Effects of Plastic Strain and Strain Rates on the Mechanical Properties and Thermal Recovery of 304 Stainless Steel," Metals Engr. Quart., Vol. 11, 47-48 (1971).

L. E. Murr

Publications for the Report Period

March - October 1971

1. "Comparison of Residual Defect Structures and Hardness in Inconel 600 Following Deformation by Explosive Shock Loading, Cylindrical (Explosive) Expansion, and Cold Reduction," with G. Wong and J. V. Foltz, Mat. Sci. Engr., Vol. 7, pp. 278-285 (1971).

2. "Comparison of Recovery, Recrystallization, and Grain-Growth Characteristics in Shock-Loaded, Explosively Expanded, and Cold-Rolled Inconel 600," with B. H. Maddala, Mat. Sci. Engr., Vol. 7, pp. 286-295 (1971).

3. "Interpretation of Some Field-Ion Micrograph Features from SEM Observations," with O. T. Inal and N. M. Hodgkin, Proc. Fourth Annual Scanning Electron Microscope Symposium, ed. O. Johari, IIT Research Institute, Chicago, April (1971), pp. 193-200.

4. "Measurement of Absolute Interfacial Free Energies in a NiCr Alloy," with R. J. Horylev and G. Wong, Surface Sci., Vol. 26, pp. 184-196 (1971).

5. "Field-Ion Microscopy of Graphite Fibers," with O. T. Inal, J. Appl. Phys., Vol. 42, pp. 3487-3493 (1971).

6. "Deformation Substructures and Terminal Properties of Explosively-Loaded Thin-Walled Stainless Steel Cylinders," with J. V. Foltz and F. D. Altman, Phil. Mag., Vol. 23, pp. 1011-1028 (1971).

7. "The Role of Transmission Electron Microscopy in Characterizing the Nature and Behavior of Grain Boundaries," Proc. Electron Microscopy Soc. America, ed. C. J. Arceneaus, Claitor's Publishing Division, Baton Rouge, La., pp. 102-103 (1971).

8. "Electron Microscopy of Thin Film Immiscible-Miscible Systems," with K. P. Staudhammer, ibid., pp. 218-219 (1971).

9. "Nucleation and Epitaxial Growth of Vapor-Deposited Films: Electron Transmission and Field-Ion Microscopy Studies," with O. T. Inal and H. P. Singh, ibid., pp. 214-215 (1971).

10. "Electron Diffraction Effects in Multi-Layered (Overlapping) Palladium Single-Crystal Films," with G. I. Wong and H. P. Singh, ibid., pp. 190-191 (1971).

11. "Nucleation and Growth Characteristics of Thin Metal Films," with H. P. Singh, ibid., pp. 216-217 (1971).

12. "The Effects of Interfacial Torque on the Geometry of Twin-Grain Boundary Intersections," with R. J. Horylev, ibid., pp. 220-221 (1971).

13. "Scanning Electron Microscopy of Earthquake-Induced Rail Fractures," with N. M. Hodgkin and B. V. Lowe, Metallography, in the press.

14. "A Field-Ion Microscope Study of Vapor-Deposited Platinum," with O. T. Inal and H. P. Singh, Thin Solid Films, in the press

15. "Effects of Plastic Strain and Strain Rates on the Mechanical Properties and Thermal Recovery of Type 304 Stainless Steel," with J. A. Korbonski, Metals Engr. Quarterly, Vol. 11, pp. 47-48 (1971).

16. "Applications of the TEM, SEM, and FIM in the Analysis of Structure and Energy of Metal Interfaces," with O. T. Inal and G. I. Wong, in The Structure and Properties of Materials - Techniques and Applications of Electron Microscopy (Proc. 5th International Materials Symposium, Berkeley, 1971).

1.5.5 Materials Research on High-Field Superconductors

AT(04-3)-113, Project #23, Atomic Energy Commission

Y. B. Kim, R. Wang, J. Savage

This research project entails an investigation of the metallurgical microstructure in relation to the superconducting properties of high-field superconductors. During the past six months our investigation has been concentrating on the superconducting properties of Nb_3Sn sintered in copper matrix.

Because of the difficulties associated with instabilities and ac losses, the present trend of superconducting technology is to fabricate conductor configurations in which the superconducting material is dispersed as finely as possible in a matrix of high conductivity normal metal.

In fact, with the latest technical development ductile superconducting alloys embedded in copper have been drawn to continuous superconducting filaments of only 0.002" in diameter. This technique is, however, not directly applicable to the high T_C but brittle intermetallic compound type superconductors, e.g., Nb_3Sn, V_3Ga, Nb-Al-Ge. This situation led us to explore the possibility of attaining practical conductor configurations by sintering Nb_3Sn powder in copper matrix. This approach is viable provided that in the sintered material (a) Nb_3Sn particles are in good metallic bond with the background matrix, and (b) the matrix of normal metal retains the high conductivity of copper.

Powder compacts were made by pressing the powder mixture of Nb_3Sn and Cu under 100,000 psi pressure. After a series of tests involving optical investigation and powder x-ray analysis, we found sintering in purified argon atmosphere at various temperatures does not completely eliminate Cu-Sn alloy phase. While alternative sintering techniques are being tested for Nb_3Sn, we are also working with Nb-Ti-C system for which Cu alloy phase is not expected to form. Tests for superconducting properties of these sintered materials are being carried out simultaneously.

1.5.6 Interaction of Kondo Systems

GP-29031, National Science Foundation

M. D. Daybell and Y. K. Yeo

The spin dependent interaction of the conduction electrons of a metal with an isolated magnetic ion dissolved in the metal gradually quenches the moment of the magnetic impurity below a temperature T_k, characteristic of each magnetic ion-host metal combination. A very strong conduction electron scattering also appears below T_k, the so-called "Kondo temperature". In materials such as a few parts per million of

chromium or iron in copper or gold, the low temperature quasi-bound state formed by the interaction has been intensively studied in recent years,[1,2] so that it is now feasible to investigate interactions between two or more of these "Kondo states" by examining the concentration dependence of various properties of these dilute magnetic alloys.

The theory of the interaction between Kondo systems is not as highly developed as that of the Kondo state itself. We have chosen to measure first the concentration dependence of the one property on which the best theoretical work is available,[3] the electrical resistivity as a function of temperature. Since it is important that the impurity-impurity interaction be strong enough to be seen, but weak enough not to completely obliterate the Kondo state, the choice of material is critical. Chromium in copper has proven to be nearly ideal, and we have seen for the first time all of the effects predicted by Suhl's theory. In addition, we have measured the average interaction energy between chromium impurities dissolved in copper. Outside the present problem, these results will be useful not only in the understanding of a class of non-dilute magnetic alloys, but also in removing some of the existing confusion about which of the properties of very dilute alloys should be ascribed to single impurity effects, and which should be ascribed to interactions between impurities.

We have measured the resistivity of copper-chromium alloys as a function of concentration c and temperature T from the dilute limit up to the limit of solubility and from 40 milliKelvin up to 77 Kelvin, using a dilution refrigerator and an a.c. bridge utilizing eddy current losses. The behavior observed for the electrical resistivity is essentially as predicted by Suhl.[3]

In the single impurity, or zero concentration limit, the Kondo effect leads to a divergence in conduction electron scattering as T is decreased below T_k, with the scattering finally saturating at a high value as T approaches absolute zero. As the concentration increases, impurity-

impurity interactions cause this divergence to be arrested at higher and higher temperatures, in fact, the increase of resistivity $\Delta\rho$ with decreasing T ceases below a temperature such that $k_B T$ is about equal to Δc, where Δ is a constant equivalent to 37 Kelvin per per cent chromium (k_B is Boltzmann's constant). As a result, the resistivity of a single impurity ($\Delta\rho/c$ as $c \to 0$) as a function of temperature and the low temperature limit of our new data ($\Delta\rho/c$ as $T \to 0$) as a function of concentration look very similar (Fig. 1). In particular, the proportionality of $\frac{\Delta\rho}{c}$ to $\log \frac{1}{T}$ over two or more decades in T when c is small is reflected in a proportionality of $\frac{\Delta\rho}{c}$ to $\log \frac{1}{c}$ when T is small. In short, the low temperature, low concentration Kondo state is destroyed in almost the same way by thermal energy or by the energy of interaction with its neighbors, which is known to depend nearly linearly on concentration.[4] Magnetic field Zeeman energy, $\mu_B H$, has a similar effect (μ_B is the Bohr Magneton).

Suhl has predicted that $\frac{\Delta\rho}{c}$ should vary as a universal function $F(\gamma)$ of the parameter γ, where $\gamma^2 = (k_B T)^2 + (c\Delta)^2$. In the presence of an external magnetic field, H, γ should be given by $\gamma^2 = (k_B T)^2 + (c\Delta)^2 + (\mu_B H)^2$. We have verified this result (approximately) for the zero magnetic field case, and for the zero concentration case.[5] Measurements now under way seek to test the behavior of the resistivity at finite concentrations in a magnetic field. In particular, it is expected that Δ may be a function of H.

References

1. M. D. Daybell and W. A. Steyert, Rev. Mod. Phys. 40, 380 (1968).
2. A. J. Heeger, Solid State Physics 23 (1969), 283-411.
3. H. Suhl, Phys. Rev. Letters 20, 656 (1968).
4. M. W. Klein, Phys. Rev. 136, A1156 (1964).
5. M. D. Daybell and Y. K. Yeo, Bull. Am. Phys. Soc. 16, 840 (1971), and to be published.

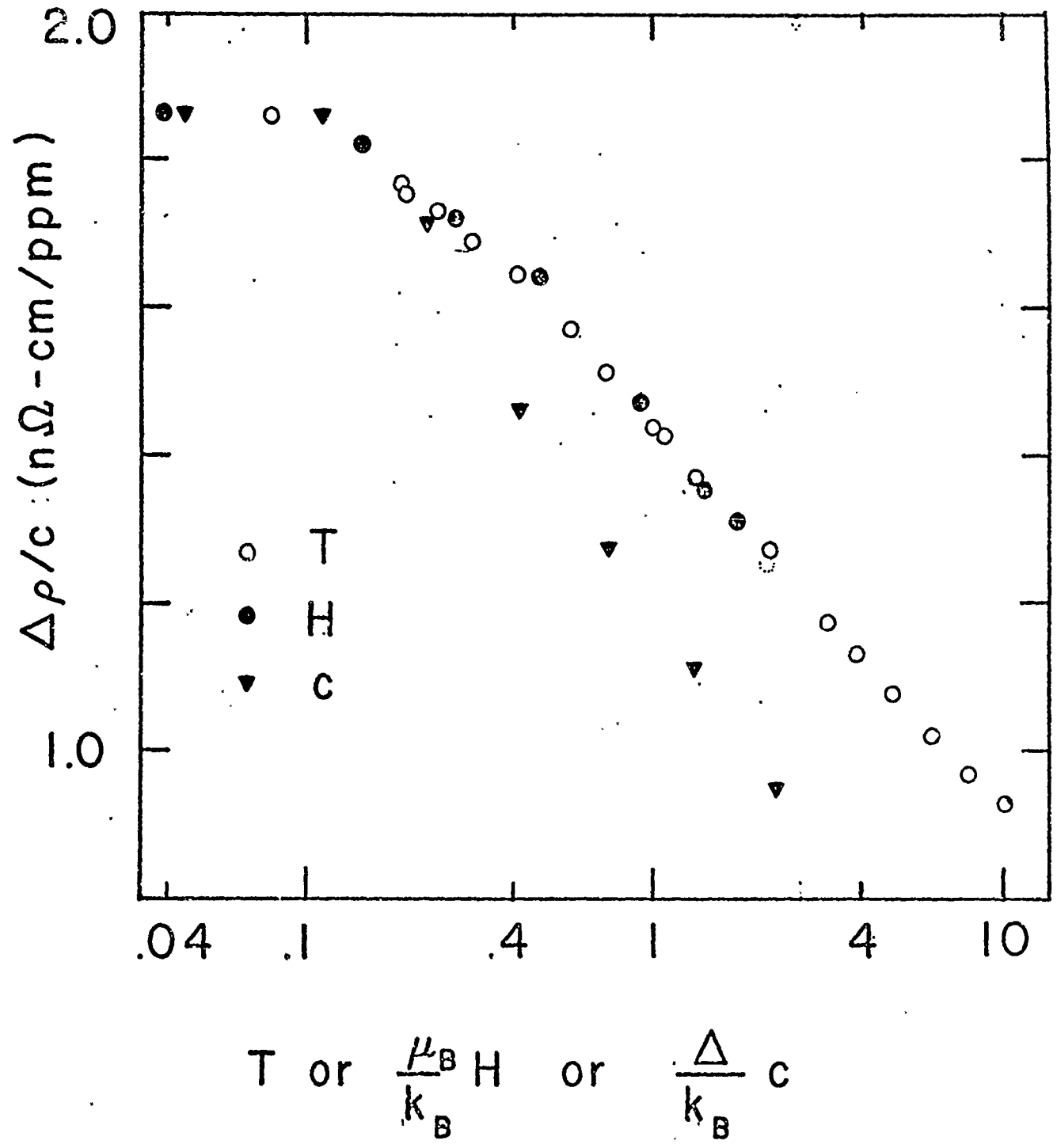
2.0
1.0
Δρ/c : (nΩ-cm/ppm)
T
H
C
.04
.1
.4
1
4
10
T or $\frac{\mu_B}{k_B}$ H or $\frac{\Delta}{k_B}$ C

FIG. 1

1.5.7 Influence of Stress on Precipitation and Coarsening in Alloys

AFOSR-71-2087, Air Force Office of Scientific Research

S. M. Copley

This is a new project just recently initiated. The objective of this research is a more complete understanding of the effect of stress on solid state processes and its concomitant effect on microstructure and properties. Specifically, we are investigating the influence of both applied and residual stresses on precipitation and coarsening in alloys. Our approach involves the application of a uniaxial stress to alloys as they are cooled through their solvus temperature or are annealed at temperatures suitable for coarsening. Electron microscopy is being employed as a tool to determine stress-induced microstructural changes. The observed changes are being interpreted by thermodynamic arguments based on continuum elastic models. Particular attention is being given to the possibility of utilizing stress as a means of producing alloys with novel microstructures and properties.

1.5.8 Rare Earth Metastable Solid Solutions

F44620-71-C-006, Joint Services Electronics Program

R. Wang and S. K. Hsiung

Introduction

It has long been known that direct quenching from liquid state can yield an extensive increase of solid solubility but yet, no principles have been found to describe the solubility limit. Based upon a step reduction of the atomic sizes of the rare earth elements and their similar chemical properties, a systematic study of the rare earth metastable

solid solutions shall contribute information for the metastable solubility limits.

Our research objective is to investigate rare earth metastable hcp solid solutions with Group IV elements and study the solubility limits and structural stabilities so that some controlling factors for governing the formation and the stability of the hcp solid solution can be determined.

Present Status of Work

In our previous reports, we have shown that the investigation of rare earth metastable solid solutions with Group IV elements has yielded interesting results. We have prepared continuous solid solutions by rapid quenching of alloys from the liquid state and the solubility limits were able to be correlated to the c/a ratios of the hcp rare earth metals. Yet, there are two basic questions about those solid solutions still remaining unclear: (1) What are the stabilities of those metastable solid solutions; and (2) Are the metastable hcp solid solutions really different from ordinary supersaturated solid solutions? In order to provide enough evidence to tackle these problems, we are studying the decomposition mechanism of the metastable solid solutions by selecting Er-Zr systems as a typical representative.

Our studies involving electric resistivity measurements, transmission electron microscopy and x-ray diffraction of the as quenched and aged alloys have provided sufficient results to show that the Er-Zr metastable solid solutions are unique in both formation as well as decomposition mechanisms.

From all the characterization methods used here, there are consistent agreements among the observations for the existence of a ready decomposition mechanism occured in as quenched alloys at composition range from ~40 at % Zr to 70 at % Zr. From the measurement of the temperature coefficient, the ordering by the formation of clusterings in this composition range is revealed. With

the reduction in resistivity, it is possible to conclude that between the composition of 40 ~ 70 at % Zr, a pre-precipitation phenomena occurs in as quenched alloys. The activation energy obtained from the experimental results was found to be close to the energy of formation of vacancies. This suggests that the pre-precipitation process is associated with a migration of vacancies.

As the decomposition is carried on at elevated temperatures, the metastable solid solution has reformed precipitates through the nucleation and growth mechanism. The decomposed solid solutions, therefore, have solid solubilities corresponding to equilibrium values. Because the decomposition has to be carried through nucleation and growth mechanism, it is possible to explain why the metastable solid solutions exhibit high thermal stability ($< 350^{\circ}C$).

It is obvious that metastable hcp solid solutions formed by rapid quenching from liquid state are unique compared to the supersaturated solid solutions prepared at solid state. As illustrated in Fig. 1, the formation theory for non-equilibrium phases is much more complex than for equilibrium phases. We have demonstrated that the c/a ratios of the rare earth elements have played an important role in the formation of rare earth metastable hcp solid solutions.

1.5.9 Thermoelectric Properties of New Materials in Metastable Crystalline and Amorphous State

F44620-71-C-006, Joint Services Electronics Program

R. Wang and S. K. Hsiung

Introduction

In the past four years there has not been much progress in developing thermoelectric materials. Continuous improvement in the

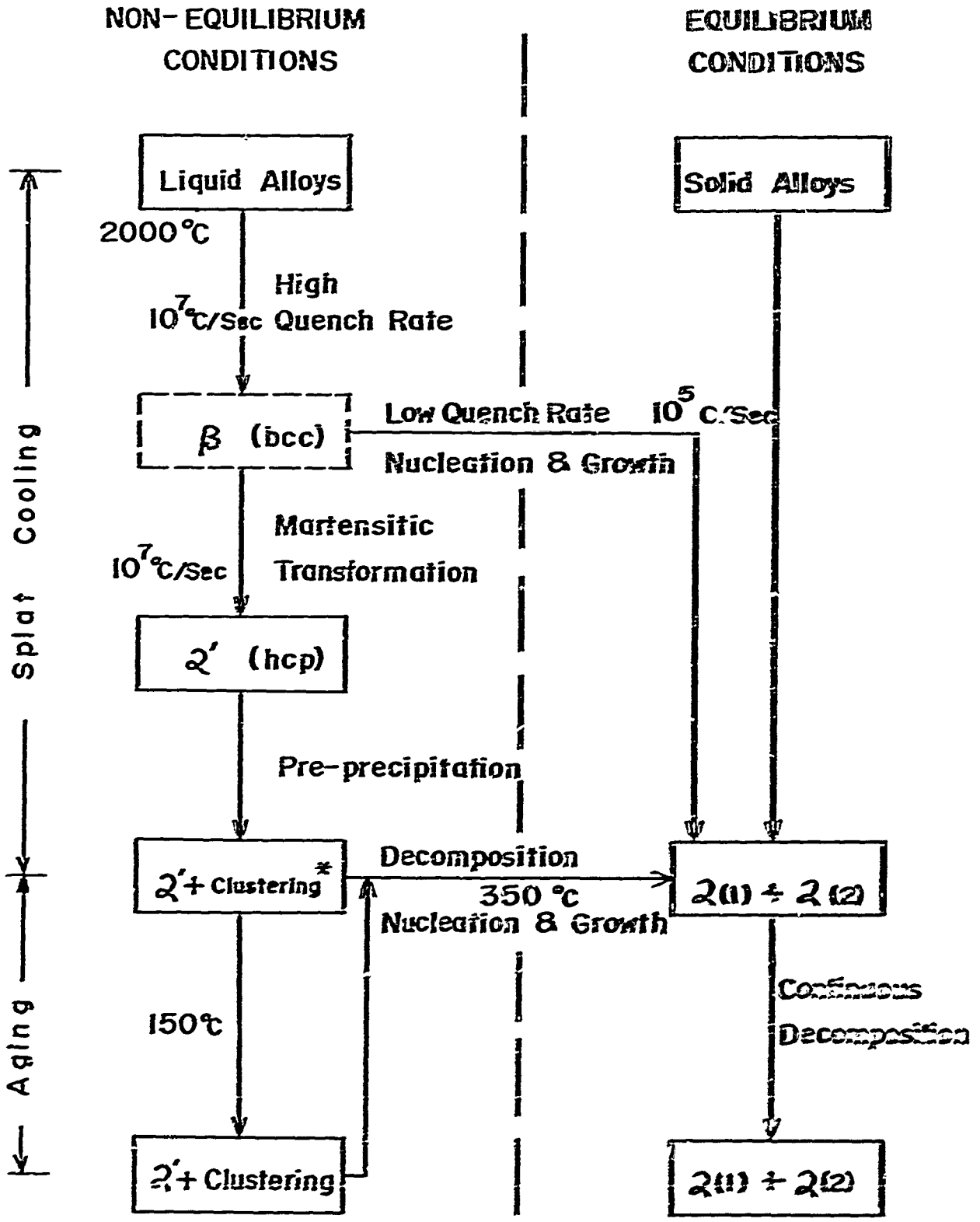

* Formation depends on system or composition

thermoelectric cooling or heating technique is important for the development of modern technology especially as applies to weapon development and space programs. Our research approach is to investigate the synthesis of new metastable crystalline phases and amorphous solids by rapid quenching from liquid state. Measurements of the thermoelectric properties and figure of merits are carried out for the structure-sensitive properties.

Present Status of Work

The recently initiated material research program contains the synthesis of new materials by rapid quenching alloys from the liquid state, characterization of the phase stability and homogeneity by x-ray diffraction and electron microscopy followed by the measurement of their thermoelectric properties. In the past few months, we have concentrated on the synthesis of single-phase metastable alloys and a specimen preparation technique. The optimum composition ranges for the preparation of single-phase materials have been studied for alloy systems of In-Sb, In-Te, Pb-Sb and Ge-Sb. We have found that the composition ranges for single-phase materials are much narrower than the reported values.[1] The metastable materials were first tested for thermal stabilities. Measurements of their thermoelectric properties and figure of merits are currently in process. Detailed results would be reported after completing more measurements. In general, compared to the same alloys in equilibrium conditions, the metastable phases have much higher figure of merits.

Reference

1. B. C. Giessen, "Constitution of Non-equilibrium Alloys After Rapid Quenching from the Melt," in "Developments in the Structural Chemistry of Alloy Phases," Giessen, ed., Plenum Press, New York (1969), pp. 227.

I.6 SOLID STATE DEVICES

I.6.1 Microwave Acoustics and Solid State Devices

AF-AFOSR, Joint Services Electronics Program
GK-5751, National Science Foundation
N00014-67-A-0269-0018, Office of Naval Research

K. M. Lakin, W. Bradford, D. Penunuri, K. Wang

Introduction

The study of microwave acoustics and related solid state devices involves sound generation and propagation in the VHF to microwave frequency ranges where the acoustic wavelengths are measured in microns. One area of microwave acoustics which has recently attracted much interest is that related to the surface or Rayleigh mode of elastic wave propagation and various modes which exist when layered thin film structures are present.

The research work here at USC involves theoretical and experimental investigations related to elastic wave propagation in piezoelectric and non-piezoelectric materials as well as layered structures, new devices and device configurations, materials evaluation for surface wave devices, and acoustoelectric interactions which give rise to traveling wave amplification.

A. Propagation Studies, Numerical Calculations

K. M. Lakin, D. Penunuri

The boundary value problem associated with surface wave and layered wave propagation has been solved using numerical techniques. These techniques have been applied to several crystals of interest for delay line and surface wave amplifier considerations. Figure 1 shows the results for the (OT12) plane of sapphire. Similar results have been

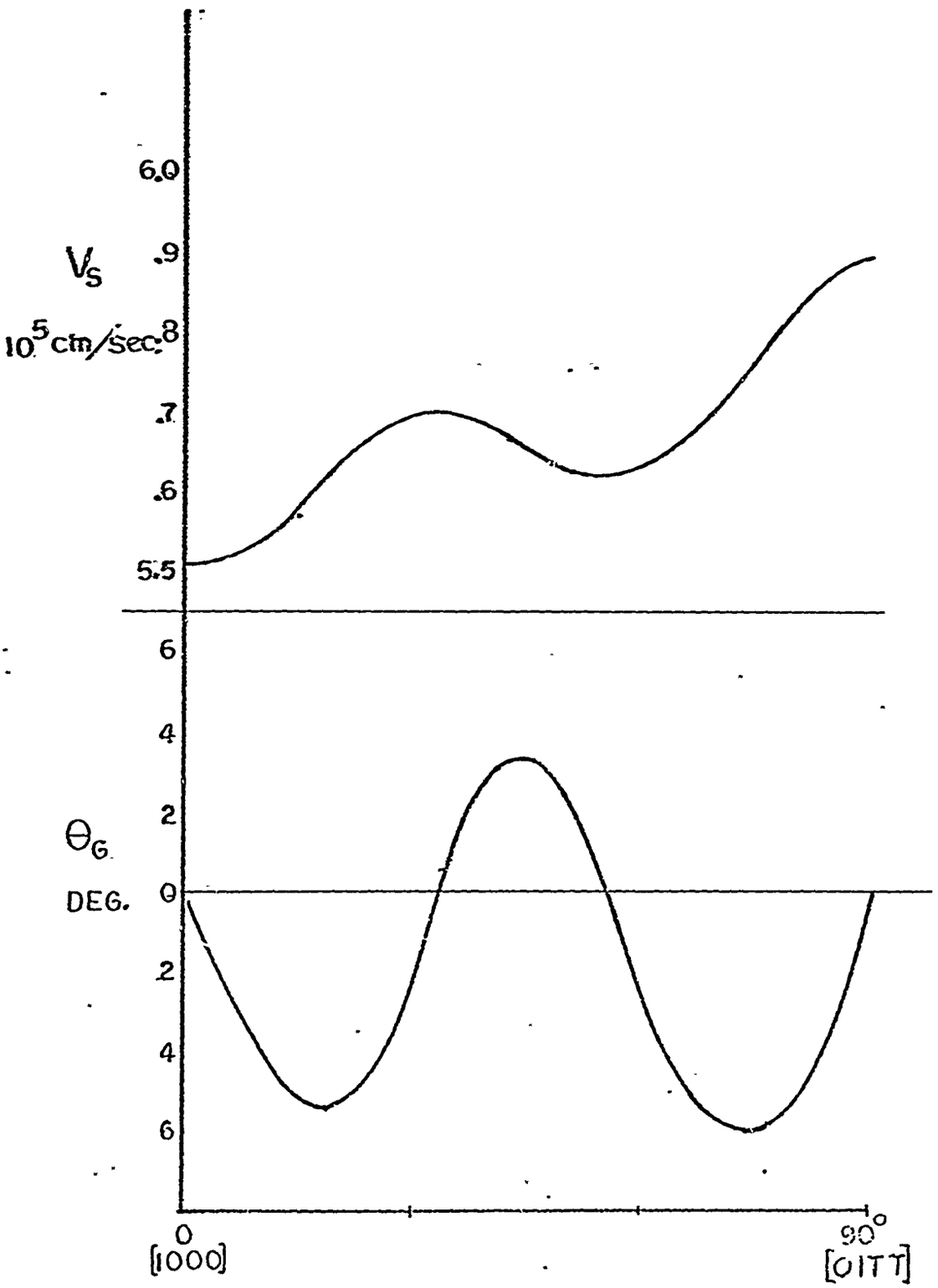

Figure 1: Numerically calculated surface wave velocity and powe: flow angle versus direction in (0 1 $\bar{1}$ 2) piane of sapphire. Similar results are obtained for the (0 1 $\bar{1}$ 2) plane.

obtained for the (01T2) plane except that "leaky" surface waves have been found. Along the [01TT] direction the normal surface wave mode is found.

The layered structure of ZnO on (01T2) sapphire has also been studied in some detail and shows the expected dispersive wave propagation of a low velocity material on high velocity substrate.

B. Epitaxial Film Growth

K. M. Lakin, K. Wang

Epitaxial films of AlN on sapphire, AlN on Si and Si on sapphire have been grown by the chemical vapor phase process. The commercial vertical reactor was modified to accept low temperature reaction gases in the AlN growth system. Figure 2 shows the orientation relations for the epitaxial layers and sapphire substrates.

The AlN films are grown at a deposition temperature of 1250°C using the trimethylaluminum ammonia process. Growth rates of 0.5 μm/min have been obtained for films up to 5μm thick on sapphire. Grown on (111) Si gives a [0001] AlN orientation with crocked surfaces for films greater than 0.5 μm thickness. The AlN/Al_2O_3 films showed strong piezoelectric coupling and were of single crystal structure as observed by reflection electron diffraction.

Work will continue on the epitaxial film growth with efforts directed toward improved surface finish.

C. Non-linear Space Charge Waves

A general approach to the problem of non-linear space charge waves resulted in a Fourier analysis approach to solve the non-linear differential equations. The results of this analysis are still being evaluated and more economical (computer time) methods are being sought.

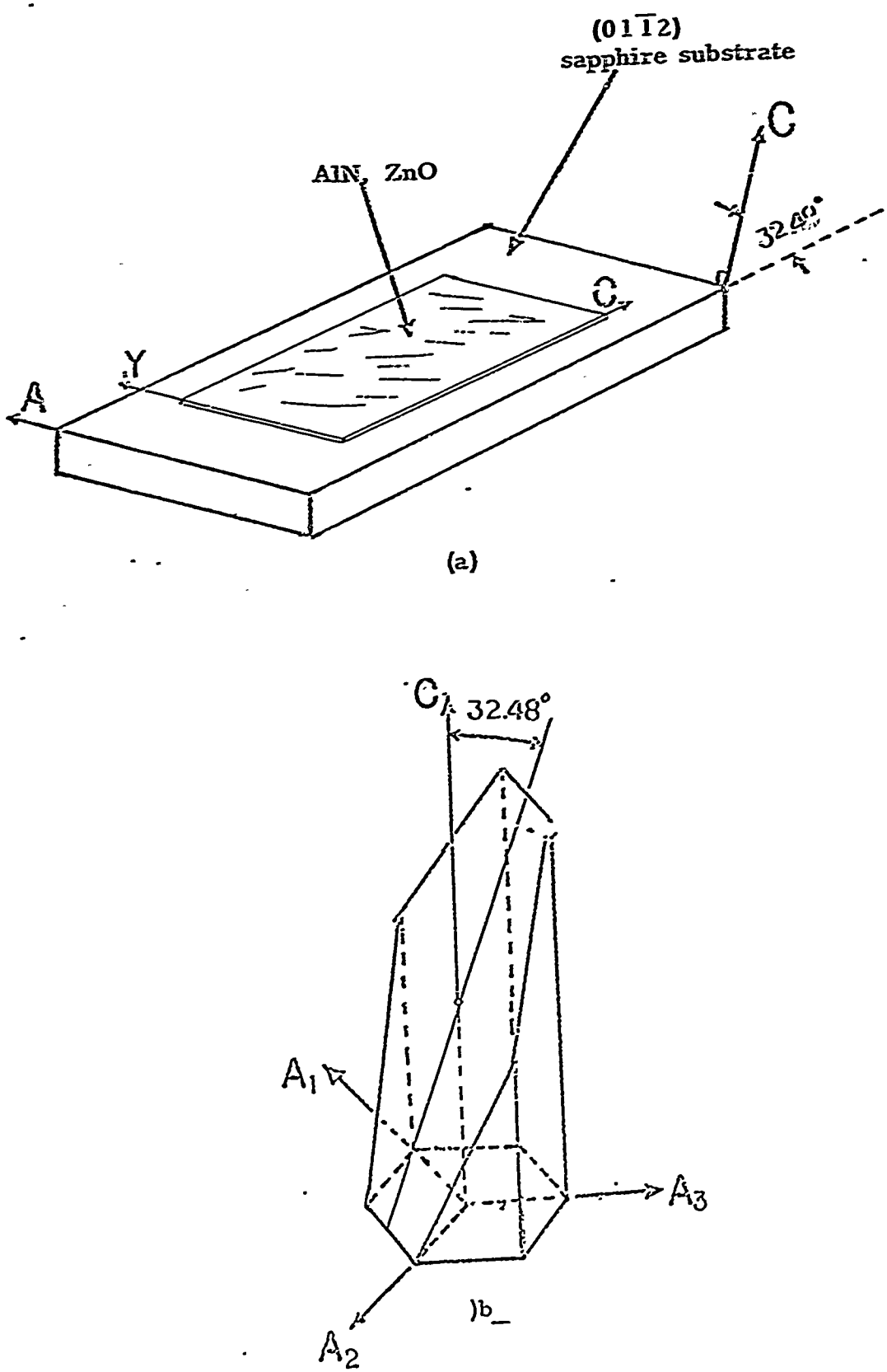

Figure 2: Orientational relationships for AlN or ZnO film and sapphire substrate; a) AlN or ZnO relative to sapphire, b) (0 1 $\bar{1}$ 2) plane definition in sapphire.

2. PLASMAS AND APPLIED ELECTROMAGNETICS

2.1 Analytic Studies of Reflector Antennas (Radar Cross-Section of Truncated Paraboloid)

F44620-71-C-0067, Joint Services Electronics Program

W.V.T. Rusch, Fu-Lai Chu

Introduction

a. Background: The radar signature of a paraboloidal reflector is useful for remote sensing applications. This interesting and valuable result is currently within the state of numerical techniques of diffraction theory although it has apparently not been reported in the literature.

b. Objective: To obtain the radar cross-section of a paraboloidal reflector using the methods of physical optics.

c. Approach: Numerical integration of the scattering integral using physical optics to approximate the currents induced by the incident wave.

Present Status of Work

The back-scattered field from a paraboloid immersed in an incident, linearly polarized wave which is polarized in the plane of scan is:

$$E_{s\theta} = -j2\pi \frac{E_o e^{-jkR}}{\left(\frac{R}{\lambda}\right)} \left\{ \cos\alpha \int_{\theta_o}^{\pi} e^{j2k\rho\cos\alpha\cos\theta'} J_o(2k\rho\sin\alpha\sin\theta') \left(\frac{\rho}{\lambda}\right)^2 \sin\theta' d\theta' - j\sin\alpha \int_{\theta_o}^{\pi} e^{j2k\rho\cos\alpha\cos\theta'} J_1(2k\rho\sin\alpha\sin\theta') \cot\left(\frac{\theta'}{2}\right) \left(\frac{\rho}{\lambda}\right)^2 \sin\theta' d\theta' \right\} \quad (1)$$

where ρ is the polar distance from the origin (focus) to the paraboloidal reflector and α is the angle of incidence (see Figure 1). The effects of aperture blocking or feed reflectivity have not been included. An identical result is obtained for the backscattered component $E_{s\varphi}$ when the incident field is polarized perpendicular to the plane of scan. The corresponding radar cross-section is then

$$\sigma = 4\pi R^2 \left| \frac{E_{s\theta}}{E_0} \right|^2 \tag{2}$$

In the special case of normal incidence the back-scattered field from physical optics becomes

$$\bar{E}_s = E_o \bar{a}_y \frac{e^{-jkz}}{z} f e^{-j2kf} \left[1 - e^{j\frac{kf}{8}\left(\frac{D}{f}\right)^2} \right] \tag{3}$$

Using special edge diffraction coefficients of Ufintsev[1] the field due to the localized edge currents is

$$\bar{E}_{edge} = E_o \bar{a}_y \frac{e^{-jkz}}{z} f e^{-j2kf} e^{j\frac{kf}{8}\left(\frac{D}{f}\right)^2} \left[1 - \sqrt{1 + \frac{d^2}{16 f^2}} \right] \tag{4}$$

Superimposing these two fields yields the total back-scattered field at nose-on incidence

$$\bar{E}_{TOTAL} = E_o \bar{a}_y \frac{e^{-jkz}}{z} f e^{-j2kf} \left\{ 1 - \sqrt{1 + \frac{d^2}{16 f^2}}\, e^{j\frac{kf}{8}\left(\frac{D}{f}\right)^2} \right\} \tag{5}$$

This result is identical to the results obtained by Laxpati, Smith, and Uslenghi[2].

The normalized radar cross-section of the reflection is plotted in Figure 2 as a function of the angle of incidence for three

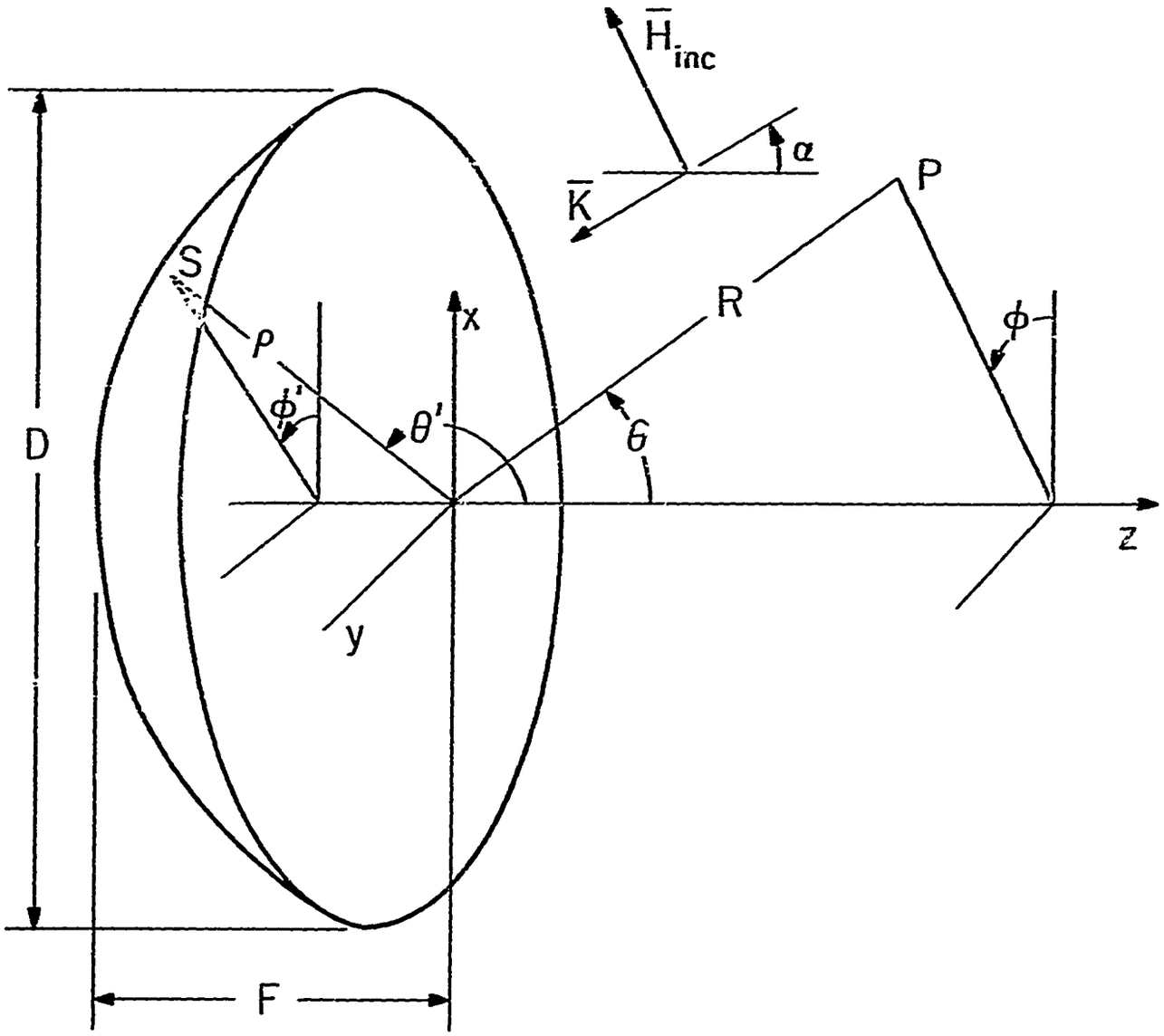

Fig. 1: Geometry of H-scan

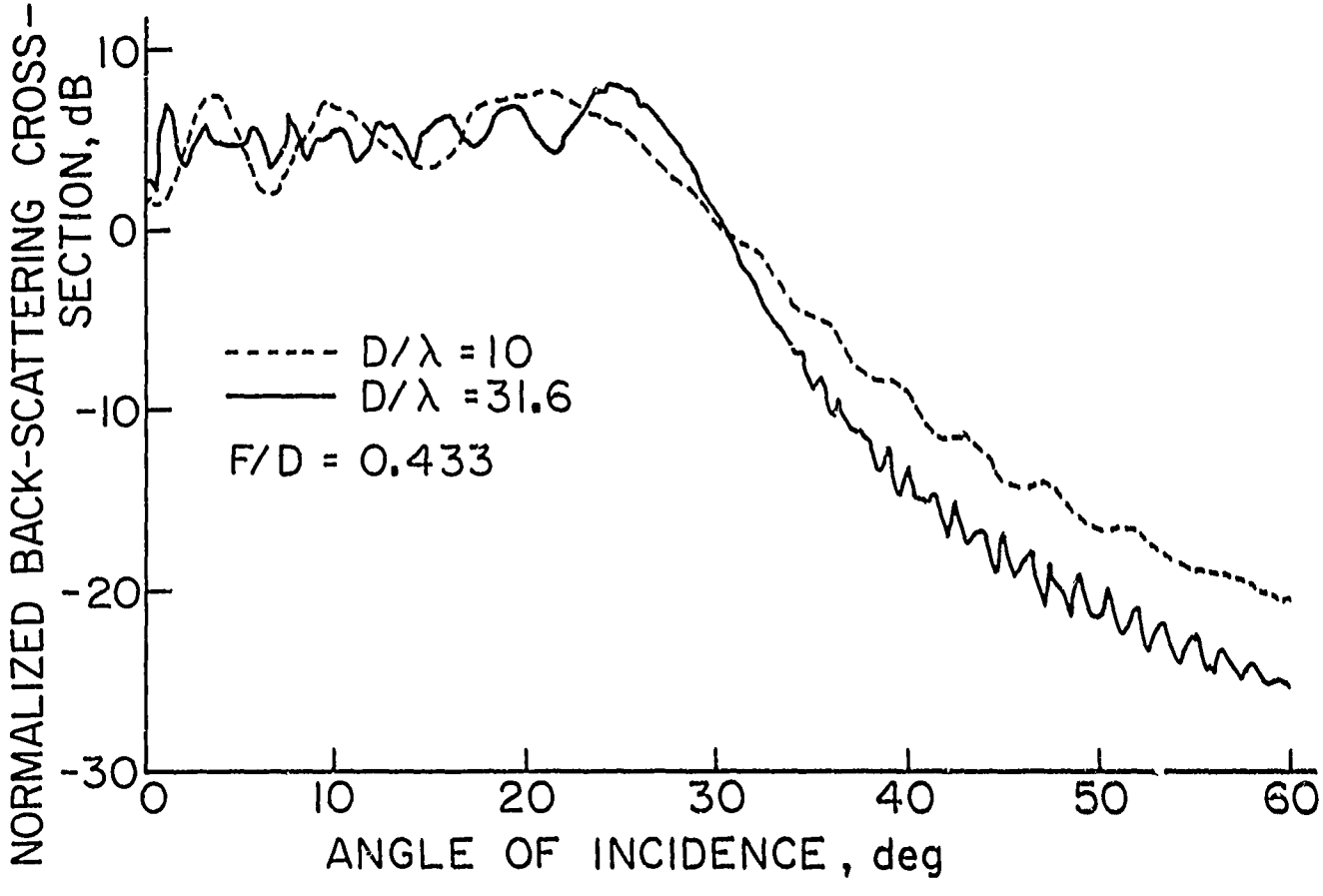

Fig. 2: Normalized backscattering cross section versus angle of incidence

different diameter/wavelength ratios and an f/D value of 0.433. The backscattering is approximately isotropic until about 30-degrees incidence, beyond which the cross section decreases monotonically. (It should be noted that the rear of the reflector was not illuminated for the angles of incidence shown.) The cross-section appears to be the superposition of the geometric, or specular return, which drops to zero at 30° for F/D = 0.433, and two or more edge rays.

References

1. P. Ia. Ufimtsev, "Approximate Computation of the Diffraction of Plane Electromagnetic Waves at Certain Metal Bodies," Sorret Physics, Part 2, July-Dec. 1957, pp. 1708-1718.

2. S. R. Laxpati, T. M. Smith, and P.L.E. Vslenghi, "The Radar Cross Section of a Parabolic Dish," URSI Symposium Digest, UCLA, 21-23 September 1971, pp. 65-66.

3. INFORMATION SCIENCES

3.1 CONTROL SYSTEMS

3.1.1 Stochastic Control

AF-AFOSR 69-1622, Joint Services Electronics Program

D. D. Sworder

Many large industrial systems have several different modes of possible operation. The dynamic characterization of such a system at any specific point in time will depend upon the operational status of a numbe· of individual components or subsystems. For example, the efficiency and stability of electrical generation and distribution system may change radically when an important generating station is lost from services because of an unexpected failure.

An initial study of problems of this type was that of Ratner and Luenberger[1]. A linear system subject to sudden stochastic parameter changes was considered. These changes were thought of as failures in elements within the system. The authors of Ref. (1) sought to find the optimal control and the best time to repair the failures when the number of repair units was limited. This combined control and repair problem proved to be rather intractable.

In Ref. (2) the policy of immediate repair or replacement was investigated. Conditions which guarantee optimality were derived and the corresponding optimal control policy was deduced.

In these references a number of assumptions were made to simplify the analysis. It was supposed that repair took place instantaneously and that there was always a work crew available to do

the work. The initial inventory was specified and no possibility of restoring a depleted stock of replacement units was admitted. Neither the cost of the repair crews nor the storage costs associated with the inventory were included in the performance index.

When some of these structural assumptions are relaxed, new problems are introduced. If repair can take considerable time to accomplish, several different failures can occur before any repairs are completed. The number of available work crews will then determine the speed with which repair can be accomplished. The workers are useful only if there are sufficient renewal units in inventory to permit them to begin repair when a failure occurs. The inventory description used in References (1) and (2) will not be adequate if time interval over which control is exercised is long, for in this event the number of replacement units would too soon be exhausted. This suggests that a policy of restocking the inventory must also be specified for the system.

The criterion functional for a system as described above must be made more complicated to account for the various costs associated with different decisions. There are costs related to the dynamic response of the controlled system. The wage rates of the repairmen determine the labor cost. There are costs for each replacement unit which are incurred when a purchase order is placed, and there are storage costs associated with the replacement unit in the interval between the time of delivery to the purchaser and the time of use in system.

The engineer in charge of such a system must not only determine the best controller to use, but he must also select the correct number of repairmen and the best inventory policy. Because the costs associated with each decision depend fundamentally on the other decisions, system design decisions are often made on the basis of "trade-offs." Thus, more repair crews improve dynamic performance by reducing "down-time," but cost more money in labor charges.

In the past reporting period an algorithm has been derived for finding the optimal control, repair, and inventory policies for a linear system. Costs are assigned to dynamic performance, labor, inventory storage, and purchase of parts. Both finite planning horizon and infinite planning horizon problems are considered. When the system has certain stationarity properties the latter class of problems is relatively easy to solve.

To test computational feasibility of the algorithm, a simple linear system was considered. It was assumed that labor and inventory costs are proportional to a normalized base labor wage rate. For a specified purchase price for renewal units, it was shown that optimal policy is a piecewise constant function of the wage rate. For wage rates below an easily determined limit several work crews are used. As wages are increased a point is reached where certain workers are eliminated. If wage rates exceed a certain bound, it is expedient to simply operate the system in a degraded mode and eliminate all costs associated with repair.

References

1. R. S. Ratner and D. G. Luenberger, "Performance-Adaptive Renewal Policies for Linear Systems," IEEE Trans. Automatic Cont., Vol. AC-14, pp. 344-351, August 1969.

2. D. D. Sworder, "Uniform Performance-Adaptive Renewal Policies for Linear Systems," IEEE Trans. Automatic Cont., Vol. AC-15, pp. 581-583, October 1970.

3.1.2 Traffic Responsive Control Systems

GK-24520, National Science Foundation

N. Nahi and H. J. Payne

3.1.2.1 Freeway Traffic Control and Surveillance

H. J. Payne and L. Isaksen

Freeway traffic can be regulated by controlling the traffic entering the freeway through on-ramps. The development of effective ramp control procedures depends upon the development of adequately descriptive models of freeway traffic and the determination of rational objectives. One traffic control problem, that of regulating traffic to maintain conditions near some set of nominal conditions, can be formulated as a linear system, quadratic cost problem. A design technique based on this approach has been developed and was reported at a conference.[1] Further details of a design for a segment of the San Diego Freeway in Los Angeles are available in reference (2).

Present efforts are concerned with (1) a second detailed design for a segment of the Hollywood Freeway in Los Angeles which will be implemented in an experimental project in cooperation with personnel of the California Division of Highways; and (2) identification of parameters of the freeway traffic model based on digitized aerial freeway data.

References

1. Payne, H. J. and L. Isaksen, "Systems Problems in Freeway Traffic Control and Surveillance," presented at the 1971 ASME-ASCE National Transportation Meeting, July 25-30, Seattle, Washington.

2. Isaksen, L., "Suboptimal Control of Large Scale Systems with Application to Freeway Traffic Regulation," unpublished Ph.D. dissertation, Department of Electrical Engineering, University of Southern California, 1971.

3.1.2.2 Solution of Large Order Lyapunov Equations

G.G.L. Meyer and H. J. Payne

The numerical solution of the Lyapunov equation

$$PA + BP = C \qquad (1)$$

for large order matrices remains as a difficult problem. Presently available techniques[1] are generally limited to matrices of order less than 20 x 20.

A new iterative procedure which converges to the solution of (1) has been developed which requires at each elemental step approximately 4n multiplications for matrices of order nxn. Application to large order matrices, therefore, is attractive. A paper[2] is presently in preparation.

References

1. Rothschild, D., and A. Jameson, "Comparison of four numerical algorithms for solving the Liapunov matrix equation", Int. J. Control, Vol. 11, No. 2 (1970), pp. 181-198.

2. Meyer, G.G.L. and H. J. Payne, "An Iterative Method of Solution of the Lyapunov Equation".

3.1.3 Bayesian Recursive Image Estimation

NGL 05-018-044, National Aeronautics and Space Administration

F08606-72-C-0008, Advanced Research Projects Agency

N. E. Nahi and T. Assefi

Certain classes of images are best characterized by statistical procedures, such as specifying the mean and correlation

functions associated with the random process representing the brightness level. A procedure for recursively estimating such images, when they are corrupted by additive noise, is introduced in this paper. The image estimation here refers to the problem of image enhancement, i.e., the attempts to eliminate the additive noise from the noisy observation. The input to the estimator is the output of a horizontal line scanner with uniform speed. The procedure is to first develop a dynamic model possessing a response characteristic which matches that of the scanner output in a statistical sense. These models will assume the form of an ordinary differential or difference equation with white noise input. Since the image is a two-dimensional object while the scanner output is only one-dimensional, the model must exhibit the vertical correlation of the image. This reveals itself in the oscillatory nature of the model responses. Although the image is assumed to have a stationary (two-dimensional) autocorrelation function, the scanner output is nonstationary due to the scanner's periodic movement. In this paper, however, this edge effect is averaged out, resulting in a constant coefficient model. It is suspected that this approximation does not have significant effect on the optimality of the estimator in most cases. Development of a nonstationary model is currently under investigation.

After the appropriate model--a vector valued difference equation with the solution representing a vector Markov process--is developed, the minimum mean square estimate of the image is obtained by utilization of a Kalman filter. Since the image estimation is an interpolation problem, two successive runs over the observation are performed in opposite directions and the resultant estimates are averaged. These results are reported in reference (1) where examples are included for illustration.

Reference

1. "Bayesian Recursive Image Estimation," N. E. Nahi, T. Assefi, Proceedings of Two Dimensional Digital Signal Processing Conference, Columbia, Missouri, Oct. 1971.

3.1.4 Decision-Directed Adaptive Recursive Estimators

NGL 05-018-044, National Aeronautics and Space Administration

N. E. Nahi and B. M. Schaefer

In recent years, minimum-variance recursive estimators, such as the Kalman filter, have been used successfully in many practical applications. However, a common problem, known in the literature as the divergence phenomenon, is often encountered in these applications. Divergence is said to occur when the error covariance calculated by the estimator becomes inconsistent with the actual error covariance.

Previous methods of dealing with this problem have involved limited memory filtering or simultaneous estimation of random process statistics. The method investigated under this study is different in that the state model and statistics are accepted as given; the form of the optimal estimator is used, but a constant check is made on the consistency of the calculated and actual error covariances[1], [2].

The method is independent of the source of error, whether it be inaccuracies in the system model, incorrect values of the a priori and random process statistics, approximations required in the case of nonlinear systems, or computational round-off. A test for inconsistency and an adaptive decision-directed procedure for adjusting the calculated covariance, shown to be optimal in a certain sense, are discussed. Several simulated examples, in which inconsistencies in the calculated and actual error covariances exist, show a significant improvement in the performance of the estimator when the given procedure is appended.

References

1. "Decision-Directed Adaptive Recursive Estimators; Divergence Prevention," N. E. Nahi, B. M. Schaefer, IEEE Transactions on Automatic Control, Feb. 1972.

2. "Adaptive Decision-Directed Recursive Estimators," N. E. Nahi, B. M. Schaefer, Proceedings of 1971 Joint Automatic Control Conference, St. Louis, Missouri, Aug. 1971.

3.1.5 Sequential Error Detection for Nonlinear Estimators

NGL-05-018-044, National Aeronautics and Space Administration

N. E. Nahi and B. M. Schaefer

Most nonlinear estimators, such as the extended Kalman filter, require approximation for the recursive computation of the error covariance. Although these approximations often work quite well in practice, they can cause the actual error covariance to become inconsistent with the calculated covariance. Unfortunately, an analysis of the errors caused by such approximations is as untractable as solving the original optimal problem itself, namely, deriving the complete density function. It is important that the actual and calculated covariances be as consistent as possible because the optimal weighting of observations is dependent on the actual covariance, and also because the calculated covariance is generally used as a measure of the quality of the estimate. In this work a paper is introduced for sequentially testing the consistency of the actual and calculated error covariances.[1] It should be noted that this method is useful for linear filters as well, where the inconsistency may be caused by modeling inaccuracies.

Reference

1. "Sequential Error Detection for Nonlinear Estimators," N. E. Nahi, B. M. Schaefer, Proceedings of Second Symposium on Nonlinear Estimation Theory, San Diego, California, Sept. 1971.

3.1.6 Design of Optimal Probing Signals for Vector Parameter Estimation

NGL 05-018-044, National Aeronautics and Space Administration

N. E. Nahi and G. A. Napjus

In the design of optimal estimators it is common to consider some function of the error covariance matrix, usually the trace, as a criterion of optimality. In the design of optimal inputs, or probing signals, for parameter estimation it is more natural to consider functions of the Fisher information matrix instead.

The input which maximizes the Fisher information measure for efficient estimation of a scalar parameter also provides the minimum error variance. The information is thus a logical choice for the optimality criterion in scalar problems. No such obvious choice is apparent for vector parameter estimation, however. In this paper we examine and compare a number of performance measures and select a useful criterion. The design of an optimal probing signal using this criterion is shown to be equivalent to an optimal control problem in which certain equality constraints must be satisfied. This problem may be solved by conventional techniques of deterministic or stochastic optimal control. The above results appear in reference (1).

Reference

1. "Design of Probing Signals for Vector Parameter Estimation," N. E. Nahi, G. A. Napjus, Proceedings of IEEE Decision and Control Conference, Miami, Florida, Dec. 1971.

3.1.7 Bounding Filters in the Presence of Inexactly Known Parameters

NGL 05-018-044, National Aeronautics and Space Administration

N. E. Nahi, I. M. Weiss

Kalman-Bucy (K/B) filtering assumes that the linear dynamic system and corresponding noise statistics are exactly known. When this information is only approximately known, an optimum bounding filter can be designed for specific versions (steady state time-invariant with scalar observations) of the K/B problem. A system is designed in which the actual estimation error covariance is bounded by the covariance calculated by the estimator. Therefore, the estimator obtains a bound on the actual error covariance which is not available and also the apparent divergence is prevented. The bounding filter can be designed to be of lower order than the original system, however, this results in a higher error covariance. Conditions for the design of the optimum (minimum mean square error) bounding filter within a permissible class are derived.

Since the specific K/B problem is formulated as an equivalent Wiener filtering problem, therefore, all the results are applicable to the design of bounding filters for Wiener problems. The design of a bounding filter is illustrated by an example. The above results appear in ref. (1).

Reference

1. "Bounding Filters in the Presence of Inexactly Known Parameters," N. E. Nahi, I. M. Weiss, Proceeding of IEEE Decision and Control Conference, Miami, Florida, Dec. 1971.

3.1.8 Models of Human Driver Behavior in Car Following

NGR-05-018-022, National Aeronautics and Space Administration

G. Burnham, G. A. Bekey and A. Phatak

This study is concerned with the human operator in one of his most common and most hazardous quasi-compensatory, quasi-pursuit tracking tasks: following the car in front of him. The objective is to determine the sensitivity of propagated disturbances in single-lane platoons of automobiles and the major parameters of both driver and vehicle.

Mathematical models of hypothetical car-following situations have been available since the work of Pipes[1] and Herman[2]. However, previous studies have been concerned with problems of predicting traffic flow, improving the man-machine system interface and automating the driving task.

The car following model used in this project is based on the hypothesis that the human operator, while following a lead car, controls the velocity of his vehicle by using only the car's accelerator, that is the human operator output is accelerator position. The vehicle dynamics are represented by a first order lag. The dynamics of the vehicle change substantially when brakes are applied and for this reason braking has not been included in our model so far. (It will be added later.)

The input to the human operator is assumed to be a weighted sum of closing velocity difference and separation distance information, between the operator's vehicle and the vehicle directly in front of him. The human operator is represented by a gain, time delay and a first order lag.

A number of identical blocks can be interconnected, thus obtaining an n-car following model. The model is presently implemented

using continuous system simulation languages (MOBSSL on the IBM 360/44 and CSMP on the 360/65).

Preliminary results obtained from the model are encouraging. Propagation of disturbances following an acceleration pulse have been computed as well as their dependence on the parameters in the driver model. Plans for model evaluation using expressway data will be presented.

References

1. Pipes, L. A., "Car-following Models and the Fundamental D Diagram of Road Traffic," Transportation Research, v. 1, pp. 21-29, 1967.

2. Herman, R. E., E. W. Montroll, R. B. Potts, and R. W. Rothery, "Traffic Dynamics: Analysis of Stability in Car Following," Operations Research, v. 7, pp. 86-106, 1959.

3.2 COMMUNICATIONS SYSTEMS

3.2.1 Communication, Synchronization and Tracking Systems

F44620-71-C-0067, Joint Services Electronics Program
DA-ARO-D-31-124-70-G51, U.S. Army Research Office - Durham

I. S. Reed, R. A. Scholtz, and C. L. Weber

Theoretical studies of several difficult problems in communication system design are now underway.

(1) Frequency Tracking

The study of frequency tracking in the presence of signal fading and additive Gaussian noise, reported in the previous semiannual progress report is almost completed. The final results are approximately optimal MMSE and MAP estimators of the frequency process, a linearized analysis of estimation error, and simulation results for the estimation error of the general nonlinear estimator (see Reference 1).

(2) Multipath Channel Problems

A tenable receiver designed to operate in conjunction with the random multipath channel has been proposed. When intersymbol interference is present, the implementation of the optimal receiver is impractical. These implementation difficulties are alleviated, to a large extent, by employing the proposed suboptimal receiver, which utilizes previous detector decisions in the receiver.

The transmitter continuously sends one of M equally likely signals of finite duration through the multipath channel. The multipath return is assumed to be sufficiently corrupt so that no direct attempt is made to use it to enhance the decision making at the receiver.

These decisions are made via the specular path. The decision directed receiver is proposed to overcome the salient drawbacks associated with implementing the optimal receiver.

The exact performance of the decision-directed receiver is determined for the steady-state probability of correct decision. The resulting performance of this type of receiver is far superior to the standard correlation receiver when 20% or more of the transmitted energy propagates via the extraneous paths (see Reference 2).

(3) On-Off Communications

With the increasing interest in optical communications and with the availability of low cost high power r.f. pulse sources, it seems logical that some attempt to definitively state the capabilities of an on-off phase-incoherent communication system should be made. Such a system may compete well with a coherent constant power system when complexity or cost are taken into account. So far we have determined error probability expressions for a PCM system, and have programmed these as a function of basic system parameters. Presently under consideration are methods for choosing the system parameters, taking into consideration synchronization problems as well as error probabilities.

References

1. T. M. Rodriguez, R. A. Scholtz, and C. L. Weber, "Frequency Tracking Loop Study," Fifth Hawaii International Conference on System Sciences.

2. R. M. Fielding and C. L. Weber, "A Digital Decision-Directed Receiver for the Multipath Channel," Fifth Hawaii International Conference on System Sciences.

3.2.2 Performance Measures for Transform Data Coding and Multidimensional Rotations for Feature Selection

GK 20258, National Science Foundation
F 08606-72-C-0008, Advanced Research Projects Agency

H. C. Andrews

The rate distortion function has been investigated for its potential as a yardstick in comparing data compression and feature selection mechanisms[1,2]. For a basis restricted assumption[3], the rate distortion function can be evaluated for a mean square error fidelity criterion and a Gauss Markov process. For two such processes (1st order and specialized 2nd order) the curves are presented below. The corresponding covariance matrices are given by

$$[\phi_1] = \left[\rho^{|r-s|}\right] \qquad 0 < \rho < 1$$

$$[\phi_2] = \left[\frac{1+(-1)^{|r-s|}}{2}\,\rho^{|r-s|/2}\right] \qquad 0 < \rho < 1$$

where r and s index the rows and columns respectively. The curves in Figures 1 and 2 indicate that for such processes and such a fidelity criterion, the Fourier, Walsh, Haar and identity transforms are decreasingly efficient respectively compared to the optimum Karhunen-Loeve transform for data compression and feature selection. For a given distortion quantitative values can be assigned each transform process. The implications from the curves are that the Fourier and Walsh transforms are not too poor a substitute for the optimum decorrelating transform.

References

1. Andrews, H. C., "Some Unitary Transformations in Pattern Recognition and Image Processing," IFIP 1971 Congress, Ljubljana, Yugoslavia (August, 1971).

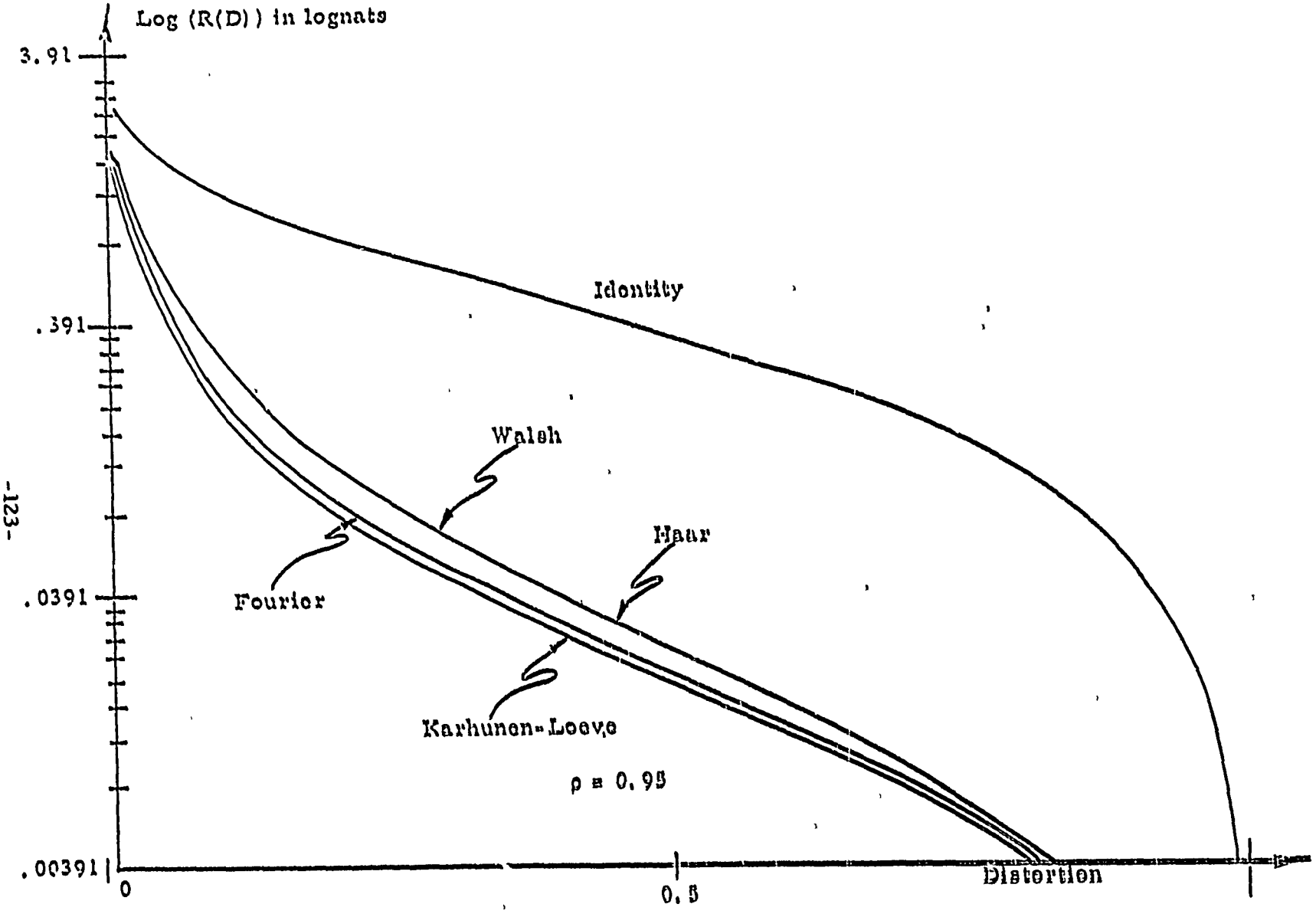

FIGURE 1. Rate Distortion for Various Transforms for First-Order Gauss-Markov Process ($\rho = .95$, $N = 256$)

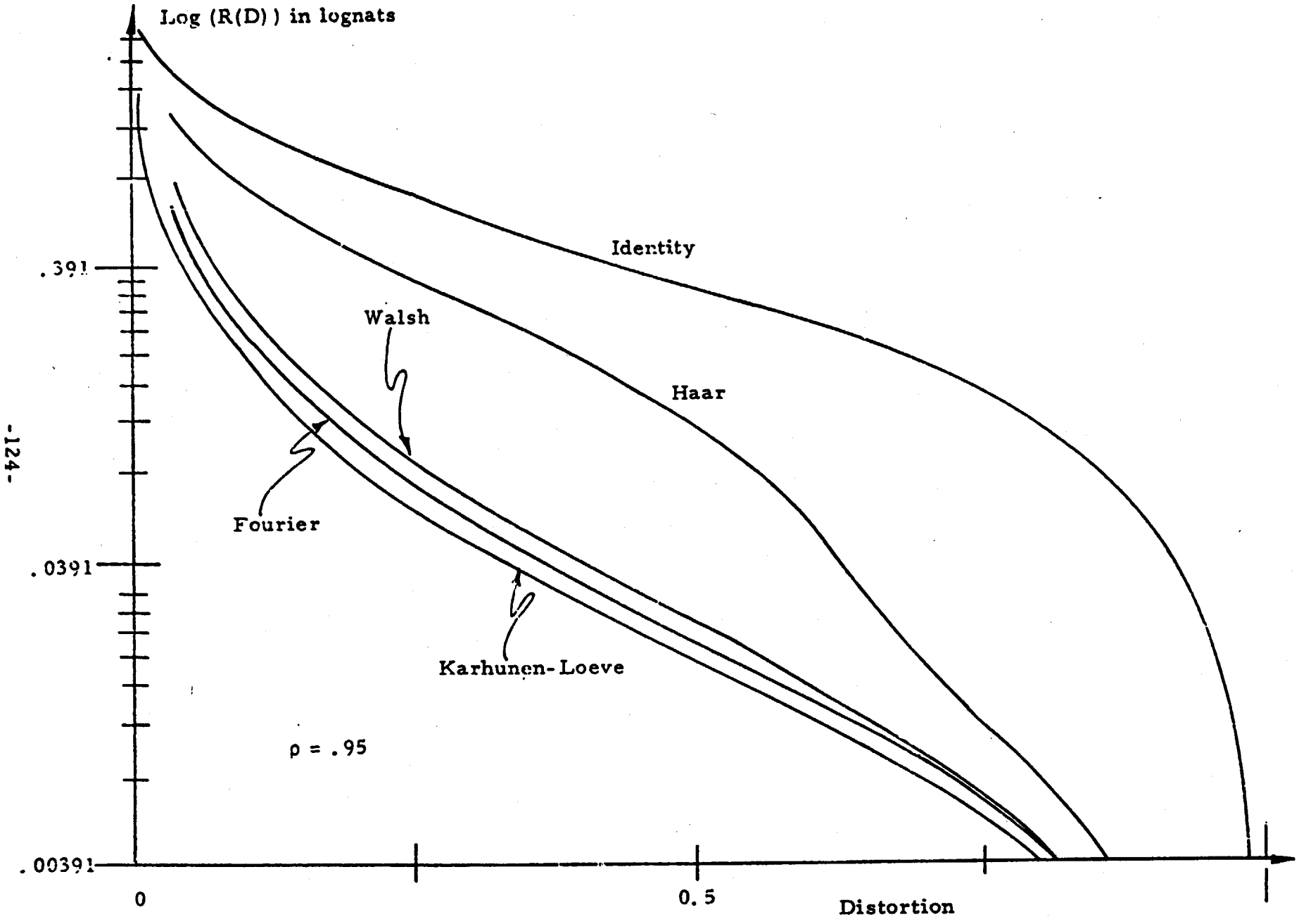

FIGURE 2. Rate Distortion for Various Transforms for a Second Order Gauss-Markov Process (N = 256)

2. Andrews, H. C., "An Experimental Comparison for Karhunen-Loeve and Other Unitary Transforms for Feature Selection Using RDT," Fifth Hawaii International Conference on System Science, (January, 1972), Honolulu, Hawaii.

3. Pearl, J., "Basis-Restricted Transformations and Performance Measures for Spectral Representations," PGIT, Vol. IT-17, No. 6, pp. 751-753, (Nov., 1971).

3.2.3 Data Enhancement of Sampled Images*

GK-20258, National Science Foundation

H. C. Andrews, A. G. Tescher (USC & Aerospace)

Introduction

While the same problem is not easily tractable in mathematical terms, it is usually a simple task for the human observer to choose a preferred image representation. Specifically, if the same scene is represented in various modes, such as through different filters and/or non-linear mapping, usually, the observer can easily select what appears to him the best image. More importantly, if the selection is made by a group of individuals, the variance in the expressed preference is usually small. The phrase, human preference is used here somewhat loosely. We do specify a better image representation where the important image details are emphasized within the constraints of the display medium. It should be noted, that the latter statement implies that the optimum image will not be photometrically accurate in the general case.

The objective of the study reported here, is to develop and analyze algorithms which can be applied for the enhancement of general class of images utilizing some of their statistical parameters.

*Research results presented at the Optical Society of America meeting, Ottawa, Canada, Oct., 1971.

Discussion

While the conclusions can be generalized, the discussed study is restricted to digital image processing. By assumption, the image is readily available in quantized form and the various statistical quantities can be calculated as they are required. Basically, the general strategy of the analysis is to utilize most efficiently the available quantum levels of the display, for mono color presentation. For full pseudo color display the separate images, corresponding to the primary colors, are remapped such that their covariance matrix becomes diagonal. Alternate interpretations of the suggested approach are the maximum utilization of the available degrees of freedom and maximization of image source entropy.

Optimization of the Intensity Image

A general technique that has been successfully used in many applications involves a non-linear intensity transform based on the first order probability density function of the image which is approximated by its intensity histogram. The most "efficient" image is the one whose histogram is a constant.

Color Display Optimization

The histogram equalization principle can be extended to color display which involves the simultaneous display of three images in three different primary colors. The pseudo color representation is obtained by the decomposition of the original single color image into three different images which are then properly combined into a single display in which they represent the primary components.

Conclusions

In this report, we have discussed some conventional and unconventional processing of intensity and color imagery. While the results are preliminary, we feel that the general approach to pseudo color generation may result in a more efficient human interpretation.

3.2.4. Digital Image Enhancement Techniques

GK-20258, National Science Foundation

H. C. Andrews, A. Jain

The use of analytic continuation has often been suggested as a means of extrapolating the frequency domain of an image for enhancement via super-resolution. Often the use of the prolate spheroidal wave functions plays a major role in the implementation of the analytic continuation concepts. For image application, two dimensional expansions into these functions becomes necessary before effective extrapolation can be achieved. In addition, a change in bandwidth suggests a novel means of computing more accurate expansions. These and related techniques are under investigation to determine the feasibility of applying the theory to digital images on large scale computer image processing facilities.

3.2.5 Generalized Wiener Filtering Computation Techniques

F44620-70-C-0113, Air Force Office of Scientific Research

F08606-72-C-0008, Advanced Research Projects Agency

W. K. Pratt

Wiener filtering is a classical technique of signal estimation that has been applied, primarily, to one dimensional, continuous signals, with analysis and implementation based upon continuous Fourier signal theory. It is possible, of course, to perform Wiener filtering operations on time sampled signals, and extend the technique to two dimensions. Furthermore, the filtering operation can be implemented by any unitary transformation, rather than the Fourier transform. Finally, it is possible to significantly reduce the computational requirements without severely affecting performance by a technique of selective

computation.

Figure 1 is a block diagram of a generalized one dimensional Wiener filtering system. A zero mean, M element, data column vector, f, composed of additive and uncorrelated zero mean signals, s, and noise, n, components is the input to the system. The signal and noise are assumed uncorrelated. A unitary transform operation is performed on the input yielding

$$F = Af = As + An \equiv S + N \tag{1}$$

The Fourier, Hadamard, and Karhunen-Loeve transforms have been studied for this application. Next, the transformed input vector is multiplied by the filter matrix, G, and an inverse unitary transform operation is performed. The resultant

$$\hat{s} = A^{-1}GF = A^{-1}GAf \tag{2}$$

is considered the estimate of the signal, with the filter matrix, G, chosen so that the mean square error

$$e = T_r \left\{ \overline{(s-\hat{s})(s-\hat{s})^T} \right\} \tag{3}$$

between the signal, s, and its estimate, $\hat{s}$, is minimized. The expression for the m.s.e. can be rewritten in terms of transform domain quantities as

$$e = Tr \, \overline{(A^{-1}S-A^{-1}G(S+N))(A^{-1}S-A^{-1}G(S+N))^T} \tag{4}$$

Making use of the fact that

$$\overline{SS^T} = C_S = AC_sA^{*T}$$

$$\overline{NN^T} = C_N = AC_nA^{*T}$$

$$\overline{SN^T} = \overline{NS^T} = 0$$

where Cs and Cn are the covariance matrices of the signal and noise vectors, respectively, one obtains

$$e = Tr\left\{ C_S - 2GC_S + GG(C_S + C_N)\right\} \tag{5}$$

Now, a straightforward minimization of eq. (9) yields the optimum filter matrix

$$G_O = C_S(C_S + C_N)^{-1} \tag{6}$$

Thus, the optimum filter matrix may be determined from the transform spectral densities of the signal and noise vectors. Alternatively, the optimum filter can be found by a two dimensional transformation

$$G_O = Ag_OA^{*T} \tag{7}$$

of a matrix

$$g_O = C_s(C_s + C_n)^{-1} \tag{8}$$

based upon the covariance matrices of the signal and noise. The matrix g_O will be called the response matrix, in analogy with the impulse response of a linear system.

Substitution of the optimum filter matrix in eq. (5) gives the minimum m.s.e.

$$e_{min} = Tr\left\{ C_SC_N(C_S + C_N)^{-1}\right\} \tag{9}$$

Alternatively, the m.s.e. can be written in terms of the data domain covariance matrices as

$$e_{min} = Tr\left\{ C_sC_n(C_s + C_n)^{-1}\right\} \tag{10}$$

Note that from eq. (10), the minimum m.s.e. is independent of the type of unitary transform employed. However, the character of the filter

matrix, G, is dependent upon the unitary transform. The conclusion is that one is free to choose the transform that will minimize the computational processes entailed in filter generation and filter operation.

Figure 2 contains magnitude displays of the Hadamard, Karhunen-Loeve, and Identity Wiener filter matrices for a vector length of sixteen elements, a Markov process signal with adjacent element correlation of 0.9 and white noise giving a signal-to-noise ratio of ten. Comparing the filter planes, it is apparent that the filter characteristic changes drastically for different unitary transforms. For the Karhunen-Loeve transform, the filtering operation is a scalar multiplication, while for the identity transform many of the elements of the filter matrix are of relatively large magnitude. The Hadamard filter matrix contains large magnitude terms along the diagonal and terms of decreasing magnitude away from the diagonal.

When considering only the amount of computation required to perform the Wiener filtering operation, as opposed to the computation requirements for the filter generation, it is obvious that the bulk of the computation for the Fourier, Hadamard, and identity transform systems can be attributed to the filter matrix multiplication operation. The Karhunen-Loeve transform system only requires a scalar filter multiplication, but entails two matrix multiplication operations for the transformations. As a compromise, consideration has been given to the development of filter matrices that contain a relatively large number of zero entries. With such matrices the filter operation could be performed with a reduced number of computations. The goal in the filter design, of course, is to maintain the m.s.e. performance as close to the optimum filter level as possible.

The generalized Wiener filtering technique has been applied to the enhancement of images as a test of its validity. Figure 3a shows an original image containing a toy tank. The image contains 256 by 256 elements and 64 grey scales. In Figure 3b uniformly distributed noise

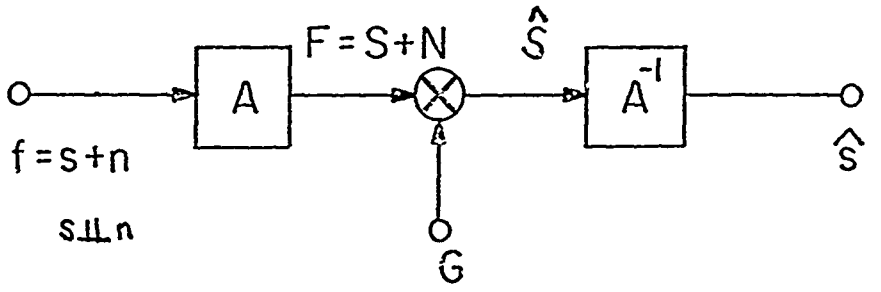

FIGURE 1. Generalized Wiener Filtering

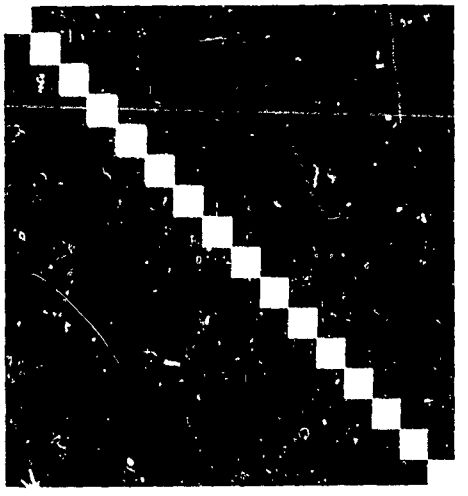

(a) identity

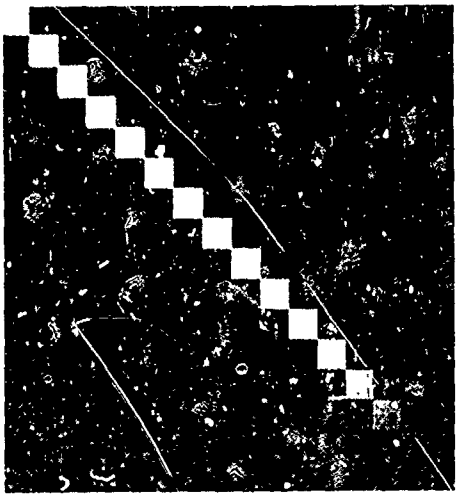

(b) Hadamard

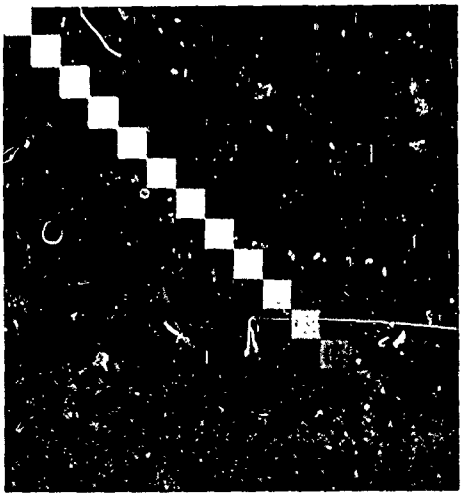

(c) Karhunen-Loeve

Figure 2. Mag·itude Displays of Wiener Filter Matrices

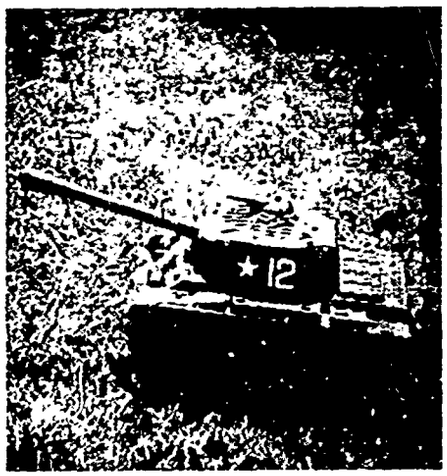

(a) Original

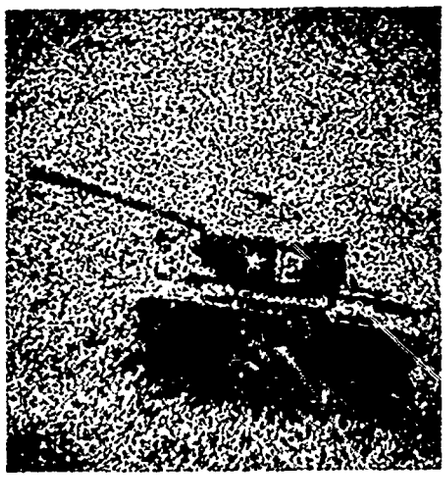

(b) Original plus noise

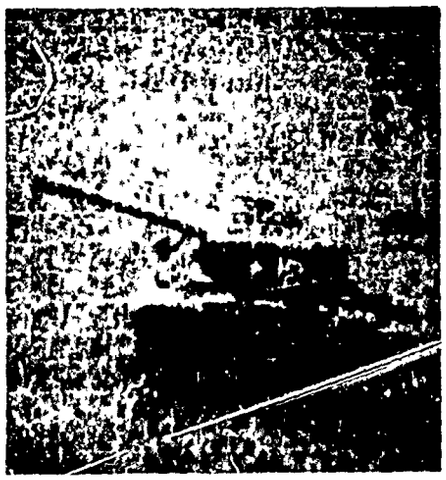

(c) Optimal Hadamard Filtering

(d) Suboptimal Hadamard Filtering

Figure 3. Image Enhancement Examples

has been added to the original to produce an image with a signal-to-noise ration of unity. Figure 3c illustrated the effect of optimal Hadamard transform Wiener filtering in 16 by 16 blocks over the image surface. There is an obvious improvement in image quality, however, the grid pattern caused by the small block size is noticeable. In Figure 3d the filtering operation was performed with only the largest 25% of the filter elements employed in the operation. There is no apparent difference in the visual results for the optimal and suboptimal filtering examples. The grid pattern in the filtered images can obviously be eliminated by filtering over the entire image, but at the expense of computational complexity. Alternatively, the grid pattern can be minimized by overlapping the filtering blocks or by spatial averaging at the interface between blocks.

3.2.6 Nonparametric and Adaptive Techniques in Communication

ENG-74190, National Science Foundation

NGL-05-018-118, National Aeronautics and Space Administration

NAS 5-21505, National Aeronautics and Space Administration

L. D. Davisson, H. C. Andrews, J. R. Velman, C. H. Tang, D. Kazakos, J. K. Kim, P. Papantoni-Kazakos, M. Reichik

This research effort is directed toward the nonparametric and/or adaptive theoretical solution and application of wide classes of problems in detection, prediction and data compression. The research may be summarized briefly as:

1. Nonparametric Detection: Both existing and new schemes for nonparametric detection are investigated; the systems include non-ordered tests, rank tests, and mixtures of both. Particular interest has centered on small sample, large signal tests and tests for continuous

time observation.

2. Stochastic Approximation, Adaptive Prediction and Filtering: Theoretical and experimental schemes for adaptive prediction and filtering are considered. Such schemes have extensive application in data compression, adaptive channel equalization, adaptive antenna arrays, and general communications.

3. Decision Directed Schemes: Methods of estimating unknown signal and/or noise distribution parameters to minimize the error probability (or some other cost function) are investigated. Particular attention is devoted to digital communications with signal-to-signal transmission dependencies.

4. Data Compression: Bounds are developed on the information rates for a given source with respect to fidelity criteria. These bounds are used to design efficient source coding techniques and to analyze the effectiveness of various compression schemes, in particular the relationships between time and transform methods. Applications are made to "real" data, in particular, video data.

Nonparametric coding methods are being studied for data compression. A real time data compression system is being developed for transmissions between Wallops Island, Virginia, and Suitland, Maryland.

Progress has been made in each of the preceding areas. Some of the completed research tasks are reported in references 1-12. Additional work is continuing on optimal small sample nonparametric tests, the distribution of signal plus noise after limiting and filtering, on the performance of adaptive algorithms and on the development of new coding methods and the application of theoretical results to video source coding.

References

1. L. D. Davisson and S. C. Schwartz, "Analysis of a Decision Directed Receiver with Unknown Prioris," IEEE Trans. on Information Theory, May 1970.

2. L. D. Davisson, "Adaptive Predictive Coding," Proc. National Electronics Conference, Nov. 1969.

3. L. D. Davisson, "Adaptive Minimum Mean Square Estimation," IEEE Trans. on Information Theory, July 1970.

4. L. D. Davisson, "Data Compression-Theory and Application," Proc. UMR Communications Conf., Oct. 1970.

5. L. D. Davisson, "Convergence Probability Bounds for Stochastic Approximation," IEEE Trans. on Information Theory, Nov. 1970.

6. L. D. Davisson, "Data Compression and Rate Distortion Theory," Proc. Princeton Conf. on Information Sciences and Systems, March 1970.

7. L. D. Davisson, "Expected Time to Error Threshold Crossing for Adaptive Algorithms," Proc. Princeton Conf. on Information Sciences and Systems, 1971.

8. J. P. Hong, A Multiclass Hypothesis Test with Applications in Pattern Recognition, U.S.C. Ph.D. Dissertation, June 1971.

9. L. D. Davisson, "Two Theorems on Minimax Equalization," IEEE Trans. on Information Theory, May 1971.

10. L. D. Davisson, "Error Threshold Crossings for Adaptive Algorithms," paper presented at the Second International Symposium on Information Theory, Tsahkadsor, USSR, Sept., 1971.

11. J. P. Hong and L. D. Davisson, "A Sequential Hypothesis Test with Applications in Character Recognition," Proc. Second International Symposium on Information Theory, Tsahkadsor, USSR, Sept., 1971.

12. J. K. Kim, Adaptive Estimation with Gradient Following Algorithm for Stationary and M-Dependent Processes, U.S.C. Ph.D. Dissertation, Sept. 1971.

3.2.7 The Study of Synchronization Techniques for Optical Communication Systems

NGR-05-018-164, National Aeronautics and Space Administration

R. M. Gagliardi

Introduction

This study program is devoted to an investigation of problems associated with synchronizing an optical communication system. The objective of the effort is to indicate design procedures, assess system performance, and predict future areas of needed study in synthesizing and improving system operation. The organization and guideline of the study, the particular problem areas, and their applications are covered in the first quarterly report, March, 1969 (submitted to NASA).

The research effort is primarily analytical in nature, and is divided into two categories. The first involves tasks with direct application to the synchronization problem, while the second involves related areas also being studied under the grant. This document reports technical progress during the fourth quarter, but detailed results will be published in separate interim reports, and are omitted here.

Current Progress

During the past quarter the following report has been completed and published.

The Effect of Timing Errors in
Optical Digital Systems

R. Gagliardi

Abstract

The use of digital transmission with narrow light pulses

appears attractive for data communications, but carries with it a stringent requirement on system bit timing. In this paper we investigate the effects of imperfect timing in direct detection (non-coherent) optical binary systems using both PPM and on-off keying for bit transmission. Particular emphasis is placed on specification of timing accuracy, and an examination of system degradation when this accuracy is not attained. Bit error probabilities are shown as a function of timing errors, from which average error probabilities can be computed for specific synchronization methods. Of significant importance is the presence of a residual, or irreducible error probability in both systems, due entirely to the timing system, that cannot be overcome by the data channel.

The material in the above report was presented as an invited paper in Optical Communications Session 12 at the International Telemetering Conference, September 1971, Washington, D.C.

Present study work has been concentrated in the following areas:

1) The Optical Power Allocation Problem (R. Gagliardi)

Earlier results (reported in the above document) have shown that bit error probability in optical digital systems depends on both the data signal count (signal power) and the synchronization signal count (sync signal power). Since the total power for the two signals must originate from the same transmitter, a power division among the two channels must be made during the transmission of the bits. In this study effort an investigation is being made to determine an optimum power split of the transmitter power for data and sync. The straightforward procedure is to attempt to find the power split that minimizes error probability (PE). Unfortunately, the analytical expression for PE is extremely complicated, and not of a closed form, and such a minimization can only be obtained via numerical computation. Alternative procedures would involve minimization over ranges of PE where portions of the PE curve can be approximated. The power allocation solution must also take

into account the format of the synchronization system, i.e., whether the sync channel involves a separate optical channel, a separate baseband channel, or is obtained directly from the modulation. Although all these methods are commonly used, solution of the power allocation problem may indicate an advantage of one of these formats over the others.

2) Optimal Synchronization of Optical Communication System. (N. Mohanty)

The problem of obtaining timing information in an optimal receiver is being investigated as a problem in optimal estimation theory. The objective is to determine if the optimal mathematical solution tends to suggest possible design procedures. Preliminary studies for the optical channel governed by Laguerre counting statistics indicate a very complicated solution for the optimal estimator, and suboptimal solutions may have to be used. A similar situation occurs in the case of an additive Gaussian channel (microwave instead of optical system), and meaningful design procedures were developed using suboptimal estimation.

3) Channel Capacity of an Optical Communication Link. (N. Mohanty, R. Gagliardi)

This area of study affords an information theoretic approach to the assessment of performance in an optical digital communication system. Such an approach would help to understand the advantages of using M level PPM as an encoding scheme. The notion of system efficiency (energy per transmitted data bit) has been studied previously from this point of view, and the present study is intended to be an extension of this work.

4) The study of optical communication systems that employ RF demodulation following noncoherent intensity demodulation of the optical beam. (R. Maag)

Particular attention is devoted to the low power operation, in

which case the count statistics must be properly accounted for. No significant results have been reported during this quarter.

3.3 SWITCHING, AUTOMATA THEORY, COMPUTERS

3.3.1 Automata and Formal Language Theory

GJ 454, National Science Foundation
GJ 28787, National Science Foundation

A. Gabrielian, S. Ginsburg, J. Goldstine, T. N. Hibbard,
D. Kiel, J. Outwater, and B. Rovan

Background

During the past five years, a multitude of different types of acceptors and the languages they recognize have been introduced. Recently, it was observed that most of these devices and languages could be subsumed and unified within the notions of an "abstract family of acceptors", abbreviated AFA, and an "abstract family of languages", abbreviated AFL. This has resulted in a flood of new questions and results, hitherto unsuspected. Whereas before the advent of AFA, there was a surfeit of devices, after AFA there was a sudden scarcity. This situation arose because there were not enough different types of extant devices to answer the new questions.

Progress

A report entitled, "On AFL Generators for Finitely Encoded AFA," was written. In it, two languages, $\tilde{L}_{\mathcal{L}}$ and $\bar{L}_{\mathcal{L}}$, are introduced for each finitely encoded AFA $\mathcal{L}$. Then two conditions on $\mathcal{L}$ are presented, each of which guarantees that $\tilde{L}_{\mathcal{L}}$ and $\bar{L}_{\mathcal{L}}$ are generators for the AFL defined by $\mathcal{L}$. Using $\tilde{L}_{\mathcal{L}}$ and $\bar{L}_{\mathcal{L}}$, generators are exhibited for a number of well-known AFL in computer science.

A report entitled, "On the Largest Full SubAFL of an AFL," was written and subsequently accepted for publication. The main result is that each AFL with the language consisting of exactly the empty word

contains a largest full subAFL.

A report entitled, "The Equivalence of Stack-Counter Acceptors and Quasi-Realtime Stack-Counter Acceptors," was written. In it, stack-counter acceptors are considered, i.e., stack acceptors whose auxiliary storage is over a one-letter alphabet. It is proved that each language accepted by a stack-counter acceptor is accepted by a stack-counter acceptor operating in quasi-realtime.

The paper, "AFL with the Semilinear Property," was published.

The papers, "Multitape AFA" and "Substitution and Bounded Languages," were accepted for publication.

References

1. S. Ginsburg and S. Greibach, "On AFL Generators for Finitely Encoded AFA," June 1971.

2. S. Ginsburg and J. Goldstine, "On the Largest Full SubAFL of an AFL," to appear in Math Systems Theory.

3. S. Ginsburg and G. F. Rose, "The Equivalence of Stack-Counter Acceptors and Quasi-Realtime Stack-Counter Acceptors," October 1, 1971.

4. S. Ginsburg and E. H. Spanier, "AFL with the Semilinear Property," Journal of Computer and System Sciences, vol. 5 (1971), pp. 365-396.

5. S. Greibach and S. Ginsburg, "Multitape AFA," accepted for publication in the Journal of the Association for Computing Machinery.

6. J. Goldstine, "Substituion and Bounded Languages," to appear in the Journal of Computer and System Sciences.

3.3.2 Detection of Faults in Combinational and Sequential Circuits

F44620-71-C-0067, Joint Services Electronics Program
GK-23886, National Science Foundation
N00014-67-A-0269-0019, Office of Naval Research

M. A. Breuer, S. Su, S. J. Chang, D. Ko

I. Introduction

In order to maintain digital equipment it is necessary to be able to detect and locate faults. This is accomplished by testing the circuits. Generating tests for large circuits is quite complex, and no algorithms exist for generating self-tests, i.e., tests for systems which test themselves. Our research deals with developing algorithms for generating fault tests and in developing design techniques for adding logic to aid in the automatic detection of faults.

II. Present Status of Work

A. Linear Networks

Work was completed on the problem of generating tests for linear logic networks[1]. The new results which were added to our first draft of this paper are:

a) A linear tree network can be completely tested for all stuck-at-faults using just three input patterns.

b) In a loop free linear circuit one can distinguish between all single stuck at faults.

B. Test Generation Program

Three papers[2], [3], [4] documenting our program for test generation were revised and have been published. This research was discussed in our previous annual report.

C. Two-Way Input Finite State Machines

The analysis of finite state machines which read from their input tape in two directions is being carried out by Mr. S. Chang. The results to date deal with three main areas, namely, the state reduction of such devices; the testing of such devices when restricted to reading in only one direction and when they are not strongly connected; the general testing problem. A few results obtained so far are:

1) conditions to identify periodic operation of a 2-way sequential machine;

2) the input and output languages to the finite state control are context sensitive languages;

3) techniques for extending the testing strategy of Hennie[7] to machines which are not strongly connected;

4) necessary and sufficient conditions have been obtained for determining when a simple experiment (rather than a multiple one) exists for testing such a machine.

D. Hardware Error Detection

The problem of adding logic to aid in fault detection is being investigated by Mr. D. Ko. The objective of this work is to append to a logic network a checking circuit with output ϵ so that $\epsilon = 1$ iff a fault exists which is producing an incorrect output. Parity checkers solve this problem if an odd number of output lines are in error. The general problem can be solved by duplicating the logic. The solution sought in our research is one which will require less logic than the duplication method.

Our results to date have been in the following areas:

1. Error Analysis

a. Circuit topological conditions required for multiple errors.

b. Input conditions required for multiple errors.

c. A model for representing multiple errors and techniques for their analysis.

2. Error Detection Strategy

Two major approaches have been studied which led to the discovery of four distinct error checking methods as described below:

a. Forced-Parity Error Detection

Two methods have been developed in which additional hardware is introduced to assure the correct generation of ODD error-parity. In this case the parity checker alone is sufficient to detect all output errors. This approach is not valid if the internal nodes of a circuit are not accessible, however, it will serve as a design criterion for initial layout of self-testing circuitry.

(1) Fanout Degenerating Method

This method can be considered as an iterative process and can be expressed by the following set of equations:

$$\mathcal{F}_\alpha(t+1) = \mathcal{F}_\alpha(t) - 1, \quad 0 \leq t \leq t_{max}, \quad \mathcal{F}_\alpha(0) \geq 2 \text{ and } \mathcal{F}_\alpha(t_{max}) = 1$$

where $\mathcal{F}_\alpha(t)$ is the fanout value of node α at time t during processing. The objective of this process is to reduce the number of output line errors (error-parity) due to a fault in α from EVEN to ODD under all input conditions. In the mean time, new signals α', α'', $\cdots$ are successively built by duplicating the α function.

(2) Fanout Enhancing Method

Contrary to the previous method, this method will not require any duplication of the fanout signal. Instead, a tapping of the fanout node along with some gating (ψ) circuitry is fed directly to the parity checker. Similarly, this process can be expressed by the

equations:

$$\mathcal{F}_\alpha(t+1) = \mathcal{F}_\alpha(t) + 1, \quad 0 \leq t \leq 1, \quad \mathcal{F}_\alpha(0) \geq 2$$

b. Supplemental Error Detection

Unless the Forced-Parity method is employed, the parity checker alone will fail in case of an EVEN error-parity exists. One way of attacking this problem is to have a supplemental error detection circuit built locally to the line pair where double errors are unavoidable. This method does not require any access to the internal nodes, but rather, like partial duplication, it duplicates what is needed on the output functions.

(1) Unconditional Sensing Method

First of all, the double-error pattern of a line pair (i,j) has to be determined. Based on this information, a minimal cost generating function $g_{ij} = g(f_i, f_j)$ is sought implemented in terms of the input variables. $\hat{g}_{ij} = g(i,j)$ is also implemented in terms of the primary output (PO) line signals. A comparison organ is used at the last stage to sense the error condition and hence serves as a supplemental error detector for the parity checker. Let ϵ_{ij} be the error signal of (i,j), ϵ_p be the error signal of the parity checker and ϵ be the overall error signal for the circuit under consideration. Then

$$\epsilon_{ij} = g_{ij} \oplus \hat{g}_{ij}, \quad \epsilon = \epsilon_p + \epsilon_{ij}$$

This method ignores the input conditions under which errors may occur.

(2) Conditional Sensing Method

In this method, the input conditions play an important role. The true logic value of an arbitrary line of (i,j) is found under input conditions when double errors can occur. Take line j for instance and

call its value $V_j(w_{ij}) \in \{0,1\}$ while under input conditions for which $w_{ij} = 1$. Thus $\epsilon_{ij} = w_{ij}(j \oplus V_j(w_{ij}))$.

E. Detection of Intermittent Faults

It is paradoxial that while almost all published papers deal with solid logic failures, the majority of logic failures in many technologies are intermittent. We have recently made significant progress on the problem of generating a fault detection test sequence for the following model:

1. Clocked (synchronous) sequential circuits
2. Multiple faults (non-redundant)
3. Intermittent faults.

Consider a clocked, synchronous sequential circuit. Assume clocked pulses occur at times $T = t_1, t_2, \ldots, t_K = T'$. We say that a fault F is race free if when clock pulse t_k occurs, $k = 1,2,\ldots,K$, the circuit is stable, whether or not the fault is present. That is, if the fault does occur between clock pulse t_{k-1} and t_k, it occurs early enough so that all signal changes caused due to the fault have stablized by time t_k. If F is present at time t_k we set $\delta_k = 1$, otherwise $\delta_k = 0$. The occurrence of the fault F can be represented by the fault pattern $\underline{\delta} = (\delta_1, \delta_2, \ldots, \delta_K)$. If $\underline{\delta} = (1,1,\ldots,1)$ we say that F is a permanent fault over the time interval $[T,T']$. If $\underline{\delta} = (1,1,\ldots,1)$ as $T' - T \to \infty$, we say that F is a permanent fault. If $\underline{\delta} = (0,0,\ldots,0)$ we say that the circuit is F fault free over the interval $[T,T']$. Let F be a fault defined by the fault pattern $\underline{\delta} = (\delta_1, \delta_2, \ldots, \delta_K)$ over the interval $[T,T']$. Then F is said to be an intermittent fault over the interval $[T,T']$ if and only if the probability of a $\underline{\delta}$ occurring such that $\underline{\delta} \neq (1,1,\ldots,1)$ or $\underline{\delta} \neq (0,0,\ldots,0)$ is non-zero.

We will denote the fault pattern $\underline{\delta} = (\delta_1, \delta_2, \ldots, \delta_K)$ by the decimal equivalent of the binary integer $\delta_K \delta_{K-1} \cdots \delta_1$. For example, $\delta(0) = (00\ldots0)$, $\underline{\delta}(1) = (1,0,0,\ldots,0)$, $\delta(2) = (0,1,0,0,\ldots,0)$, and

$\underline{\delta}(2^K-1) = (1,1,\ldots,1)$.

There may be many causes for the occurrence of an intermittent fault, such as loading (data dependent), temperature, radiation, marginal power voltages, vibration, etc. For this discussion, we will consider a very simple model for describing the occurrence of a fault, namely, we assume that $\delta_k = 1$ with probability p. The occurrence of the fault during interval $t_k + \epsilon \leq t \leq t_{k+1}$ is statistically independent of its previous history of occurrence. In addition, we assume the fault is race free.

Note that there are 2^K possible fault patterns, each of which defines a circuit $C^{\underline{\delta}(t)}$, $t = 0,1,\ldots,2^K-1$, where $C^{\underline{\delta}(0)}$ is the fault free circuit. Let $\underline{x} = x_1 x_2 \ldots x_K$ be an input sequence and $Z^{\underline{\delta}(t)}$ be the response of $C^{\underline{\delta}(t)}$ to $\underline{x}$ starting in initial state $\gamma^{\underline{\delta}(t)}$. Then $\underline{x}$ detects fault pattern $\underline{\delta}(t)$, $t \neq 0$, if and only if $Z^{\underline{\delta}(t)} \neq Z^{\underline{\delta}(0)}$. Fault pattern $\underline{\delta}(0)$ is non-detectable. $\underline{x}$ is a fault detection test for intermittent fault F if and only if $Z^{\underline{\delta}(t)} = Z^{\underline{\delta}(0)}$ for $t = 1,2,\ldots,2^K-1$.

Since errors due to faults may require many clock periods to propagate to a primary output, we will consider only a specific subclass $\Delta(Q,K)$ of fault patterns having parameters Q,K. That is, $\underline{\delta} = (\delta_1, \delta_2, \ldots, \delta_{K'}) \in \Delta(Q,K)$ if and only if $K = K'$ and $\delta_q = 1$ for some $q \leq Q$. Therefore $|\Delta(Q,K)| = 2^K - 2^{K-Q}$. We have found that for a given intermittent fault F and parameter Q, for any value of K it is not always possible to construct a fault test $\underline{x}$. For this reason one must consider the probability of detection.

Let $|\delta|$ be the number of one elements in fault pattern $\underline{\delta}$. During any interval $[T,T']$ the probability of fault pattern $\underline{\delta}$ occurring is $p(\delta) = p^{|\delta|}(1-p)^{K-|\delta|}$. For a given $\underline{x}$, let $m(\underline{x}) = \{k \mid z^{\underline{\delta}(k)} = z^{\underline{\delta}(0)}, k \neq 0, \underline{\delta}(k) \in \Delta(Q,K)\}$. The probability P that $\underline{x}$ detects intermittent fault F is $P = p_1 p_2$ where p_1 = prob. $\underline{\delta}(k) \in \Delta(Q,K)$ occurs for some k, and p_2 = prob. $k \notin m \mid \underline{\delta}(k) \in \Delta(Q,K)$. Now $p_1 = 1 - (1-p)^Q$ and $p_2 = 1 - \sum_{k \in m(\underline{x})} p(\underline{\delta}(k))$.

The probability p_2 is called the miss value of $\underline{x}$ since it is the probability that a fault pattern of interest occurred and was not detected. If $\underline{x}$ is repeated R times, then the probability of detecting fault F is P(R), where $P(R) \geq 1 - (1-P)^R$, and where we have " $\geq$ " due to the assumption on the initial conditions. Assume $P(R) \cong 1 - (1-P)^R$. If we require a probability of detection of P*, then we must select R such that

$$R \geq \frac{\ln (1-P^*)}{\ln (1-P)}$$

A few of the results obtained so far are:

1. Results indicating how the length of a test sequence varies as a function of Q in order to obtain a given probability of detection P*.

2. Results concerning the properties and existence of tests for intermittent fault patterns, such as

a. If a test exists for $\underline{\delta}$, then there exists a test for $\delta_0 \underline{\delta} = (\delta_0, \delta_1, \delta_2, \ldots, \delta_K)$;

b. The value of K-Q need only be as large as the memory bound of the circuit;

c. It is sufficient to consider only the case Q = 1 for seeking the existence of a test.

3. (Main Result). For a given value of Q and K, we have developed an algorithm for generating a test $\underline{x}$ with the smallest miss value. To solve this problem we employed three extensions of classical testing techniques, namely:

a. Mapping of sequential circuits to iterative combinational circuits (previously known).

b. Developed an algorithm for generating a test for a multiple fault in a combinational circuit.

c. Developed an algorithm for generating a test for a

set S of faults in a combinational circuit, i.e., $\underline{x}$ is a test for all faults in S. (These faults do not occur simultaneously in time.)

References

1. M. A. Breuer, "Generation of Fault Tests for Linear Logic Networks," IEEE Trans. on Computers, vol. C-21, January 1972 pp. 79-83.

2. M. A. Breuer, "Generation of Fault Detection Tests for Sequential Circuits," Digest 1971 International Symposium on Fault-Tolerant Computing, (IEEE), pp. 18-21.

3. M. A. Breuer, "A Random and an Algorithmic Technique for Fault Detection Test Generation for Sequential Circuits," IEEE Trans. on Computers, vol. C-20, November 1971, pp. 1364-1371.

4. M. A. Breuer, "An Algorithm for Generating a Fault Detection Test for a Class of Sequential Circuits," presented at the International Symposium on the Theory of Machine and Computation, Haifa, Israel, August 1971, and published in Theory of Machines and Computations, Z. Kohavi (ed), Academic Press, 1971, pp. 313-326.

5. M. A. Breuer, "Recent Developments in the Automated Design and Analysis of Digital Systems," Proc. IEEE, (to be published).

6. M. A. Breuer, "A Note on Three-Valued Logic Simulation," IEEE Trans. on Computers, vol. C-21, (to be published).

7. F. C. Hennie, "Fault Detection Experiments for Sequential Circuits," Proc. Fifth Annual Symp. on Switching Circuit Theory and Logical Design, pp. 95-110, October 1964.

3.3.3 Computer Techniques of System Identification

AFOSR 71-2008

G. A. Bekey and J. Seo

The major objective of this research is to develop computationally efficient algorithms for determining unknown parameters in mathematical models of dynamic systems. Resulting techniques are of

great importance in synthesizing such mathematical representations as aircraft dynamics, human pilot behavior, flight control systems, and structural dynamics. During the past year major effort was devoted to improving the efficiency of such techniques as the Fletcher-Powell method[1] and stochastic approximation[2]. Results to date have demonstrated that use of hybrid computer techniques in connection with the Fletcher-Powell-Davidon algorithm may result in a reduction of computation time of the order of 100 to 1, as compared to all digital methods.[1]

In the course of our work on system identification, a broad survey of the field has recently been published[3].

Currently, attention is devoted to the problem of developing an interactive and highly automated technique of constructing mathematical models from system input-output data.

References

1. Bekey, G. A. and J. C. Maloney, "Parameter Identification with a Hybrid Computer Implementation of the Fletcher-Powell Method," Proc. 3rd International Conf. on System Sciences, Hawaii, pp. 175-177, January 1970.

2. Bekey, G. A. and C. B. Neal, "Estimation of the Parameters of Sampled Data Systems by Means of Stochastic Approximation," International Journal of System Science, v. 1, pp. 63-74, 1970.

3. Bekey, G. A., "System Identification--An Introduction and a Survey," Simulation, v. 15, pp. 151-166, October 1970.

3.3.4 Digital Simulation Techniques

AFOSR 71-2008

G. A. Bekey

A promising technique for improving the computer processing of engineering data is in the development of digital simulation

methods, particularly as these are combined with graphic oriented interactive computer systems. In cooperation with personnel of the Rand Corporation, computer techniques for dynamic systems simulation[1] have been developed. An outcome has been a set of guidelines evaluating new digital simulation languages termed "natural simulation languages"[2]. It is our view that new simulation languages should use the capabilities of modern computers not only to obtain numerical solutions to equations, but to assist the user to understand the interrelationships between complex subsystems.

References

1. Bekey, G. A. and E. C. DeLand, "Interactive Simulation of Continuous Systems: Progress and Prospects," Proc. Mexico International Conference on Systems, Networks and Computers, pp. 641-648, 1971.

2. DeLand, E. C., G. A. Bekey and G. P. Moore, "Toward a Natural Simulation Language," Proc. of 1971 Summer Computer Simulation Conf., Boston, July 1971.

4. MATHEMATICAL BIOSCIENCES AND BIOMEDICAL ENGINEERING

(This section is omitted from this edition.)

APPENDIX A

Recent Publications

Allred, W. B.

"An Infrared Localized Vibrational Mode Technique for Measuring Segregation Coefficients," J. Phys. Chem. Solids, Pergamon Press, 1971, 32, pp. 1-14, 1970.

Andrews, H. C.

"Walsh Functions in Image Processing, Feature Selection and Pattern Recognition," 3rd Annual Walsh Symposium, April 1971, Washington, D.C., also see IEEE Trans. Electromagnetic Compatibility, Vol. EMC-13, No. 3, p. 26-32 (August, 1971).

"Multidimensional Rotations in Feature Selection," IEEE Trans. on Computers, Vol. 20, No. 9, pp. 1045-1051, (September, 1971).

"Some Unitary Transformations in Pattern Recognition and Image Processing," Proceedings IFIP Congress 71, Ljubljana, Yugosloavia (Aug. 23-28, 1971).

"Computer Image Manipulation for Restoration and Enhancement," International Telemetry Conference (Sept. 27-29, 1971), Washington, D.C.

Azen, S. P.

"Solution of Fredholm Integral Equations with Displacement Kernals that Satisfy a Linear Ordinary Differential Equation," with H. Kagiwada and R. Kalaba, to appear in Journal Approximation Theory.

Book: Statistical Analysis: A Computer Oriented Approach, with A. Afifi, Academic Press, New York, to appear, April, 1972.

"Asymptotic and Small Sample Behavior of Estimated Bayes Rules for Classifying Time-Dependent Observations," with A. Afifi, submitted to Biometrics.

"A Longitudinal Predictive Study of Success and Performance of Law Enforcement Officers," with H. Snibbe and H. Montgomery, submitted to Journal of Personality and Social Psychology; also as a chapter in Urban Policeman and Transition Studies, Snibbe and Snibbe, eds., Charles C. Thomas, Springfield, Illinois, to appear 1972.

Bekey, G. A.

"Control Theory in Biological Systems," with M. B. Wolf, Chapter 2 in Biomedical Engineering, ed. by J.H.U. Brown, J. E. Jacobs, and L. Stark, F. Davis Press (1971).

"Interactive Simulation of Continuous Systems: Progress and Prospects", with E. C. DeLand, in Proc. Mexico Intern. Conf. on Systems Networks and Computers, pp. 641-648 (1971).

Breuer, M. A.

"An Algorithm for Generating a Fault Detection Test for a Class of Sequential Circuits," presented at the International Symposium on the Theory of Machine and Computation, Haifa, Israel, August, 1971, and published in Theory of Machines and Computations, Z. Kohavi (ed.), Academic Press, 1971, pp. 313-326.

"A Random and an Algorithmic Technique for Fault Detection Test Generation for Sequential Circuits," IEEE Trans. on Computers, vol. C-20, November 1971, pp. 1364-1371.

"Generation of Fault Tests for Linear Logic Networks," IEEE Trans. on Computers, vol. C-21, January 1972, pp. (to be published).

"Recent Developments in the Automated Design and Analysis of Digital Systems," Proc. IEEE, (to be published).

"A Note on Three Valued Logic Simulation," IEEE Trans. on Computers, vol. C-21, (to be published).

"Recent Developments in Design Automation," Computers, to be published.

Crowell, C. R.

"Deep Level Impurity Effects on the Frequency Dependence of Schottky Barrier Capacitance," with K. Nakano, to be published.

"Threshold Energies for Electron-Hole Pair Production by Impact Ionization in Semiconductors," with C. L. Anderson, to be published.

"High Field Impact Ionization in the Baraff Approximation," with Y. Okuto, to be published.

Daybell, M. D.

"Anomalous Concentration Dependence of Kondo Resistivity Below T_K in Cu Cr," Bull. Am. Phys. Soc. 16 (1971) 840.

Gilbert, P.

"Interference Between Communicating Parallel Processes," with W. J. Chandler, to appear in Communications of the ACM.

Ginsburg, S.

"AFL with the Semilinear Property", J. of Computer and Systems Sciences, Vol. 5, pp. 365-396 (with E. H. Spanier) (1971).

"Images of AFL Under Certain Families of Homomorphisms", to appear in Mathematical Systems Theory (with J. Hopcroft).

"Multi-Stack-Counter Languages," to appear in Math. Systems Theory (with R. Book).

"Multitape AFA", to appear in the Journal of the Assoc. for Computing Machinery (with S. A. Greibach).

"On the Largest Full Sub AFL of an AFL", to appear in Math. Systems Theory (with J. Goldstine).

Golomb, S. W.

"A New Number-Theoretic Function of Combinatorial Significance," Journal of Number Theory, to appear, 1971/72.

"How to Number a Graph", chapter in Graph Theory and Computing, Edited by R. C. Read, Academic Press, 1971/72.

"On the Survival of Sequence Information in Filters", IEEE Trans. on Information Theory, to appear, 1972.

Grodins, F. S.

"Comparison of Parameter Identification Methods Applied to a Study of Peripheral Vascular Function", with S. M. Yamashiro and T. Sato, Fed. Proc. 30: 698 Abs., 1971.

"Estimation of Capillary Hydrostatic Pressure and Filtration Coefficient Using Sinusoidal Perturbation of Isogravimetric State," with T. Sato and S. M. Yamashiro, Fed. Proc. 30: 661 Abs., 1971.

"Effect of Simulated Metabolic Loading on Respiration," with S. M. Yamashiro and M. Gordon, Physiologist 14: 255, 1971.

Hurrell, J. P.

"Nuclear Induced Electron-Spin-Echo Decay in Solids", Solid State Comm. 9, 461 (1971).

Hellwarth, R. W.

"Intensity Induced Changes in Optical Polarization in Glasses," with A. Owyoung and N. George (to be published in Phys. Rev.).

"Origin of the Nonlinear Refractive Index of Liquid CCl_4," with A. Owyoung and N. George (to be published in Phys. Rev.).

Kashef, R. S.

"A Formal Approach to the State Assignment of Asynchronous Sequential Machines," submitted to IEEETC, July 1971.

"On the Race-Free Assignments and Classifications of 9 to 16 Rows Asynchronous Sequential Machines," submitted IEEETC, July 1971.

"On the Race-Free Assignment and Classification of Asynchronous Sequential Machines," to be presented at the Annual International Conference on System Sciences, Jan. 1972.

Kim, Y. B.

"Alternating Current Losses in Hollow Cylinders," J. Appl. Physics, 42, 550 (1971).

Kuehl, H. H.

"Reflection and Transmission Measurements on a Magnetized Plasma Slab," with B. O'Brien, Phys. Fluids 14, 1187 (1971).

Lakin, K. M.

"Perturbation Theory for Electromagnetic Coupling to Elastic Surface Waves on Piezoelectric Substrates," Journal of Applied Physics, 42, 899, (1971).

Lamont, J. W.

"The Mini Computer--Its Role in Power Systems," with M. Couchman, to be published in Electrical World.

Lindsey, W. C.

"Double Loop Tracking Systems," with J. H. Yuen, Proceedings of the 1971 IEEE Conference on Engineering in the Ocean Environment, San Diego, Calif., Sept. 1971.

"Coherence of Random Nonlinear Oscillations," with M. J. Siman, pending publication, IEEE Transactions.

"Nonlinear Analysis of Cascaded Tracking Systems," with J. H. Yuen, ITC/7/, Sept. 1971, Wash., D.C., June, 1971. Also pending publication in IEEE Transactions.

"Carrier Synchronization and Detection of Polyphase Signals," pending publication, IEEE Transactions.

"An Application of the Nonlinear Theory of Generalized Tracking Systems to a Third-Order Phase-Locked Loop, April, 1972, pending publication, IEEE Transactions on Com. Tech.

"Block-Coded Communications," NASA Tech. Brief, 70-10242 Paper Award, April, 1971.

Marburger, J. H.

"OGO-V Magnetic Field Data Near the Earth's Bow Shock: A Correlation With Theory," with J. Guha and D. Judge, Journal Geophysical Research (1971).

"Observation of Moving Self-Foci in Sephire," with C. Giuliano, Phys. Rev. Letters 27, 905 (1971).

"Theory of Self Focusing for Fast Nonlinear Response," in Damage in Laser Material, edited by A. J. Glass, et. al. Proceedings of 3rd Symposium on Damaged in Laser Material, NBS Special Publication, Page 51 (1971).

"IR Window Criteria; 'Exact' Analysis of the Thermal Distortion Problem," with M. Flannery in Proceedings of Coherence on "High Power IR Laser Window Materials" (1971).

Moore, G.

"Models for the Release of Transmitter Agent at the Neuromuscular Junction," with M. Anderson and J. C. Watts, 9th Annual Symposium on Biomathematics and Computer Science in the Life Sciences, Houston, Texas, March 1971.

Murr, L. E.

"Effects of Plastic Strain and Strain Rates on the Mechanical Properties and Thermal Recovery of Type 304 Stainless Steel," with J. A. Korbonski, Metals Engr. Quarterly, Vol. 11, pp. 47-48 (1971).

"Applications of the TEM, SEM, and FIM in the Analysis of Structure and Energy of Metal Interfaces," with O. T. Inal and G. I. Wong, in The Structure and Properties of Materials--Techniques and Applications of Electron Microscopy (Proc. 5th International Materials Symposium, Berkeley, 1971).

Nahi, N.

"Adaptive Decision-Directed Recursive Estimators," with B. M. Schaefer, Proceedings of Joint Automatic Control Conference, St. Louis, Missouri, August 1971.

"Bayesian Recursive Image Estimation," with T. Assefi, Proceedings of Two-Dimensional Digital Signal Processing Conference, Columbia, Missouri, Oct. 1971.

"Sequential Error Detection for Nonlinear Estimators," with B. M. Shaefer, Proceedings of Second Symposium on Nonlinear Estimation Theory, San Diego, Calif., September 1971.

"Decision-Directed Adaptive Recursive Estimators: Divergence Prevention," with B. M. Schaefer, IEEE Transactions on Automatic Control, Feb. 1972.

"Bounding Filters in the Presence of Inexactly Known Parameters," with I. M. Weiss, Proceedings of 1971 IEEE Decision and Control Conference, Miami, Florida, Dec. 1971.

"Design of Probing Signals for Vector Parameter Estimation," with G. A. Napjus, Proceedings of 1971 IEEE Decision and Control Conference, Miami, Florida, Dec. 1971.

Payne, H. J.

"Systems Problems in Freeway Traffic Control and Surveillance," invited paper presented at the 1971 National Transportation Engineering Meeting, Seattle, Wash., July 26-30.

"Suboptimal Control of Large Scale Systems with Application to Freeway Traffic Regulation," Proceedings of the Fourth International Conference on System Sciences (1971), 332-334 (with L Isaksen).

Reed, I. S.

"The Effect of Envelope Limiting in Adaptive Array Control Loops", with L. E. Brennan, IEEE Trans. on Aerospace and Elect. Systems, Vol. AES-7, No. 4, July 1971.

"Path Sensitization, Boolean Difference and Automated Fault Diagnosis," with A.C.L. Chiang and A. V. Banes, IEEE Trans. on Computers, to be published, January 1972.

"Coding Versus Noncoding Redundancy for Failure-Tolerant Sequential Circuits," with R. W. Larsen, IEEE Trans. on Computers, to be published, January 1972.

"Notes on the Arithmetic BN Modulo A Codes," IEEE Trans. on Computers, to be published in 1972.

"An Information Theoretic Measure of Image Similarity", with L. A. Liporace, IEEE Trans. on Info. Theory, to be published.

"The Systematic Selection of Cyclically Equivalent Codes," with C. T. Wolverton, accepted for publication in IEEE Trans. on Info. Theory, 1972.

Scholtz, R. A.

Book Review: "Theory of Synchronous Communications," by J. J. Stiffler, IEEE Transactions on Information Theory (to appear).

"Frequency Tracking Loop Study," with T. M. Rodriguez and C. L. Weber, submitted to the 5th Hawaii Inter. Conf. on System Sciences, January 1972.

Shlichta, P. J.

"Movement of Crystal Inclusions in a Centrifugal Field," with W. R. Wilcox, J. Appl. Physics, Vol. 42, No. 5, pp. 1823-7 (1971).

"Relationship Between T-O-T Angle and Metastability of $LiAlSi_2O_6$-III," with C. T. Li, submitted to American Mineralogist.

"Three- and Four-Dimensional Hadamard Matrices," Bull. Amer. Phys. Soc., Series II, Vol. 16, No. 8, pp. 925-6 (1971).

Silverman, L. M.

"Structure and Stability of Discrete-Time Optimal Systems," IEEE Trans. on Automatic Control, Vol. AC-16, pp. 227-233, 1971 (with D. Rappaport).

"Realization of Linear Dynamical Systems," to appear in special issue of IEEE Trans. on Automatic Control, December 1971.

"Exact Model Matching by State Feedback and Dynamic Compensation," to be presented at the 1971 Decision and Control Conference (with B. C. Moore).

"Structure of Index Invariant Systems," to be presented at the 1971 Decision and Control Conference (with A. S. Morse).

Smit, J.

"Phonon Coupling and Angular Dispersion in Biaxial $NaNO_2$," with C. M. Hartwig, E. Wiener-Arnear and S. P.S. Porto, Phys. Rev. B 3, 2078 2080 (1971).

"Mössbauer Effect in Lithium-2 inc Ferrites," with J. W. Young, J. Appl. Phys. 42, 2345-48 (1971).

"Theory of Raman Scattering in Solids," Phys. Rev. B, 3, 4330-37 (1971).

Smith, T. I.

"Superconducting Microwave Cavities and Josephson Junctions," Bull. Am. Phys. Soc. 16, 843 (1971).

"Magnetic Fields Produced by a Hollow Superconducting Cylinder and a Coaxial Solenoid," Bull. Am. Phys. Soc. 16, 843 (1971).

Spitzer, W. G.

"Investigation of Te-Doped GaAs Annealing Effects by Optical and Channelling Effect Measurements," with I. V. Mitchell, J. W. Mayer, and J. K. Kung, J. Appl. Phys. 42, 3982 (1971).

"Infrared Localized Vibrational Mode Absorption of Ion Implanted Aluminum and Phosphorus in GaAs," with L. H. Skolnik, A. Kahan, and R. G. Hunsperger, to be published, J. Appl. Phys.

"Localized Vibrational Modes in Semiconductors: Infrared Absorption," Advances in Solid State Physics/Festkörperprobleme, Vol. 11, Pergamon Press, 1971.

"Localized Vibrational Mode Absorption of Ion Implanted Silicon in GaAs," with L. Skolnik, A. Kahan, F. Euler, and R. G. Hunsperger, to be published, J. Appl. Phys.

Steier, W. H.

"Simultaneous Mode Locking and Pulse Coupling of the CO_2 Laser," with R. G. Eguchi, M. M. Mann and W. B. Lacina, Appl. Phys. Letters 18, pp. 406-408 (May 1, 1971).

"Rotating-Waveplate Optical-Frequency Shifting in Lithium Niobate," with J. P. Campbell, IEEE Journal of Quantum Electronics QE-7, pp. 450-457 (September 1971).

"Bandwidth and Threshold Calculations for Angle Tuned Parametric Oscillators," with Ramen Basu, to be published.

Su, S. Y. H.

"A Digital Modeling and Design Language," with M. B. Baray, Proceedings of the 8th Annual Design Automation Workshop, June 28-30, 1971, Atlantic City, New Jersey, pp. 1-22.

"A System Modeling Language Translator," with M. B. Baray and R. L. Carberry, Proceedings of the 8th Annual Design Automation Workshop, June 28-30, 1971, Atlantic City, New Jersey, pp. 35-49.

"The Structure and Operation of a System Modeling Language Compatible Simulator," with M. B. Baray and R. L. Carberry, Proceedings of the 8th Annual Design Automation Workshop, June 28-30, 1971, Atlantic City, New Jersey, pp. 23-34.

"Digital System Fault Diagnosis Package," with R. L. Carberry, Proceedings of 1971 Summer Computer Simulation Conference, July 19-21, 1971, Boston, Massachusetts, pp. 83-95.

"The Role of a Logic Level Simulator as a Teaching Aid," with R. L. Carberry, presented at the Annual ASEE (American Society for Engineering Education) Conference, June 21-24, 1971, Annapolis, Maryland, to be published in ASEE Journal.

Sworder, D. D.

"Suboptimal Control of Linear Systems Derived from Models of Lower Order," 1971 Joint Automatic Control Conference, pp. 926-935, 1971; also AIAA Journal, Vol. 9, No. 8, pp. 1461-1467, August 1971 with R. O. Rogers.

"Constrained Linear Filtering as a Multistage Process," 1971 Joint Automatic Control Conference, pp. 135-139, 1971, with A. Jain.

"Feedback Estimation Systems and the Separation Principle of Stochastic Control," 1971 Joint Automatic Control Conference, pp. 834-840, 1971; also IEEE Trans. on Automatic Control, Vol. AC-16, No. 4, pp. 350-354, August 1971, with S. C. Sworder.

"Optimal Control, Repair and Inventory Strategies for a Linear Stochastic System," 1971 IEEE Conf. on Decision and Control, pp. 393-394, 1971 (abstract); also IEEE Trans. on Systems, Man and Cybernetics, July 1972, with T. Kazangey.

"Bayes Controllers with Memory for a Linear System with Jump Parameters," IEEE Trans. on Automatic Control, Vol. AC-17, No. 1, February 1972.

"Simulation of Societal Systems," Simulation Councils Proceedings, Vol. 1, No. 2, 1971.

Weber, C. L.

"Frequency Tracking Loop Study," Proc. of the Fifth Hawaii Conf. on System Sciences, with T. Rodriguez and R. A. Scholtz, January, 1972 (submitted).

"A Digital Decision-Directed Receiver for the Multipath Channel," Proc. of the Fifth Hawaii Conf. on System Sciences, with R. Fielding, January 1972 (submitted).

"Bounds on the Free Distance of Convolutional Codes," Proc. of the International Symposium on Information Theory, Asilomar, Calif., with G. K. Huth, Feb. 1972 (submitted).

"Minimum Weight Code Words of Given Length," Proc. of the International Symposium on Information Theory, Asilomar, Calif., with G. K. Huth, Feb. 1972 (submitted).

Wang, R.

"Martensitic Transformation in Metastable Y-Zr Alloys," with G. H. Narayanan, to be published.

"Preparation of Rare Earth-Cobalt Permanent Magnetic Fire Powders by a 'Liquid Spring and Quenching' Technique," with K. S. Kim and S. A. Shei, Apply. Phys. Letters (1972).